INVESTIGATION OF THE ROLE OF THE RNA-DEPENDANT RNA POLYMERASE IN THE TRANSCRIPTION AND REPLICATION OF THE 1918 PANDEMIC INFLUENZA A VIRUS

BY

SARAH JANE BOW

A THESIS SUBMITTED TO THE FACULTY OF GRADUATE STUDIES OF

THE UNIVERSITY OF MANITOBA

IN PARTIAL FULFILLMENT OF THE REQUIREMENTS FOR THE DEGREE OF

MASTER OF SCIENCE

IN

MEDICAL MICROBIOLOGY

UNIVERSITY OF MANITOBA

WINNIPEG, MANITOBA

ABSTRACT

INVESTIGATION OF THE ROLE OF THE RNA-DEPENDANT RNA POLYMERASE IN THE TRANSCRIPTION AND REPLICATION OF THE 1918 PANDEMIC INFLUENZA A VIRUS

By

Sarah Jane Bow

University of Manitoba, August 2013

The 1918 “Spanish Flu” pandemic was cause by an Influenza A virus that infected 500 million people and nearly 50 million people died. Influenza viruses utilize a RNA-Dependant RNA Polymerase (RdRp) complex, composed of the PA, PB1 and PB2 proteins along with the viral nucleoprotein (NP) to mediate viral transcription and replication. The 1918 PB1 gene has been linked to increased virulence in mice and ferrets. We have investigated the role of PB1 in the transcription and replication of the 1918 virus and its relation to pathogenicity by comparing its RdRp to the RdRp of a low virulence conventional H1N1 human virus isolate, A/Canada/RV733/2007 (RV733). Contrary to previous studies, our dual-luciferase reporter assay revealed the 1918 RdRp had lower transcriptional activity than the RV733 RdRp *in vitro*. The 1918 NP seems to be the key determinant for the difference in transcriptional activity of the 1918 and RV733 RdRp complexes. The 1918 PB1 in the RV733 RdRp maintained high reporter expression while the RV733 PB1 in the 1918 RdRp abolished reporter expression. 1918/RV733 chimeric PB1 proteins were also generated and evaluated with the reporter assay. Recombinant RV733/1918 viruses were generated by reverse genetics and we determined that PB1 is a key determinant of the high growth phenotype of the 1918 virus, but only a minor contributor to pathogenicity. A novel role for the 1918 NP in the high growth phenotype and pathogenicity of the 1918 virus is also described.

ACKNOWLEDGMENTS

I would like to begin by thanking my supervisor Dr. Darwyn Kobasa. Your guidance and expertise have helped me be successful and reach my goals. I have learned so much during my time in your lab and I am truly thankful for your support throughout my graduate studies.

To my graduate committee, Blake and Steve, your continued encouragement and guidance over that past three years has been much appreciated. Thank you for being part of Team Sarah. To the department of Medical Microbiology and Infectious Disease and the Faculty of Graduate Studies at the University of Manitoba I appreciate all of the dedication and support you showed to me over the years.

To Special Pathogens, I am very grateful to have had the opportunity to work with such a fine group of scientist. Each of you has taught me something and helped me achieve my academic and research goals in one way or another. So for this I sincerely thank you.

Phil. I don't think I could have survived it all without your constant reassurance and inappropriate jokes just to make sure I smiled (and rolled my eyes) at least once every day. You have been my rock to get me through Grad School. To all of my friends: fellow graduate students, Goodlife peeps, treasured girlfriends and my loyal country gang, thank you for your continued support, love and encouragement. I couldn't have done it without each and every one of you.

Finally, and most importantly, I would like to thank my family. I could never have accomplished my goals and so much more without you. You always had faith in me and supported me through all my successes and failures. You always encouraged me to strive for more. More importantly, you have instilled in me values, which will help me in all aspects of my life.

There are so many other people who have contributed to this dissertation; to all of you I extend my sincere thanks and gratitude.

TABLE OF CONTENTS

LIST OF TABLES

LIST OF FIGURES

ABBREVIATIONS

293T	Human embryonic kidney cells
aa	Amino acid
ATP	Adenosine triphosphate
BSA	Bovine Serum Albumin
BSL	Biosafety Level
$C0_2$	Carbon dioxide
CPE	Cytopathic effect
cRNA	Complementary Ribonucleic acid
C-terminal	Carboxyl-terminal
ddH20	Double distilled water
DMEM	Dulbecco's Modified Eagles Medium
DNA	Deoxyribonucleic acid
dNTP	Deoxyribonucleotide triphosphate
et al	et alli (latin for "and others")
E.coli	*Escherichia coli*
FBS	Fetal Bovine Serum
GFP	Green fluorescent protein
H_20	Water
HA	Hemagglutinin
HA0	Hemagglutinin polypeptide precurser
hr	Hour
i.e.	id est (latin for "that is")
IgG	Immunoglobulin G
kb	Kilobase
M	Matrix Protein
MDCK	Madin-Darby Canine Kidney cells
MgCl2	Magnesium chloride
min	Minute
ml	Millilitre
mM	Millimolar
MOI	Multiplicity of infection
mRNA	Messenger RNA
NA	Neuraminidase
NaCl	Sodium chloride
NEP	Nuclear export protein
NLS	Nuclear localization signal
nm	Nanometer
NP	Nucleocapsid protein
NS1/2	Non-structural protein 1 and 2
N-terminal	Amino-terminal
ºC	Degrees Celsius
OD	Optical density
ORF	Open reading frame

PA	Acidic Protein
PB1	Polymerase Basic Protein 1
PB2	Polymerase Basic Protein 2
PBS	Phosphate buffered saline
PCR	Polymerase chain reaction
PFU	Plaque forming unit
pPol	RNA pol I vector for reverse genetics
pCAGGS	DNA expression vector for minigenome studies
RNA	Ribonucleic acid
RNP	Ribonucleoprotein
rpm	Revolutions per minute
RT	Reverse transcription
RT-PCR	Reverse transcription polymerase chain reaction
Sec	Seconds
UTR	Untranslated Region
UV	Ultraviolet
V	Volts
vRNP	viral ribonucleoprotein
α	Alpha
µg	Microgram
µl	Microlitre
µM	Mircromolar

1.0 Introduction

1.1 Influenza Virus

The *Orthomyxoviridae* family includes influenza virus types A, B, and C, as well as two tick-borne mammalian viruses in the *Thogotovirus* genus and the Salmon Anaemia Virus in the *Isavirus* genus [1,2]. Influenza type A viruses are the most extensively studied of the family, and are responsible for most flu epidemics. They are quite widespread globally and are able to infect many avian and mammalian species [3]. Influenza type B infects can infect humans and seals [4] and type C can infect both pigs and humans [5]. The three influenza virus genera differ in host range and pathogenicity, and are likely to have diverged evolutionarily from a common ancestor [2,6] (Figure 1).

Influenza virus strains are named according to their genus (type A, B, or C), the species from which the virus was isolated, the geographic site of isolation, isolate number, the year of isolation, and, for the influenza A viruses, the hemagglutinin (H) and neuraminidase (N) subtypes. There are currently 17 different hemagglutinin (H1 to H17) subtypes and 10 different neuraminidase (N1 to N10) subtypes for influenza A viruses [7,8,9].

In 1930, Richard E. Shope isolated the first influenza virus, A/swine/Iowa/30 [10], but it was not until 1933 that the first human virus was isolated by Wilson Smith, Sir Christopher Andrews, and Sir Patrick Laidlaw of the National Institute for Medical Research in London, England [11]. Influenza viruses were first propagated in embryonated hens' eggs [8], which continue to be the medium of choice for growth of large quantities of virus for vaccine production [12,13]. Influenza viruses can also be grown in cell culture [14]. The most commonly used cell line is the Madin-Darby canine kidney (MDCK) cells, which support efficient replication of many influenza A and B viruses and can be used to show isolated viruses from humans [7,8,15,16,17,18].

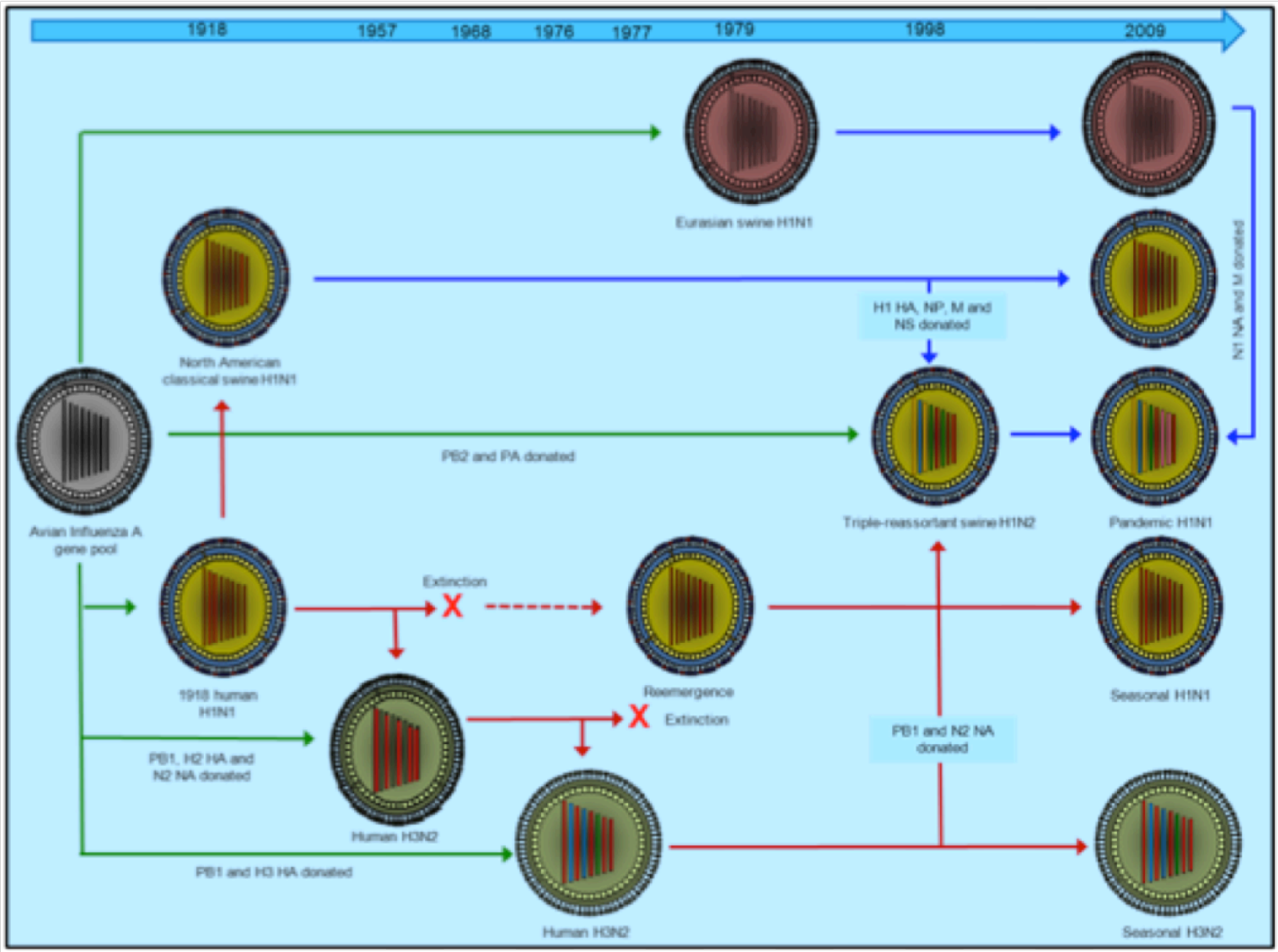

Figure 1: The genetic relationship among human and relevant swine Influenza Viruses, 1918-2009. The green arrows indicate the incorporation of one or more genes from the avian Influenza A virus gene pool. The red arrows indicate the evolutionary path of human Influenza virus lineages and the blue arrows for swine Influenza virus lineages. All Influenza viruses contain 8 viral gene segments that encode for the following proteins (shown from left to right within each virus schematic): polymerase basic protein 2 (PB2), polymerase basic protein 1 (PB1), Acidic polymerase protein (PA), hemagglutinin (HA), nuclear protein (NP), neuraminidase (NA), matrix proteins (M), and non-structural proteins (NS1 and NEP/NS2). Adapted from Morens and Taubenberger, 2009.

Orthomyxoviruses share a common structure and mode of replication. Virions are pleomorphic and can be either spherical or filamentous. The spherical particles have a diameter of about 100 nm, and the filamentous particles, which have elongated viral structures (greater than 300 nm), are commonly observed in clinical isolates [19,20].

Influenza A viruses possess a segmented, negative-sense, single-stranded RNA genome composed of 8 linear genome segments that code for up to 13 viral proteins. Viral particles have a complex structure and possess a lipid membrane derived from the host cell (Figure 2). This lipid envelope contains two glycoproteins, the hemagglutinin (HA) and the neuraminidase (NA) as well as the ion channel (M2) protein that project from the surface of the virus. The matrix protein (M1), forming the viral protein shell, lies just beneath the envelope, and the core of the virus particle is comprised of the ribonucleoprotein (RNP) complex. Within the virus particle, the individual gene segments are assembled into ribonucleoprotein (RNP) complexes that contain viral RNA (vRNA) encapsulated by viral nucleoprotein (NP) and a single copy of the RNA-dependant RNA Polymerase (RdRp) [21]. The influenza RdRp is a heterotrimeric complex, composed of the polymerase basic protein 1 (PB1), polymerase basic protein 2 (PB2), the polymerase acid protein (PA) and together with the nucleoprotein (NP) mediates viral transcription and replication. The nuclear export protein (NEP), also known as nonstructural protein 2 NS2) protein is also present in purified viral preparations [19].

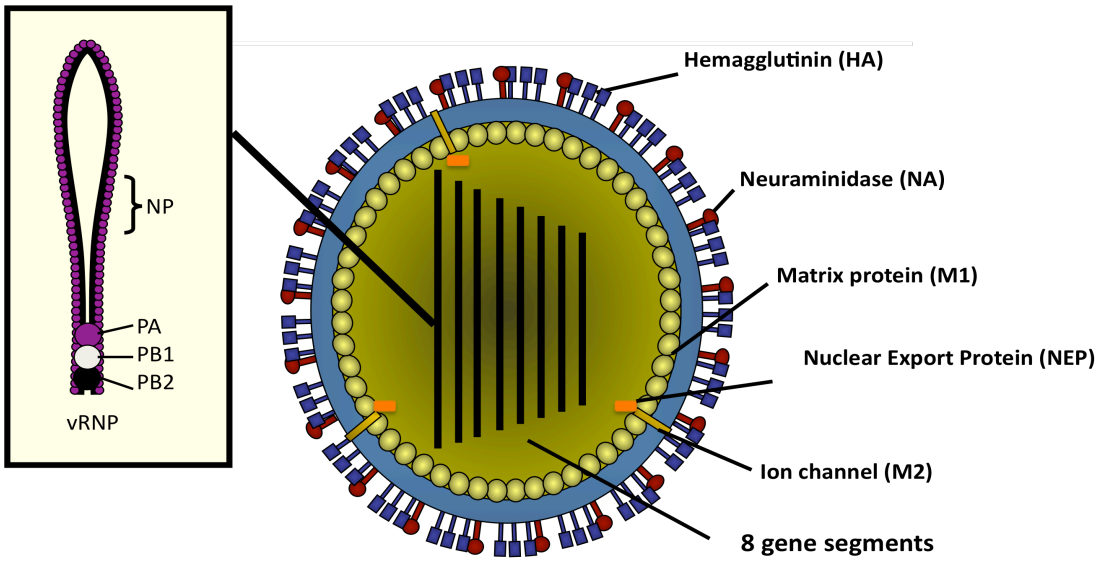

Figure 2: A schematic representation of an Influenza virus particle. Reproduced with permission from DK.

1.2 Influenza Viral Replication

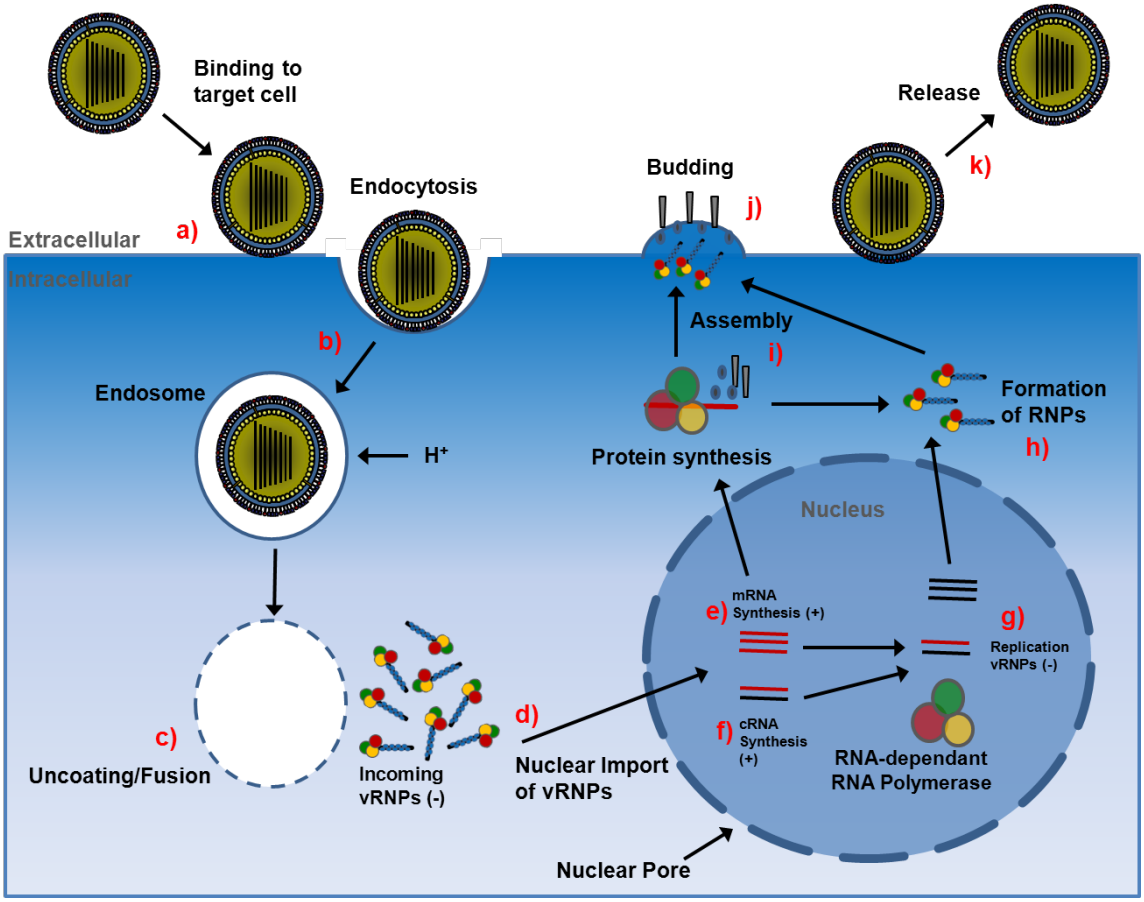

Figure 3: Overview of the Influenza Virus Life Cycle.(a) Entry of the virus into the host cell through receptor-mediated endocytosis: mediated by the viral HA binding to the cellular receptor, sialic acid (*N*-acetyl neuraminic acid) on host glycoproteins. (b) Endocytosis: receptor mediated endocytosis of virions into acidified vesicles (c) Uncoating/fusion: Fusion occurs via the low pH mediated conformational change in HA that results in fusion of the viral and endosomal membranes. At the same time an influx of H+ ions from the endosome into the virus particle, mediated by the M2 ion channel results in disruption of protein-protein interactions, resulting in the release of vRNPs into the host cell cytoplasm. (d) Specific and highly regulated trafficking of the vRNPs into the nucleus. (e) vRNA is transcribed into messenger RNA (mRNA) by a primer-dependent mechanism. (f) Replication occurs through a two-step process. First, a full-length, complementary RNA (cRNA) is generated which is then used as a template to produce more negative-sense vRNA in the second step (g). (h) NEP mediates export of vRNPs from the nucleus to the cytoplasm, ensuring they are available for packaging into new virions. (i) HA, NA, and M2 will accumulate at the same spot under the plasma membrane and determine the maturation site of the virus and where virus budding occurs. (j) Budding occurs when M1 accumulates at the inner leaflet of the lipid bilayer and forms a bridge between the inner core components and the membrane proteins. (k) The enzymatic activity of the NA protein is then required to remove the sialic acid from host glycoconjugates and the viral glycoproteins, and thereby releases the virus from its host cell.

1.2.1 Attachment

Influenza virus replication begins with the entry of the virus into the host cell through receptor-mediated endocytosis (Figure 3a). The major surface viral glycoprotein, hemagglutinin

(HA) can recognize and bind to sialic acid residues on the surface of the host cell facilitating attachment. These sialic acid residues are found on a wide variety of cell types, including red blood cells and epithelial cells of the respiratory system and intestinal tract. The HA is first proteolytically cleaved by cellular proteases into HA1 and HA2 [1], a step that is essential for the generation of infectious virus as it generates a hydrophobic fusion peptide at the amino-end of HA2. There is a sialic acid binding pocket on HA1, which binds to sialic acid, the cellular receptor for attachment. Clathrin-mediated endocytosis has traditionally been the model for influenza virus entry [1]. However, a nonclathrin, noncaveolae-mediated internalization mechanism has also been described [22]. Once the virus has been internalized into an acidified endosome, the HA undergoes a conformation change, exposing the hydrophobic fusion peptide on HA2 which then mediates fusion between the viral envelope and the cellular membrane. This results in the entry of the virus particle into the host cell cytoplasm and the beginning of the uncoating process (Section 1.2.3).

1.2.2 The Hemagglutinin (HA)

The hemagglutinin protein (HA) is the major surface glycoprotein of influenza viruses. The HA protein exists as a trimer in the virus envelope and is responsible for virus attachment and the subsequent fusion of viral and cellular membranes [5]. It is synthesized as a single polypeptide chain (HA0) that undergoes posttranslational cleavage by cellular proteases generating the two active forms of the hemagglutinin protein, HA1 and HA2. This cleavage is essential for infectivity because it exposes the hydrophobic amino terminus of HA2, which mediates the fusion between the viral envelope and the endosomal membrane [8,23]. HA is also a critical determinant of the pathogenicity, with a clear link between the cleavage of HA and virulence [24].

HA recognizes sialic acids (*N*-acetyl neuraminic acid), that are bound to underlying sugars on the ends of host cell glycoproteins [6]. These sialic acid residues are present on a wide variety of cell types, including red blood cells and epithelial cells. HAs of the different influenza virus

strains isolated from various animal species will have differing preferential specificities for the glycosidic bond isomerization on the sialic acid receptors that is dependent on the major species of sialic acid found at the sites of replication in a given host [6]. This is a major factor that drives host specificity of influenza virus strains as avian virus HAs bind α-2,3 sialic acid receptors while mammalian virus HAs bind to α-2,6 sialic acids [25]. Early studies demonstrated that epithelial cells in human trachea contain α-2,6 sialic acids on their cell surface but lack glycoconjugates with an α-2,3 linkage [8,26]. Thus, viruses with α-2,6 linkage specificity, but not those with α-2,3 linkage specificity, bind with high affinity to the epithelial cells lining the human trachea [27]. Conversion to preferential recognition of the human-type receptor (α-2,6 linkage) is, therefore, required for development of efficient human-to-human transmission of avian-derived viruses that are transmitted into humans. This is supported by the findings in early isolates from the 1918, 1957, and 1968 pandemics that preferentially recognized α-2,6, rather than α-2,3 sialic acids [28], even though the HAs in those viruses were originally derived from avian viruses.

1.2.3 Entry and Uncoating

After binding to the target cell surface and endocytosis of the virion, the low pH of the endosome activates fusion of the viral membrane with that of the endosome (Figure 3b). This fusion activity is induced by a structural change in the HA of influenza viruses, but in order for this to occur the HA0 precursor must have first been cleaved into two subunits, HA1 and HA2, prior to entry. The low pH-driven conformational change exposes the fusion peptide at the N-terminus of the HA2 subunit, enabling it to interact with the membrane of the endosome. The concerted structural change of several hemagglutinin molecules then opens up a pore that will permit release of the contents of the virion (i.e., viral RNPs) into the cytoplasm of the cell. This process is known as uncoating (Figure 3c). Effective uncoating also depends on the presence of the M2 protein, which has ion channel activity [29] that is essential for effective uncoating of the virus particle [29]. The role of M2 will be discussed in detail in the following section.

1.2.4 The M2 Protein

The M2 protein is an essential component of the virus envelope because it forms a highly selective transmembrane ion channel that allows H+ ions to penetrate the membrane. M2 forms tetramers by lining up four parallel transmembrane alpha-helices, thus creating a small pore in the viral envelope. This ion channel is essential for effective uncoating of the virus particle [29]. The influx of H+ ions through the ion channel from the endosome into the virus particle disrupts the protein-protein M1-M1 interactions and interactions between M1 and the vRNPs which results in the release of vRNPs that are free of the M1 protein into the cytoplasm (Figure 3c)[30]. The HA-mediated fusion of the viral membrane with the endosomal membrane and the M2-mediated release of the RNP constitute the virion uncoating process and the result is the appearance of free RNP complexes in the cytoplasm of the infected cell [31]**.** The M2 protein is the target of the adamantine class of antiviral drugs which blocks the M2 ion channel activity thus preventing effective uncoating of the virions [6,8,32].

1.2.5 Nuclear Import of vRNPs

One distinct characteristic of the Influenza life cycle over most other RNA viruses is that it replicates and transcribes its genome entirely in the nucleus of the host cell. Thus it is essential that there is a specific and highly regulated trafficking mechanism to import the viral genome into the nucleus (Figure 3d). Each of the eight viral gene segments exists as a viral ribonucleoprotein (vRNP) complex in which the vRNA is complexed by homo-oligomers of NP and tightly associated with the three protein subunits of the RdRp [21,33]. The three polymerase proteins bind to the vRNAs by associating with its panhandle region. The panhandle structure is formed by the complementary ends of each vRNA segment coming together at one end and forming a loop at the other (Figure 2)[34]. vRNPs are quite large structures (10-20nm wide) [21] and thus rely on an active nuclear import mechanism [35]. All proteins in the RNP complex possess nuclear localization signals (NLSs) that mediate their interaction with cellular nuclear import machinery

[36,37,38]. There are also NLSs present on the NP protein that have been shown to be both sufficient and necessary for the import of viral RNA [39,40].

1.2.6 The Nucleoprotein (NP)

The NP protein interacts directly with the viral RNA as well as each of the polymerase protein subunits. Each NP molecule interacts with 20-25 nucleotides of vRNA through its phosphate-sugar backbone [12,41] and serves as the structural protein in the viral RNPs by forming homo-oligomers [42]. NP is almost an entirely alpha-helical protein that has a head, body and tail domain [42,43]. NP homo-oligomers are formed when the tail-loop structure of one NP molecule inserts into the body domain on a neighbouring NP molecule [33,44]. These homo-oligomers form a strand of NP monomers that folds back on itself creating a stem loop structure at one end [33,41]. Crystallography has revealed that there are approximately nine NP molecules in each vRNP complex (Figure 4) [41,45], two of which associate directly with the PB1 and PB2 subunits of the trimeric RdRp complex to aid in the initiation of transcriptional activity [42].

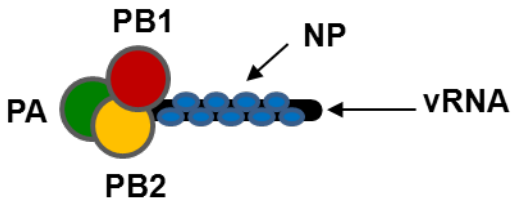

Figure 4: A schematic representation of Influenza viral ribonucleoprotein (vRNP) complex.

In addition to its structural role, the NP protein is also required for efficient elongation of RNA chains and is thought to be involved in the switch from transcription to replication by steric interactions with vRNAs [78]. At early times post infection NP is localized predominantly to the nucleus, whereas at later times it is found in the cytoplasm, which reflects the trafficking of RNPs during the virus life cycle. NP is primarily nuclear when expressed alone, and three potential NLSs have been identified that dictate nuclear localization [46,47].

1.2.7 Overview of RNA Synthesis

Over the course of an Influenza virus infection, mRNA transcription occurs first followed by genome replication. Once in the nucleus, the incoming negative-sense vRNA is transcribed into messenger RNA (mRNA) by a primer-dependent mechanism (Figure 3e). Replication occurs through a two-step process. First, a full-length, positive-sense copy of the vRNA is generated (Figure 3f). This is positive-sense strand is called the complementary RNA (cRNA) which is then used as a template to produce more negative-sense vRNA in the second step (Figure 3g). All of these reactions, vRNA→mRNA, vRNA→cRNA, and cRNA→vRNA are catalyzed by the RNA-dependent RNA viral polymerase complex with the distinct functions of each subunit being performed at each step [48,49].

1.2.8 Viral RNA Transcription

The viral polymerase complex synthesizes viral mRNAs using short, capped primers derived from cellular transcripts by a unique 'cap-snatching' mechanism. The PB2 subunit binds the 5' cap of host pre-mRNAs, which are subsequently cleaved after 10-13 nucleotides by the viral endonuclease, located in the *N*-terminus of the PA subunit [50,51]. The production of primers is activated only when the 5′ and 3′ end sequences of vRNA bind sequentially to the PB1 subunit. vRNA has been used as a template to transcribe the mRNA joined by the PB1 subunit. To simplify, transcription of influenza virus can be divided into the following steps: (i) binding of the 5′ and 3′ vRNA sequences to the PB1 subunit, which is likely to cause a conformational change in the polymerase complex [52,53]; (ii) binding of the 5′ cap of a host pre-mRNA to the PB2 subunit [54]; (iii) cleavage of a phosphodiester bond 10 to 13 nucleotides downstream of the cap by the PA subunit; and (iv) activation of the transcription of viral mRNAs at the cleaved 3′ end of the capped fragment. Polyadenylation of viral transcripts also occurs through a polymerase stuttering mechanism which involves an oligo (U) signal that is adjacent to the RNA panhandle structure [55,56,57] This polymerase complex catalyzes both mRNA transcription and replication of

negative-strand vRNAs, producing a full-length replicative intermediate cRNA. This cRNA is then replicated to produce more vRNA [51,58].

1.2.9 RNA-dependant RNA Polymerase

The influenza RNA-dependent RNA polymerase (RdRp) is a trimeric complex that consists of three proteins: polymerase basic protein 1 (PB1), polymerase basic protein 2 (PB2), and polymerase acidic protein (PA) [58,59,60]. Three-dimensional imaging of the trimer complex reveals that the three subunits are tightly associated to form a compact structure [61]**.** Protein interaction studies have shown that PB1 binds to both PA and PB2 through its N- and C-terminal domains, respectively [62,63,64]. No interaction has been reported between PA and PB2, but the condensed nature of the complex suggests that these subunits most likely do make contact with one another [65]. It has been proposed that PB1 and PA enter the nucleus as a dimer and then bind to PB2, which is imported independently (Figure 5)[66,67,68].

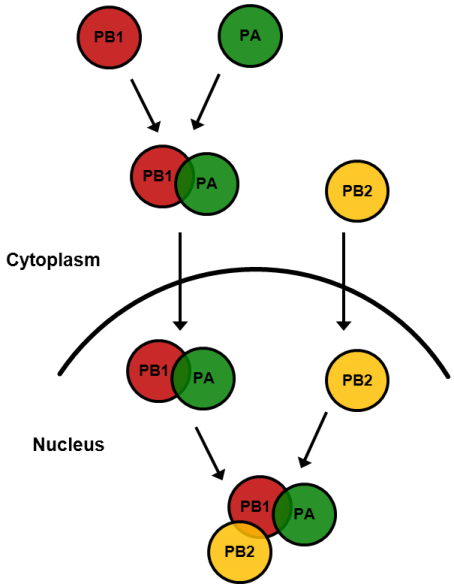

Figure 5: A model for the assembly of the influenza virus polymerase subunit proteins to form a functional RNA-dependent RNA polymerase (RdRp) in the nucleus of the host cell.

1.2.10 The Polymerase Basic Protein 1 (PB1)

The PB1 protein is that best characterized functionally of all the influenza polymerase subunits and contains amino acid motifs that are common to all RNA-dependent RNA and DNA polymerases [55,59]. The PB1 subunit is a key component of the viral RdRp complex and catalyses the sequential addition of nucleotides during RNA chain elongation [1,69,70]. The PB1 protein contains the active site for polymerase activity, an S-D-D motif at positions 444 to 446 [1,71]. PB1 is 757 amino acids long and four highly conserved regions have been identified (motifs I, II, III, IV) (Figure 6) [59]. It is also responsible for binding to the terminal ends of both vRNA and cRNA for initiation of transcription and replication [72,73].

The PB1 subunit has PA and PB2 binding domains at its N- terminus and C-terminus, respectively (Figure 6) [18,59,74]. Ghanem and coworkers have reported that blocking the N-terminal 25 amino acid resides of PB1 with a sequence-specific derived peptide, the PA-PB1 interaction can be disrupted and viral polymerase activity will be impaired [75,76]. And similarly, Li and coworkers have reported a peptide that can bind to the C-terminal 27 amino acid residues of PB1 interferes with its interaction with PB2, and thus effectively inhibits polymerase activity and viral replication [77]. These two studies reveal the importance of the PB1 protein and its interactions with the other proteins of the RdRp and how critical these interactions are to competent viral replication.

Several studies have also implicated the PB1 protein as a key virulence factor for such highly pathogenic H1N1 human viruses as the 1918 pandemic virus [69,78]. Interestingly, the 1918 PB1 gene differs from the conserved avian influenza consensus sequence by only seven amino acids [79]. It has been shown that, in a minireplicon system, the avian PB1 gene can support high transcriptional and replicative activity better than conventional human PB1 genes [80]. Thus, it has been speculated that the high similarity of the 1918 virus PB1 gene to many of the PB1 genes of avian origin may provide an explanation for the increased transcriptional activity

of the RdRp and greater virus replication that is seen in the 1918 influenza virus over many other H1N1 viruses[69].

Recently, an N-terminal truncated version of the PB1 protein has been identified, PB1 N40. This protein lacks transcriptase function but is still able to interact with the other subunits of the polymerase complex [81]. So far it seems that PB1 N40 is nonessential for viral viability but may have a regulatory role on virus replication [81].

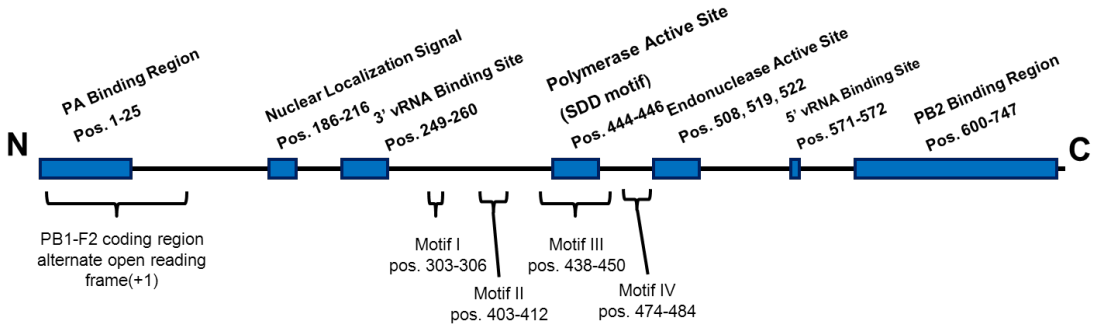

Figure 6: A schematic representation of major functional regions the Influenza virus PB1 protein and the four highly conserved motifs (motifs I, II, III, IV) associated with other RNA-dependent RNA polymerases and RNA-dependent DNA polymerases.

1.2.11 The PB1-F2 Protein

PB1-F2 is another small 87-90 amino acid viral protein (~10.5kDa) that is variably encoded within the PB1 gene by an alternative open reading frame (Figure 6) [81]. PB1-F2 is truncated and functionally inactive in all contemporary human H1N1 viruses but is functional in the 1918 pandemic virus and may contribute to its virulence by functioning as a proapoptotic protein though regulated posttranslational phosphorylation, mediated by protein kinase c [69,81]. PB1-F2 is exclusively found in infected cells (usually localized to the mitochondria) [82] and is not incorporated into virions [81]. PB1-F2 is not required for viral replication but it has been proposed that replication efficiency within epithelial cells may be altered by PB1-F2 interacting with PB1 to

increase polymerase activity [69,71,73]. Reduced polymerase activity and small plaque phenotype is observed *in vitro* when MDCK cells are infected with influenza virus mutants that lack the PB1-F2 reading frame [82]. However, transient expression of PB1 has shown to be sufficient to produce comparable levels of PB1-F2 expression as infected cells [82]. This suggests that PB1-F2 expression from the PB1 mRNA is mediated by cellular factors and does not require additional viral components.

It has been observed that the prolonged nuclear localization of PB1 during the late stages of infection seem to correlate with the presence of PB1-F2. Mazur and coworkers [82] suggest that the binding of PB1-F2 to PB1 is responsible for the prolonged nuclear retention and that this is done to ensure that efficient RNA replication during the later stages of infection are maintained, even when RNP export is at its most efficient. This is supported by their study that shows the enhanced polymerase activity when PB1-F2 is present in infected cells [82]. Also, they suggest that PB1-F2 is likely to compete with other components of the polymerase complex for binding to PB1. Thus, PB1-F2 may be sequestering PB1 for other functions within the nucleus that have not been identified yet [82].

The immunopathology associated with the PB1-F2 protein has recently been investigated and is thought to play a role in influenza pathogenesis by inhibiting viral clearance and thus increasing cytotoxicity in infected cells [83,84]. The specific mechanisms are unknown, but studies have suggested that PB1-F2 regulates pathways involved in the innate immune response by inhibiting the type I interferon response in infected cells [71,72]. PB1-F2 also seems to directly target professional antigen presenting cells for destruction. This contributes to influenza virus pathogenicity by increasing the probability of an opportunistic secondary bacterial infection, which is a major source of mortality associated with Influenza virus infection [85].

PB1-F2 has been shown to also target the mitochondrial inner membrane and may play a role in apoptosis during viral infection [6,81]. PB1-F2 does not induce apoptosis directly, but acts

to sensitize the host cell in response to apoptotic stimuli [86,87]. It has been shown to interact with the mitochondrial permeability transition pore complex components ANT3 (adenine nucleotide translocator 3) and VDAC1 (voltage dependent anion channel 1). These cellular components are involved in the permeability of the mitochondrial membranes and thus it is suggested that the role of PB1-F2 is in the induction of mitochondria-mediated apoptosis of the host cell [82,87].

1.2.12 The Polymerase Basic Protein 2 (PB2)

The PB2 protein recognizes and binds to type I cap structures of cellular pre-mRNAs. It has emerged as an important determinant of virulence and host range restriction [74,75]. The amino acid at position 627 of PB2 largely determines the replicative ability in mammalian cells [88]. Viruses with lysine at this position grow better in mammalian cells than those with glutamic acid. Studies using viral ribonucleoprotein complexes reconstituted from human or avian polymerase and NP proteins demonstrated that lysine at position 627 of PB2 supports replication at a higher efficiency in mammalian cells than does glutamic acid at this position [88]. This implies that when avian viruses transmit to humans, mutants with Glu627Lys mutations are preferentially selected and generate a virus that can replicate more efficiently and overwhelm the host immune response [89].

1.2.13 The Polymerase Acidic Protein (PA)

The PA protein is proposed to be involved in replication rather than transcription, but there is evidence that it plays a role in both [90]. The best characterized function of PA is the RNA-endonuclease activity associated with the amino-terminal portion of the protein which cleaves capped RNA fragments from cellular pre-mRNAs to provide primers for viral transcription [50,91,92]. This key N-terminal region has been shown to be multifunctional, initiating transcription and replication through different mechanisms [77]. The PA protein forms a dimmer

with PB1 in the cytoplasm, after which they are transported to the nucleus where they associate with PB2 to form the trimeric polymerase complex [67]. PA in complex with PB1 has been reported to be highly resistant to tryptic digestion compared to monomeric PA proteins [77], suggesting a conformational change in PA upon binding to PB1. This conformational change in PA is thought to enhance interactions with cellular proteins that results in nuclear translocation of the PA-PB1 dimer [67].

The most recently described influenza protein, PA-X, is derived from a +1 frameshift in the open reading frame of the PA gene which results in a polypeptide with a N-terminus that corresponds to the PA endonuclease domain [92,93]. This protein is thought to have roles in host-cell shut off, modulation of host gene expression, and, thus limitation of viral pathogenesis [93]. PA-X has been implicated as a virulence factor for the 1918 H1N1 pandemic virus [93]. Only very low amounts of PA-X protein are expressed during viral infections and it seems not to be required for viral replication. Therefore, PA-X has been identified as an accessory influenza viral protein that plays a role in the virus-host interface [92].

1.2.14 Regulation of Influenza Virus Transcription and Replication

Over the course of an influenza virus infection, mRNA transcription occurs first followed by genome replication. vRNA synthesis takes place through a cRNA intermediate, also made by the RdRp from vRNA but representing a full-length complement of the vRNA (Figure 3e,f,g). Thus, the virus must prioritize its replicative cycle to favor mRNA synthesis early in infection, then switching to the production of vRNA when new virions are to be assembled [79]. This has been confirmed in several studies where mRNA is detected in the early stages of infection (as early as 2 hours post infection), whereas cRNA is not detected until the later stages of infection. But more recently, it has been shown, using a novel strand-specific real-time RT-PCR assay that both mRNA and cRNA are detectable as early as 2 hours post infection [94](ref). Then as the infection progresses, mRNA levels decrease while vRNA levels steadily increase. This all suggests that

both transcription and replication occur simultaneously in early stages of infection and then replication dominates over transcription in the later stages of infection [94].

As discussed in section 1.2.8, the viral polymerase complex synthesizes viral messenger RNAs using short, capped primers derived from cellular transcripts by a unique 'cap-snatching' mechanism. Briefly, transcription of influenza virus begins with the binding of the 5′ and 3′ vRNA sequences to the PB1 subunit [53]; followed by the binding of the 5′ cap of a host pre-mRNA to the PB2 subunit [54]; cleavage of a phosphodiester bond 10 to 13 nucleotides downstream of the cap by the PA subunit; and finally the activation of the transcription of viral mRNAs at the cleaved 3′ end of the capped fragment. This polymerase complex catalyzes both mRNA transcription and replication of negative-strand vRNAs, producing a full-length replicative intermediate cRNA. This cRNA is then replicated to produce more vRNA [51,58].

Several studies have proposed a “switching” mechanism that regulates the transition from transcription to replication that is mediated by the availability of NP, the stability of cRNA mediated by the vRNP complex, and NS2/NEP, but the precise involvement of each of these viral proteins and the molecular mechanism remains unknown [51,95]. Two models have been proposed for the regulation of transcription and replication of the Influenza virus genome (Figure 7).

The classic model for switching between influenza virus transcription and replication says that during the early stages of infection, vRNA is transcribed to mRNA (primary transcription) and then expression of NP triggers the switch to replication (synthesis of cRNA and vRNA) and subsequent vRNA transcription by blocking the secondary structure of the vRNA panhandle and allowing complete cRNA synthesis (Figure 7A)[95,96].

More recently, a new “stabilization” model has been proposed, where, in the early stages of infection mRNA and cRNA are synthesized, but cRNA is degraded. mRNA is protected from

cellular degradation by the presence of a 5’ cap and a 3’ poly(A) tail, whereas nascent cRNA is rapidly degraded by host cell nucleases. The transition from the transcription phase to the replicative phase occurs in the later stages of infection, when PB1, PB2, PA, and NP are synthesized and cRNA is stabilized by the binding of the RNA polymerase to the cRNA promoter. The cRNA-polymerase promoter complex then serves as a nucleation point for binding of free newly synthesized NP, leading to the formation of active and stable cRNPs that can be replicated to vRNA (Figure 7B)[25,82].

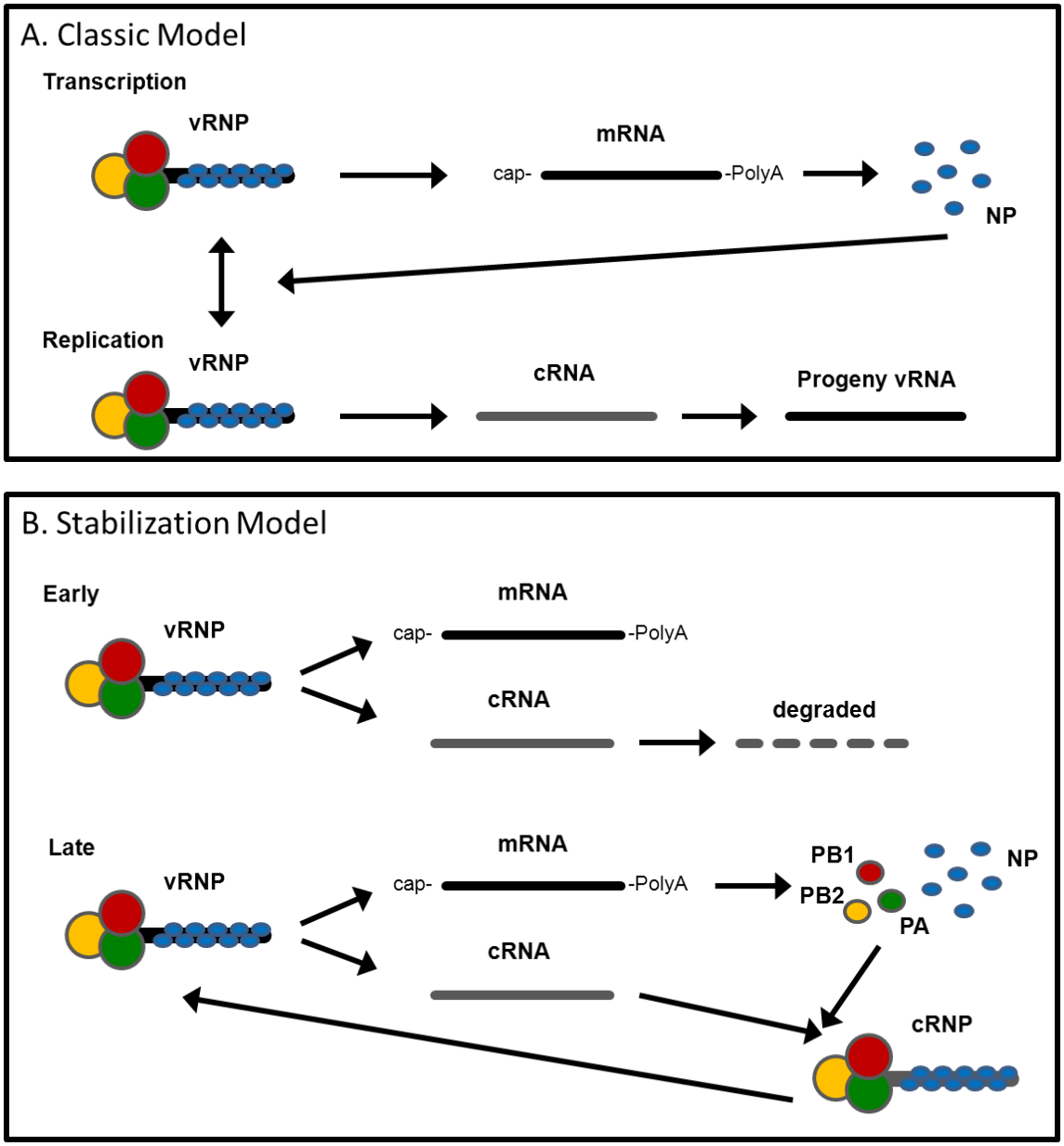

Figure 7: The two current models for Influenza virus switching mechanism between transcription and replication. **A.** The classic model. Early in infection, vRNA is transcribed to mRNA (primary transcription). It is the NP that determines the switching from primary transcription to replication (synthesis of cRNA and vRNA) and then subsequent secondary transcription. **B.** The stabilization model. At early time point in infection, mRNA and cRNA are both synthesized, but cRNA is degraded. Then at later time points, once PA, PB1, PB2, and NP have been made, cRNA is stabilized as cRNP complex that is used as the template to make progeny vRNA.

The most recent contribution to the understanding of the switching mechanism is the discovery of influenza A virus-derived small virus RNAs (svRNAs). svRNAs are 22-27 nucleotides in length and correspond to the 5' end of each of the viral gene segments [97]. Expression of these svRNAs correlates with the accumulation of vRNAs in the host cell cytoplasm and the shift

in the activity of the RNA polymerase (RdRp) from transcription to genome replication. svRNAs are synthesized by the RdRp using cRNAs as templates [97]. Synthesis of svRNA from cRNA is a stochastic event in which cRNA is produced in a svRNA-independent manner. This model is supported by the "stabilization model" of viral transcription (described above) where cRNA stability is essential for the switch between viral transcription and replication [58]. Alternatively, the "classic model" in which NP initiates the switch between viral transcription and replication also supports svRNA synthesis from cRNA as NP function is required for complete cRNA synthesis [96,97].

1.2.15 Nuclear Export of Viral Ribonucleoproteins

After the viral genome has been replicated, the newly formed RNP complexes are assembled in the nucleus and then exported into the cytoplasm. Two viral proteins, the matrix protein (M1) and the nuclear export protein (NEP/NS2) are involved in directing the nuclear export of RNPs [80,81].

M1 associates with RNPs in the nucleus and may actually promote the formation of RNP complexes [98]. M1 has been shown to make contact with both the vRNA and NP [99,100]. Relatively little is known about how M1 promotes the nuclear export of RNPs. More is known about the involvement of the NEP.

1.2.16 Nuclear Export Protein/Non-Structural Protein 2 (NEP/NS2)

The non-structural protein (NS) gene segment not only encodes the NS1 protein, but also a 121 amino acid polypeptide that is a spliced form of the mRNA transcript called the non-structural protein 2 (NS2) [101]. Originally this protein was thought to have no structural role for the virus, but then it was later noticed that small amounts of NS2 were present in virions and seemed to interact with the viral matrix protein M1 [102]. After much study on this protein it was

later renamed the Nuclear Export Protein (NEP) as it was found to be essential for mediating export of vRNPs from the nucleus to the cytoplasm, thus ensuring that they are available for packaging into new virions (Figure 3h)[103]. Recent studies have shown that NEP has the ability to regulate viral transcription and replication processes by influencing the accumulation of the various viral RNA species at various times during infection [104,105]. It has been shown that NEPs ability to regulate RNA levels translates to contributing to the switching from viral transcription to replication by favouring the production of genomic vRNPs [104,105]. This is a novel function for the NEP and appears to be independent from the vRNP nuclear export mechanism [93].

1.2.17 Virus Assembly

Influenza viruses assemble and bud from the apical plasma membrane of polarized cells (e.g., lung epithelial cells of the infected host) [43]. The individual viral envelope proteins, HA, NA, and M2 will accumulate at the same spot in the plasma membrane and determine the maturation site of the virus and where virus budding occurs (Figure 3i)[106].

Correct assembly and packaging of a full complement of RNA genome segments is a requirement for a fully infectious virion. The precise mechanism of packaging of the eight viral RNA segments is not well understood, however two different models have been proposed. The first is the random incorporation model which assumes that a common packaging signal is present on all vRNAs (vRNPs), which enables them to be randomly incorporated into budding virions [41,107,108]. These packaging signals should differentiate between vRNAs and cellular RNAs, but not among the various vRNAs. Thus any number or combination of vRNAs could be incorporated into virions [41]. This model is supported by evidence that virions may possess more than the required eight vRNPs. This ensures that there will be at least a full complement of eight vRNPs in a significant percentage of virus particles [107,108]. The second model, the selective incorporation model, suggests that each vRNA segment has a specific packaging signal which

allows each segment to be packaged selectively [41]. This model suggests that each vRNA segment contains a unique “packaging signal” in the 5’ and 3’ coding and noncoding regions of each genome segment that are required to incorporate the segment into virions [109,110]. These packaging signals serve to enhance the likelihood that every virion possesses a full complement of the eight vRNP segments [1,109]. In general, Orthomyxovirus virions must contain at least one copy of each of the eight genome segment to be infectious [107,111].

1.2.18 Budding and Release

Initiation of the budding process requires the outward curvature of the plasma membrane, which is stimulated by the accumulation of M1 at the inner leaflet of the lipid bilayer in the same region where the HA and NA accumulate (Figure 3j). The virus bud is then extruded until the inner core is enveloped. The budding process is completed when the membranes fuse at the base of the bud and the enveloped virus particle is released following fission from the cell membrane [112,113]. The M1 protein has been shown to be essential for effective and complete budding of new influenza viruses [114]. Influenza virus particles must then be actively released after the viral envelope has separated from the cell membrane. The HA protein anchors the virus to the host cell by binding to the sialic acid receptors. The enzymatic activity of the NA protein is then required to remove the sialic acid from both host cell glycoconjugates as well the newly synthesized HA and NA, and thereby releases the virus from its host cell and prevent viral aggregation (Figure 3k)[1,115].

1.2.19 The M1 Protein

M1 is the most abundant virion protein and lies just beneath the lipid envelope, where it makes contact with the cytoplasmic tails of the glycoproteins and with the RNPs, thereby forming a bridge between the inner core components and the membrane proteins (Figure 3j) [112,113]. The M1 protein consists of two globular helical domains that are linked by a protease-sensitive

region [116,117]. As mentioned above, M1 interacts with both vRNPs and NEP/NS2 and it is known to be an essential component in both the assembly processes, by recruiting the viral components to the site of assembly at the plasma membrane, as well as in the budding process [114].

1.2.20 The Neuraminidase (NA)

The neuraminidase protein (NA) is the second most abundant surface glycoprotein of influenza viruses, after the HA. NA has sialidase (neuraminidase) activity that cleaves terminal *N*-acetyl sialic-acid residues, the cellular receptor that binds HA, which results in the dissociation of the virus from an infected cell [5,118]. Like HA, the NA protein shows preference for certain types of sialyloligosaccharides according to the host animal species. Avian virus NAs cleave α2,3-linked, but not α2,6-linked, sialic acids [25]. After their introduction into the human population, N2 NAs, which were derived from an avian virus prior to the appearance of the H2N2 viruses in the 1957 pandemic, acquired the ability to cleave α2,6-linked sialic acids in addition to α2,3-linked sialic acids (15). This acquired ability likely represents adaptation to the respective recognition pattern of the HA protein, which is in turn influenced by the dominant species of sialic acid found in the human respiratory tissues. NA substrate specificity is determined by the nature of the amino acid at position 275 in the N2 NA subtype [119]. Both HA and NA are the major antigenic targets of the humoral immune response to influenza viruses. NA is the target of the antiviral drugs Oseltamivir and Zanamivir which inhibit the neuraminidase activity of the NA protein and thus inhibit further viral spread[6].

1.2.21 The Non-Structural Protein 1 (NS1)

The NS1 protein is the most abundant viral protein in influenza virus-infected cells and depending on the virus strain, encompasses 202 to 238 amino acids [120,121]. NS1 blocks the activation of RNA-dependent protein kinase (PKR) [6,122] by functioning as an antagonist if the

cellular interferon (IFN) response that allows efficient virus replication in IFN-competent hosts [123,124]. It targets both IFN-β production and the activation of IFN-induced antiviral genes [121]. Deletion of NS1 leads to increased induction of IFN and a virus that is highly attenuated [125].

In virus-infected cells, double-stranded RNA (dsRNA) triggers the activation of transcription factors, such as ATF-2/c-Jun, NFκB, and IFN regulatory factors (IRFs) that stimulate IFN-β production [121]. The nature and origin of this dsRNA has not been characterized but may arise from double-stranded promoter regions and/or replication/ transcription intermediates. NS1 interferes with the dsRNA-triggered activation of transcription factors through an as yet unknown mechanism. Possible mechanisms include interaction with a component of the IFN activation pathway or direct binding to the dsRNA, thereby masking it [8,121].

1.3 Influenza Immunology

The respiratory tract has many nonspecific protective mechanisms against influenza virus infection, including the mucin layer, ciliary action, and protease inhibitors. These barriers are in place to prevent the virus from getting into the host cells. The extremely short incubation period (1-4 days) [126] between infection and clinical illness implies that innate immunity is important for early response to infection. A role for neutrophils and alveolar macrophages in the innate immune response and limiting virus replication has been suggested in murine infection with a reconstructed 1918 virus [5,89].

The adaptive immune response to Influenza virus infection is a highly specific response that is relatively slow upon first encounter the virus. The initial infection with one strain of influenza virus results in the formation of immunological memory and the response to subsequent influenza infections is more rapid and robust. This adaptive immune response consists of humoral (virus-specific antibodies) and cellular (virus-specific $CD4^+$ and $CD8^+$ T cells) immunity [127]. Influenza virus infection induces the production of influenza virus-specific antibodies by B cells [128]. These antibodies are targeted to the viral HA glycoprotein, which contains the primary

antigenic determinants. For this reason, the seasonal influenza vaccine is formulated to stimulate a strong antibody response to the HA of the current circulating strain. The antibodies bind to the HA receptor binding site, located in its antigenic region, blocking virus attachment to host cells and/or block receptor-mediated endocytosis [129,130,131]. Antibodies are also generated to the other major glycoprotein, the NA. These antibodies interfere with the last phase of the viral replication cycle and exert protective immunity [132]. Unlike HA-specific antibodies, NA-specific antibodies do not neutralize the virus but inhibit the enzymatic activity of NA. Through this mechanism these antibodies limit the viral spread and thus shorten severity and duration of illness [132,133,134].

Influenza A virus infection also induces a cellular immune response that involves virus-specific $CD4^+$ T cells and $CD8^+$ T cells. Memory $CD4^+$ T cells, induced after a primary influenza A virus infection, contribute to faster control of subsequent influenza A virus infections and thus play a role in long-term protective immunity [135,136]. The role of $CD8^+$ T cells in influenza infections has been mainly described for long-term protection and antigen-specific memory. This also allows for a more rapid and robust immune response to secondary influenza virus infections [127].

Although immunity mediated by influenza virus infection can be long lived, re-infection with antigenetically related influenza A viruses occurs, indicating that immunity induced by a single infection is incomplete. Two mechanisms have been identified that can contribute to this incomplete immunity. First, there is a gradual decrease in the total amount of serum antibodies (IgG), local IgA antibodies, and antibody secreting cells within the first year after the first infection [94,95]. Second, the strongest immunological response is mounted during the initial influenza infection. Then each subsequent infection with different strains of the influenza virus will elicit only a limited response due to the antigenic variability of the HA protein [137]. This is why we see a greater degree of resistance to infection with antigenic drift strains in humans previously infected twice with prototype virus than in those with only one previous infection [8] (Discussed further in sections 1.8 and 1.9).

1.4 Influenza Antivirals

Zanamivir and Oseltamivir are the two neuraminidase inhibitors presently available to inhibit influenza virus infection (Figure 8). Without a functional neuraminidase enzyme, the virus progeny are not cleaved from the host cell membrane glycoproteins and the virions remain attached to the surface of the infected cell, unable to spread to other cells [5]. Zanamivir is a specific inhibitor of the NA of all influenza A and B viruses and must be administered intranasally or inhaled. Oseltamivir utilizes a hydrophobic pocket in the enzyme-active center that can accommodate lipophilic groups that are necessary to improve the inhibitor's oral bioavailability [138,139]. Both Zanamivir and Oseltamivir have been approved for use in humans [138] and studies have shown that prophylactic treatment is 96% effective against viral shedding, 82% effective against infection, and 95% effective in preventing febrile illness [8,140].

Amantadine and Rimantadine inhibit virus replication by blocking the acid-activated ion channel formed by the virion-associated M2 protein (Figure 8)[32]. The antiviral action of these compounds is to block the flow of H+ ions from the acidified endosome into the interior of the virion, preventing release of the transcriptionally active vRNPs into the host cell cytoplasm [8,32]. In addition, a second effect of these compounds is to block maturation of the HA during transport from the endoplasmic reticulum to the plasma membrane. Both Amantadine and Rimantadine have antiviral properties against all subtypes of influenza A virus, but not against influenza B or C viruses [141].

Ribavirin, an FDA-approved antiviral, and several other nucleotide analogs are known to inhibit influenza in humans, but toxicity remains a problem [142]. These compounds target the viral polymerase, specifically inhibiting the endonuclease activity of the PA subunit (Figure 8). Ghanem and coworkers as well as Li and coworkers have recently made advancements in the use of peptide derivatives to inhibit polymerase activity by blocking the interactions of the PB1

subunit with the other subunits of the RdRp complex [76,77] but these therapies are still in the laboratory phase of testing and are not approved for use in humans or animals.

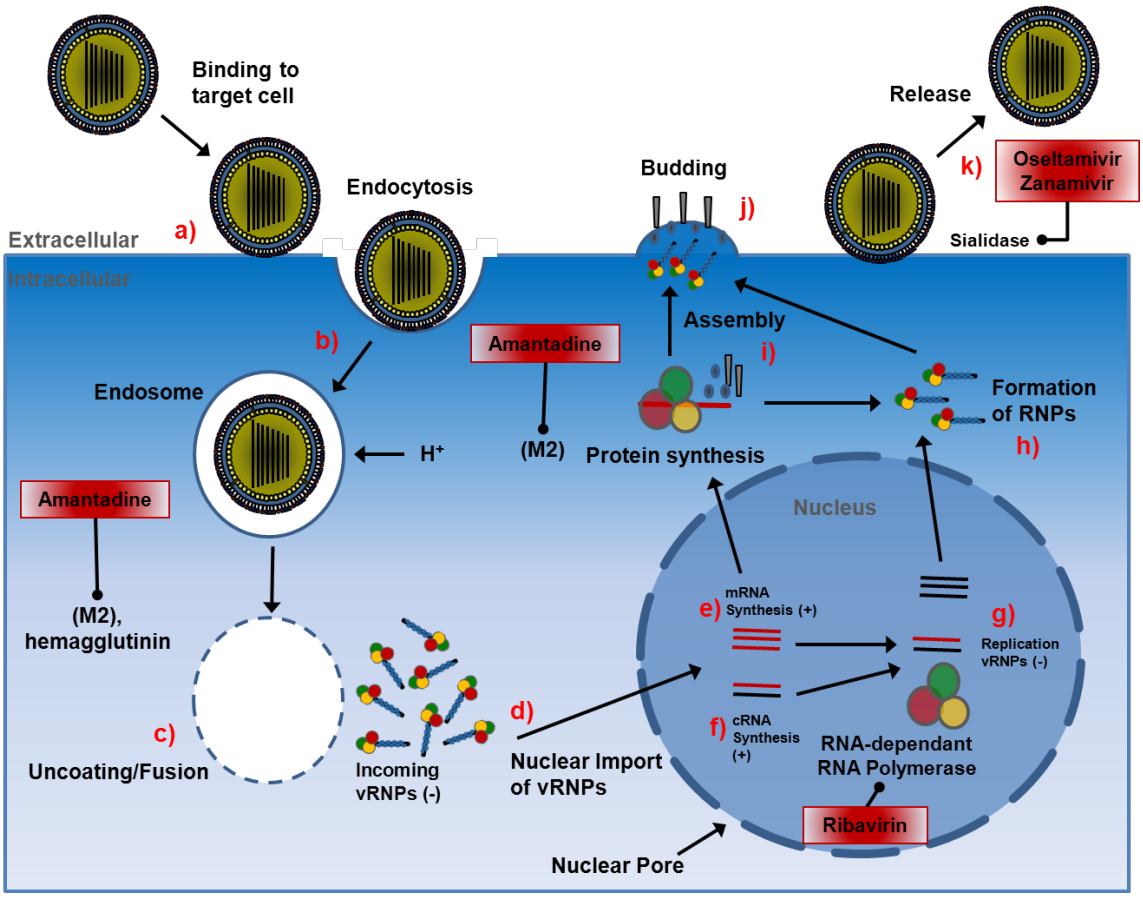

Figure 8: The targets of Influenza virus antivirals in the virus replicative cycle. Amantadine and Rimantadine inhibit virus replication by blocking the acid-activated ion channel formed by the virion-associated M2 protein. Zanamivir and Oseltamivir are the two neuraminidase inhibitors presently available to inhibit influenza virus infection and Ribivirin targets the viral polymerase.

1.5 Influenza Vaccines

In Canada, the National Advisory Committee on Immunization, the group that advises the Public Health Agency of Canada, in 2008 recommended that everyone aged 2 to 64 years be encouraged to receive annual influenza vaccination, and that children between the age of six and 24 months, and their household contacts, should be considered a high priority for the flu vaccine. Vaccination in healthy adults is 60-90% effective in preventing clinical illness associated with the virus strains similar to those used to manufacture the current seasonal vaccine [5].

Inactivated influenza virus vaccines are manufactured and administered to humans each year. The vaccines currently in use are designated whole virus (WV) vaccine or subvirion (SV) (split or purified surface antigen are alternative terms) virus vaccine. The WV vaccine contains intact, inactivated virus, whereas the SV vaccine contains purified virus disrupted with detergents that solublize the lipid containing viral envelope, followed by chemical inactivation of residual virus [8]. Inactivated viruses can retain their ability to induce an immune response but are replication incompetent and thus do not cause disease. The route of immunization for all inactivated vaccines is intramuscular.

A live attenuated intranasally administered influenza virus vaccine has recently been approved for use between the ages of 5 and 55 years and there is great interest in expanding the use of live vaccines in humans. The current live attenuated influenza vaccine is a cold-adapted vaccine which is produced by combining the HA and NA genes of the targeted seasonal virus strain with the other viral gene segments of another influenza virus that has restricted growth at 37°C [5]. This reassortant virus cannot replicate in the lungs at core body temperature, but grows at the cooler temperatures found in the nasal mucosa. For this reason the vaccine must be administered as an inhaled vaccine. This is where an efficient immune response is elicited without causing any harm to the vaccinated individual [5].

The current inactivated vaccines are recommended primarily for those at high risk of influenza virus infection and yet do not, in those groups, provide complete protection [103]. In contrast, live vaccines appear to have the potential to broaden the indications for influenza vaccines and hence to have an impact on the overall morbidity and perhaps spread of the disease. Also, local immunity is increasingly recognized to play a major role in resistance to most respiratory pathogens [103]. Respiratory tract infection with a live attenuated vaccine has been found to be the most efficient method of stimulating such immunity [8].

1.6 Clinical Presentation and Transmission

The natural reservoir of influenza A viruses is thought to be numerous species of wild birds, predominantly of the orders *Anseriformes* and *Charadriiformes* [143]. The mechanisms by which avian influenza viruses stably adapt to mammalian hosts and the key mutations that allow for efficient infectivity, replication, and transmission in the new species remains poorly understood.

Infection with an Influenza virus causes a severe acute disease in all age groups with symptoms of sore throat, cough, fever, headache, and muscular ache and pains. The acute stage can last 3-5 days, while the cough and malaise may last for several weeks [126] and the virus is maintained within human populations by direct person-to-person spread during the acute infections. The incubation period can be as short as 24 hours to 4 or 5 days [126], depending in part on the dose of virus and the immune status of the host. The most effective means of spread among humans are aerosols.

The virus initially infects the epithelial cells of the upper respiratory tract [5]. Influenza virus infection causes loss of ciliated epithelium, leading to the loss of the ability of the respiratory tract to clear virus or bacteria by mucociliary flow that normally traps these agents in mucus and disposes of them [126]. The loss of ciliated epithelium allows for the easy entry of bacteria into the lower respiratory tract, resulting in secondary bacterial pneumonias that cause many deaths attributed to influenza virus infection [5]. Virus replication induces production of interferons, cytokines, and other soluble response factors, leading to local and systemic inflammatory responses. This results in symptoms that define the “flu” syndrome: fever, headache, chills, malaise, and muscle aches [126].

Human influenza viruses replicate almost exclusively in superficial cells of the respiratory tract. Influenza virus is released from the apical surface of the cell, which may limit more systemic

spread but facilitate accumulation of virus in the lumen of the respiratory tract for transmission to the next susceptible host [8]. Alveolar macrophages and dendritic cells can also be infected and play a role in the response to influenza by processing antigens and presenting them for immune recognition. Influenza virus replicates throughout the respiratory tract, with virus being recoverable from the upper and lower tracts of people naturally or experimentally infected with virus. The site of optimal growth in the respiratory tract for each subtype of influenza virus is determined by the prevalence of the α-2,3 or α-2,6 sialic acid glycocongugates [144].

1.7 Influenza virus Host-Range and Pathogenicity

Influenza A viruses infect a wide variety of animals, including humans, birds, swine, horses, dogs, cats, whales, and seals. Viruses of all known HA and NA subtypes are maintained in aquatic birds and, therefore, they are considered the natural reservoir of influenza A viruses [92,143]. Although human pandemics have been associated with viruses of the H1 to H3 subtypes, the ability of avian viruses of the H5, H7, and H9 subtypes to infect humans could make these subtypes potential candidates of future influenza virus pandemics.

Three influenza virus proteins, HA, PB2, and NS1, have been identified as major determinants in the host range restriction and pathogenicity of these viruses [24]. Although it has been suggested that NP participates in host range restriction, direct experimental evidence is lacking.

It has been shown that the 1918 HA protein is a primary determinant of pathogenicity [24]. Recently, it was demonstrated that the 1918 PB1 and NA proteins are also contribute to the exceptional virulence of this virus in mice [69]. The virulence seen in the mouse model also correlates with the ability of the 1918 virus to replicate efficiently in mouse lungs and human airway cell lines [69]. Pappas and co-workers have showed that the 1918 PB1 has a role in pathogenicity. In their study they compared the 1918 virus to a low pathogenic contemporary

human H1N1 virus (A/Texas/36/91) and they found that by substituting the 1918 PB1 for the TX/91 PB1 in the 1918 background, resulted in complete attenuation of the 1918 virus (170-fold less) [69]. The link between the high pathogenicity of the 1918 virus and the PB1 gene has also been demonstrated in ferrets [78]. Watanabe and co-workers have investigated the role of the 1918 polymerase complex in the growth of the virus. In this study they compared the 1918 virus to A/Kawasaki/173/2001 (K173), another contemporary human H1N1 virus. They showed that when the K173 PB1 is replaced with the 1918 PB1, this recombinant virus had higher replication efficiency and was able to grow in both the upper and lower respiratory tract of macaques like the 1918 virus whereas, the K173 can only grow in the upper respiratory tract at relatively low titres. This shows that the 1918 PB1 is able to confer the 1918 virus high growth phenotype to another virus system but the complete 1918 RdRp complex is required for full pathogenicity of the 1918 virus [78].

The NEP viral protein has recently been shown to be an important factor for the adaption of highly pathogenic avian H5N1 viruses to mammalian hosts, in addition to its regulatory roles in viral transcription and regulation [93,105]. One of the factors that is known to cause host-range restriction is the reduced activity of an avian polymerase complex within a mammalian host [88,93,145] which can be attributed to impaired cRNA synthesis by the avian polymerase complex [105].

1.8 Influenza virus Genetics

Influenza viruses are evolutionarily dynamic viruses and have high mutation rates [145,146] Antigenic drift results from the accumulation of point mutations within regions of the envelope glycoprotein genes that code for the antigenic domains of these proteins [5,8]. RNA polymerases do not possess the proof reading mechanism, thus errors can be made and propagate as the virus replicates [146]. Antigenic drift has resulted in the generation of numerous influenza A subtypes with antigenically distinct HA and NA surface glycoproteins. In mammals,

influenza A virus drift variants result from the positive selection of spontaneous mutants by escaping neutralizing antibodies. These variants can then no longer be neutralized by antibodies to the original virus strain. Mutations in the human virus HA or NA amino acid sequence occur at a frequency of less than 1% per year. Nevertheless, antigenic drift variants can cause epidemics and typically prevail for 2 to 5 years before being replaced by a different variant [8]. To date, there are seventeen HA subtype (HA1-HA17) and ten NA subtypes (N1-N10) identified in naturally occurring influenza A viruses [1,8,9].

Antigenic shift results from reassortment of influenza virus genes during mixed infections with two or more virus subtypes [5,8]. Reassortment is the mixing of whole gene segments of multiple influenza strains into new combinations. In a mixed influenza infection, one or more of the eight genome segments of one virus can combine with segments of another influenza virus in one host. Reassortment between a human strain and a non-human strain (mammalian or avian) can create a virus that can replicate in humans but has an HA and/or NA subtype from the non-human virus. In many scenarios, reassortant viruses are not viable in humans. However, if a reassortant virus is capable of efficient human infection and human-to-human transmission, this virus will likely spread throughout a population if antibodies against the new subtype are not present. These are the viruses that are likely to have epidemic or pandemic potential.

Phylogenetic evidence suggests that all mammalian influenza virus strains, such as the 1918 H1N1 pandemic virus, ultimately derive from entirely avian-like viruses that have adapted to humans through accumulation of mutations in the various viral proteins that enhance viral fitness in the new host. One important adaptation is changes in one or more amino acid residues in the receptor binding domain of HA. These amino acid changes would then result in changes in receptor specificity, which allowed this virus to recognize the human HA receptors, α-2,6 sialic acids [25]. This virus then would evolve further within the human population by antigenic drift, acquiring mutations that changed the antigenicity of the virus enough that the antibodies of the original avian-like virus no longer recognized it. This makes the virus highly pathogenic to

humans. Viruses like these can continue to evolve by acquiring more mutations that enhance replication in mammalian host. The 1918 H1N1 pandemic virus likely adapted to humans in this way, but there is also evidence that suggests that the specific mutations that allowed it to adapt to the human host were acquired in an intermediate swine host [147].

A swine influenza virus was actually first clinically detected in 1918 in association with the 1918 pandemic [6]. Recent research has suggested the strain may have originated in a nonhuman, mammalian species. An estimated date for its appearance in mammalian hosts has been put at the period 1882–1913. This ancestor virus diverged about 1913–1915 into two clades, which gave rise to the classical swine and human H1N1 influenza lineages (Figure 1)[2]. The similarity of this swine virus to the classical swine virus, avian viruses as well as human viruses that have emerged over the past century leads us to believe that they are all descendants of the 1918 H1N1 pandemic Influenza virus strain [6,7]. Pigs are susceptible to infection with both avian and mammalian influenza viruses as they possess both the α-2,6 and α-2,3 sialic acid receptors on the epithelial cells of the upper respiratory tract. They are considered a “missing vessel” or intermediate host in which reassortment events can occur easily [147]. In addition, it is thought that pigs might serve as an intermediate host for adaptation of avian viruses that could eventually become transmitted to humans, as may have happened in the generation of the 1918 pandemic virus. There have been several lineages of triple reassortant influenza viruses of H3N2, H1N2, and H1N1 subtypes, that all contain genes from the classical swine H1N1, human H3N2 and several avian influenza viruses [147]. A triple reassortant virus is what caused the pandemic in 2009 [2].

1.9 Influenza Pandemics

Influenza viruses are among the most common causes of human respiratory infections and are the most significant because they can cause high morbidity and mortality. In the United

States, influenza causes approximately 36,000 deaths in a typical epidemic season [6]. In addition to the annual epidemics, pandemic influenza viruses can emerge as global outbreaks due to novel antigenic subtypes that are generated by antigenic shift. In the last 500 years, there have been approximately fourteen confirmed or suspected influenza virus pandemics, including those in 1918, 1957, 1968, 1977, and 2009 [6]. However, there have likely been many more epidemics or even pandemics throughout history that have not been as well documented or misdiagnosed as an unspecified respiratory disease.

The first influenza viruses to be isolated in the laboratory by Shope and the 1930s were determined to be descendants of the virus that was observed in pigs in 1918 and that was believed to be the causative agent of the pandemic [6]. In 1957, a new influenza A virus appeared in Southeast China of the subtype H2N2 and caused the “Asian flu” pandemic. During this pandemic, H1N1 strains seemed to disappear and were no longer prevalent in the human population. H2N2 strains persisted in humans until 1968, when another new virus subtype, H3N2, appeared in China. This H3N2 virus had a new HA gene and caused the “Hong Kong” pandemic, during which time the H2N2 viruses disappeared. In 1977, the H1N1 virus reappeared in the human population in China and spread worldwide [148]. Presently, variants of H3N2 and H1N1 viruses continue to circulate throughout the human population and cause the seasonal flu epidemics that we see each year (Figure 1).

1.9.1 1918 “Spanish Flu”

The 1918 flu pandemic (the "Spanish flu") was the worst pandemic in recorded history. Nearly three percent of the world's population (which was 1.86 billion at the time) died of the disease and as many as 500 million, or 27%, were infected, making it one of the deadliest natural disasters in human history affecting people in all corners of the globe [6]. Most victims that succumbed to the disease were healthy young adults, in contrast to most influenza outbreaks, which predominantly affect juvenile, elderly, or weakened subjects. The majority of deaths were

from bacterial pneumonia, a secondary infection caused by influenza, but the virus also killed people directly, causing massive hemorrhages and edema in the lung [8]. In early 2007, Kobasa and coworkers reported that monkeys (*Macaca fascicularis*) infected with the recreated strain showed classic symptoms of the 1918 pandemic, and died from a cytokine storm—an overreaction of the immune system [87]. This may explain why the virus that caused the 1918 pandemic caused an unusually severe disease in young adults, a population that is typically not susceptible to severe infection with influenza viruses [36,88,89].

The 1918 pandemic received its nickname "Spanish flu" because of the early perceptions of the disease's severity in Spain. Spain was a neutral country in World War I and had no censorship of news regarding the disease and its magnitude. Germany, the United States, Britain and France all had media blackouts on news because they did not want to disclose information about the disease and the number of deaths to their enemies. But in Spain, people were free to report about the disease, including the grave illness of King Alfonso XIII of Spain, giving the false impression that Spain was the most-affected area and that the virus originated there, when in fact it likely originated in an army base in the United States [149].

Human influenza viruses had not yet been identified in 1918 and no viral isolates were obtained during the 1918-1919 pandemic. It was not until the modern molecular biology era that the genome of the 1918 pandemic virus could be sequenced from small viral RNA fragments isolated from lung tissues of victims on the 1918 pandemic and reconstructed by reverse genetics to evaluate its characteristics [9,80,149]. Taubenberger and coworkers confirmed the identity of the causative agent of the 1918 pandemic to be an H1N1 virus. Viral RNA was recovered from an Inuit woman whose body was exhumed from a mass grave in Alaska [150], and from formalin-fixed, paraffin-embedded tissues of two soldiers who died in 1918 [86]. RT-PCR amplification of the viral RNAs led to the reconstruction of the viral genes and regeneration of the whole virus by reverse genetics [151].

As mentioned above, phylogenetic analyses revealed that 1918 “Spanish influenza” virus genes are avian-like, however some of the proteins contain “human-like” signature amino acids. The polymerase proteins PA, PB1, and PB2 of the 1918 human virus differ by a total of only ten amino acids from the consensus sequences of the same proteins of conventional avian viruses [69]. The large number of synonymous changes as compared to avian viruses seems to suggest that the ancestor donor of the 1918 “Spanish influenza” virus genes had been in evolutionary isolation before virus transmission to humans occurred [146,151] and that this pandemic virus arose from an avian virus by mutation, rather than by reassortment alone [84].

Understanding the origin of these pandemic viruses can help us understand when and where they may emerge again in the future. The appearance of each pandemic over the last century has followed a logical progression with the evolution of the causative influenza strains. If we can better understand the mechanisms of influenza virus evolution (ie, antigenic shift and antigenic drift) and just what gives a specific strain that pandemic potential, then we could improve our ability to predict what the next pandemic strain would be and we can adjust our annual vaccination strategies accordingly.

1.10 Molecular Biology Tools for Studying Influenza Viruses

1.10.1 Reverse Genetics

The development of reverse genetics systems allows for a more detailed study of the genome of many RNA viruses. The genome is more easily manipulated by using the stable complimentary DNA (cDNA) and the development of a full-length infectious clone system is often the most desirable tool for studying the genome of RNA viruses. This has already been well established and characterized for many RNA viruses including several strains of Influenza [48,150]. These systems rely on the intracellular synthesis of influenza viral RNAs by a cellular

enzyme, RNA polymerase I, that transcribes ribosomal RNA in the nucleus of eukaryotic cells [152]. The influenza viral segments are encoded by cDNAs flanked by the RNA polymerase I promoter and the RNA polymerase I terminator or a ribozyme sequence. RNA polymerase I transcription in transfected cells results in the efficient synthesis of RNA transcripts with defined 5′ ends, whereas the integrity of the 3′ ends is achieved using the nucleotide-specific RNA polymerase I terminator or a self-cleaving ribozyme. RNA polymerase I transcripts are neither capped nor polyadenylated; therefore, they exactly resemble influenza viral transcripts. To generate influenza viruses, cells are transfected with eight plasmids to provide all eight viral RNAs, as well as with four helper plasmids for the expression of the polymerase and NP proteins that are required to initiate viral replication [105,106]. Although this approach requires the co-transfection of cells with 12 plasmids, it is highly efficient, routinely yielding 10^8 plaque-forming units (PFUs) of influenza A virus per millilitre of cell culture supernatant [7,47].

1.10.2 The Minigenome

The minigenome system has proven to be an effective complement to the full-length infectious clone system by allowing for the analysis of the roles of individual viral genes and proteins that are important in virus transcription, replication and genome packaging *in vitro*. In general, the coding regions of the genomes are removed and replaced with that of a single reporter gene that is detectable, a Green fluorescent Protein (GFP) or Luciferase gene are commonly used [59]. This reporter gene product can be assayed and quantified, producing a simple way to analyse the contribution of single or multiple viral gene contributions to transcription and replication processes. In the case of high-containment pathogens, such as the 1918 pandemic strain of influenza, minigenome systems allow for effective manipulation in the biosafety level 2 setting.

1.10.3 Animal Studies

1.10.3.1 Mice

Balb/c mice are the best studied experimental animal model of influenza A virus pathogenicity [143]. Studies with these mice have shown that the gene encoding the hemagglutinin and those encoding the ribonucleoprotein polymerase complex act as virulence factors in the 1918 pandemic virus [143].

Although mice are not naturally infected, they can be experimentally infected with influenza A or B viruses. Most human influenza viruses cause indiscernible infection of the upper and lower respiratory tract and do not cause lethal disease without adaptation. Notable exceptions include the recently isolated H5N1 viruses, which can cause lethal infections without prior adaptation. Most mouse strains are susceptible to infection with influenza A viruses and have been used widely to study the pathogenesis of and the immune response to influenza viruses. Knock-out mice are useful tools for deciphering the molecular basis of virus–host interactions [8].

1.10.3.2 Ferrets

Ferrets can be infected with influenza A or B viruses. The pathology is usually confined to the nasal mucosa, but infection of the lower respiratory tract has been demonstrated. The pathological changes of bronchitis and pneumonia resemble those seen in humans, which makes ferrets a valuable animal model to study various aspects of influenza virus infection. Unlike mice, ferrets can also be used to study the transmissibility of influenza viruses [7,8].

1.10.3.3 Nonhuman Primates

Influenza viruses can infect a variety of non-human primates (NHPs), such as chimpanzees, gibbons, and baboons, as well as rhesus, squirrel, African green, and cynomolgus monkeys. Illness can be observed many species (e.g., cynomolgus, rhesus) experimentally infected with influenza virus. Several viruses known to be virulent in humans also produce illness in squirrel monkeys, indicating that NHPs can be a useful animal model for the study of influenza virus infections. Indeed, cynomolgus macaques (*Macaca fascicularis*) were recently tested as an animal model for H5N1 viruses and found to develop acute respiratory distress syndrome with fever, similar to that seen in H5N1-infected humans [7,8].

1.11 Experimental Rationale

The H1N1 subtype virus that caused the the 1918 “Spanish Flu” pandemic is the focus of this study as nearly 50 million people died, with 500 million people being infected [67]. The identification of the specific viral genes associated with the unique growth properties of the 1918 virus may help to correlate the transcription/replication properties to the high virulence associated with this pandemic virus. The 1918 virus replicates more rapidly and to higher titers than many other influenza viruses suggesting that this virus has efficient transcriptional activities, which yields high replication activity. We have investigated the role of the RdRp complex in viral transcription by comparing the RdRp of the 1918 virus to the RdRp of a low virulence conventional H1N1 human virus isolate, A/Canada/RV733/2007 (RV733) using a minigenome approach.

1.12 Hypothesis

The RNA-Dependent RNA Polymerase of the 1918 Influenza A H1N1 virus has unique properties that contribute to the exceptionally high replication efficiency of the virus. One or more of the individual components of the RdRp contribute to the unique efficiency of the RdRp complex as a whole and may contribute to the unusually high pathogenicity of the virus.

1.13 Experimental Outline

Aim 1: Evaluate the contribution of each polymerase gene to the transcription by the polymerase complex in vitro by use of a minigenome reporter system

Aim 2: Evaluate the contribution of each polymerase gene to viral replication by generating recombinant viruses

Aim 3: Evaluate the pathogenicity of each recombinant virus using a mouse model

2.0 Materials and Methods

2.1 Cells and Viruses

293T (human embryonic kidney) cells (ATCC) were cultured in Dulbecco's modified Eagle's medium (DMEM, Sigma) with 10% heat inactivated fetal bovine serum (FBS). Tissue culture plates were coated with poly-D-lysine (1mg/ml, Sigma) for 30 minutes (min) at 37°C to enhance cell attachment. Culture plates were subsequently washed with PBS prior to seeding of cells. 293GT human embryonic kidney "Grip tight" cells (obtained from Invitrogen) were cultured in DMEM supplemented with 10% FBS, 1% L-glutamine, 1% non-essential amino acids and 1% geneticin (Gibco). 293GT cells are a modified lineage of 293T cells with high adherence to cell culture substrates and it was not necessary to treat culture plates with poly-D-lysine prior to seeding of cells. Madin-Darby canine kidney (MDCK, obtained from ATCC) cells were cultured in minimal essential medium (MEM) supplemented with 10% FBS and 1% L-glutamine. All cells were incubated in 5% CO_2 and H_20-saturated atmosphere conditions at 37°C. Cells were passaged by treatment with trypsin [0.25% Trypsin-EDTA (ethylenediamine tetra-acetic acid), Gibco^{TM}] and diluted in culture medium every two to three days.

Influenza A virus A/ South Carolina/1/1918(H1N1) NML stock was generated by reverse genetics. Tracy Taylor (TT) and Darwyn Kobasa (DK) generated the constructs used for this virus rescue. Briefly, the complete viral and complementary sequences were synthesized as 40-mer oligonucleotides (Table 1), with a 20-nucleotide overlap between each forward and reverse primer [127]. Ligase chain reaction was used for initial assembly of subgenomic fragments from the pooled primers for each gene, and the full length genes were assembled by amplification from the pool of gene fragments using PCR (as described by Rouillard et.al. [153]). Each gene was then further amplified by PCR using the gene-specific universal primer set described by Hoffman and colleagues (2001) and subcloned into the pPolI vector for reverse genetics [113,154]. The

1918 virus was rescued by the standard protocols [24] and titres were determined by standard plaque assay on MDCK cells (see section 2.12.1).

Influenza A virus (A/Canada/RV733/2007(H1N1)) was a clinical isolate that was tissue culture (TC) adapted by serial passaging on MDCK cells (by DK). Gene sequences for the RV733 virus were obtained from the TC adapted virus by standard Sanger dideoxy sequencing. The RV733 virus was then regenerated by reverse genetics using the same protocol employed for the 1918 virus [127].

Table 1: Influenza virus nucleotide reference sequences, mRNA, complete, GenBank Database

Virus	Gene	Ascension No.
A/ Brevig Mission /1/1918(H1N1)	Polymerase Acidic (PA)	DQ208311
A/ Brevig Mission /1/1918(H1N1)	Polymerase basic protein 1 (PB1)	DQ208310
A/ Brevig Mission /1/1918(H1N1)	Polymerase basic protein 2 (PB2)	DQ208309
A/ Brevig Mission /1/1918(H1N1)	Nucleoprotein (NP)	AY744935
A/Canada/RV733/2007(H1N1)	Polymerase Acidic (PA)	n/a
A/Canada/RV733/2007(H1N1)	Polymerase basic protein 1 (PB1)	n/a
A/Canada/RV733/2007(H1N1)	Polymerase basic protein 2 (PB2)	n/a
A/Canada/RV733/2007(H1N1)	Nucleoprotein (NP)	n/a

2.2 Primers

See appendix 1 for a list of all primers used. Primers were designed against the Influenza virus PA, PB1, PB2 and NP gene sequences of A/ Brevig Mission /1/1918(H1N1) and A/Canada/RV733/2007(H1N1) (Table 1 for ascension numbers).

2.3 Polymerase Chain Reaction (PCR)

PCR reactions described in this thesis were performed using iProof™ High-Fidelity DNA polymerase (Bio-Rad) in a Biometra T-personal thermocycler. The iProof™ High-Fidelity DNA polymerase was chosen because it comprises a unique *Pyrococcus*-like proofreading enzyme that has been shown to be fast and accurate when producing long amplicons (15-30 sec/kb). It

also produces blunt-end DNA products which allows for ease of sub-cloning. PCR was used to amplify viral genes from plasmid DNA. In general, a typical 50.0µl reaction consisted of 10.0µl 5x High-Fidelity reaction buffer, 1.0µl deoxynucleotide triphosphate (dNTP) solution (10mM each), 1.0µl dimethyl sulfoxide (DMSO), 1.0µl magnesium chloride ($MgCl_2$), 2.5µl of 10µM forward primer, 2.5µl of 10µM reverse primer, 10-20ng/µl of template plasmid DNA, 0.5µl (1 enzyme unit) of iProof™ polymerase and the volume was brought up to 50.0µl with Ultrapure double-distilled water (ddH_2O; Invitrogen). All reactions were prepared on ice. See appendix 1 for list of primers that were used. General cycling conditions are outlined in table 2.

Table 2: General thermocycling parameters for PCR

Number of cycles	Time	Temperature	Cycle description
1x	30sec	98°C	Activation of DNA polymerase
40x	10sec 30sec 45sec	98°C 65°C 72°C	Denaturation Annealing Elongation
1x	10min	72°C	Final elongation
1x	hold	4°C	Final cooling

2.3.1 Amplicon Analysis

Amplicons generated by PCR were verified for size and quality by electrophoresis of a sample of the DNA on a 0.7% agarose (Invitrogen) gel, at 120 volts (V) for approximately 30 min, followed visualization of DNA bands under UV or using a Blue light SafeImager™ (Invitrogen). Gels were made in 1x Tris acetate EDTA (TAE) buffer and SYBR® Safe DNA gel stain (Invitrogen) (5.0µl/100ml gel). SYBR® Safe stain is highly sensitive and specifically formulated to be a less hazardous alternative to ethidium bromide that can be used with either blue-light or UV excitation. Five microliters of SYBR® Safe is also added to the 1x TAE running buffer during electrophoresis. A molecular weight marker, TrackIt 1Kb plus DNA ladder (Invitrogen, Appendix 2), was also included when loading the gel to verify the size of the amplicon.

2.3.2 Addition of 3' A-overhangs

The addition of 3' A-overhangs is necessary to clone blunt end inserts (as such were generated with iProof™ High-Fidelity DNA polymerase) into the pCR2.1 TOPO vector (Invitrogen). A typical reaction mixture contains all 50.0µl of purified PCR product (Section 2.3), 5ul 10x buffer, 1.0µl deoxynucleotide triphosphate (dNTP mix) solution (10mM each), and 0.5µl (0.5 units) of a non-proofreading Taq DNA polymerase (Invitrogen). The reaction mixture was incubated at 72°C for 10 minutes.

2.4 Cloning

2.4.1 DNA Digestion

PCR-amplified DNA inserts were digested in parallel with appropriate vector constructs and restriction enzymes (New England Biolabs). A typical 5.0µl digestion was prepared: 1.0µl of restriction enzyme fast digest buffer, 100ng of vector DNA / 200ng insert DNA, 0.3µl of restriction enzyme (Fast Digest), 0.1µl DTT and 1.6µl of ddH_2O. Digestions were incubated at 37°C for 1hr. DNA was purified using either a QIAquick® PCR purification kit or QIAquick® gel extraction kit (Qiagen).

2.4.2 pCR2.1 TOPO Ligation

PCR products (with appropriate 3' A-overhangs) were cloned into the pCR2.1 TOPO vector (Invitrogen) according to manufacturer's protocol (Invitrogen). Up to 4.0µl of fresh PCR product is mixed with 1.0µl Salt Solution (Sterile water is added to bring reaction mixture up to 5.0µl if using less than 4.0µl PCR product) and 1.0µl pCR2.1 TOPO vector is added last. The PCR product and vector mixture was ligated at room temperature for 20 minutes.

2.4.3 DNA Ligation

Following DNA digestion, 5µl of the reaction mixture was loaded onto a 1% agarose gel, electrophoresed at 100V for 30 min, and visualized under blue light to estimate the quality and quantity of digested DNA present (Section 2.3.1). The remaining reaction mixture was purified using a QiaQuick PCR purification kit (Qiagen) according to the manufacturers' protocol. The purified DNA was resuspended in 50.0µl ddH_20. The insert and vector was ligated using T4 DNA ligase (1 unit/µl, Invitrogen). A typical 20µl DNA ligation reaction consisted of 2µl of 10x ligation buffer, 1.0µl of digested vector DNA, 5- 15µl of digested insert DNA, 1.0µl of T4 DNA ligase in a final reaction volume of 20 µl. Ligation reactions were incubated at 16°C overnight.

2.4.4 DNA Plasmid Transformation

Escherichia coli (*E.coli*) Top 10 chemically competent cells (Invitrogen^{TM}) were commercially supplied (One Shot® TOP10 Chemically Competent *E. coli*, Invitrogen^{TM}). Competent cells were transformed by thawing cells on ice, addition of 2-4ul of the ligation reaction, followed by a 30 min incubation on ice. Cells were then heat shocked at 42°C for 30 seconds (sec), 250.0ul SOC medium (Appendix 3, Invitrogen) was added and cells were then incubated at 37°C with horizontal shaking for 1 hour. The bacterial culture was then spread on LB (Appendix 3)-agar plates containing Ampicillin (100µg/ml) plates and incubated for 16 hours at 37°C.

2.4.5 Plasmid DNA Extraction

Selected bacterial clones were used to inoculate 3-4ml of LB broth containing 100µg/ml of ampicillin and grown overnight at 37°C in a shaking incubator. Plasmid DNA was extracted from the bacterial cells using a DNA plasmid Mini prep kit (Qiagen) following the manufacturer

protocol. Plasmid DNA was eluted in 50.0µl ddH_2O and concentration was determined using a NanoDrop ND-1000 spectrophotometer.

2.4.6 Digest Screening and Verification of Constructs

Bacterial colonies were cultured in 4ml of LB broth (Appendix 1) overnight at 37°C with shaking and plasmid DNA was subsequently extracted using a plasmid DNA miniprep kit (QIAprep Spin Miniprep Kit, Qiagen). Extracted plasmid DNA was digested with appropriate restriction enzymes (New England Biolabs and Fermentas) (Section 2.4.1) in order to verify the presence of the insert. Positive screened colonies were then sequenced, using the dideoxy technique based on Sanger et al., (1977) and ABI3100 Genetic Analyzer, in order to ensure the presence and quality of the insert. Sequencing was carried out by an in-house DNA core facility.

2.5 Cloning Strategy: Plasmid Construction for Minigenome Assay

To analyze the contribution of each component of the influenza RdRp complex to viral transcription, a cloning strategy for the expression of each protein of the influenza RNP complex in a minigenome system was designed. Sequence specific primers were used to generate inserts by PCR (Section 2.3). The generated viral gene inserts were full length cDNAs of each polymerase and NP genes. Previously constructed pPol constructs (by DK and TT) for each individual viral gene were used as the template. Each amplicon was verified by gel electrophoresis (Section 2.3.1) and bands were visualized using a blue light SafeImager™ (Invitrogen). The desired band was extracted from the agarose gel and purified using a QIAquick Gel Extraction kit (Qiagen), and eluted in 50µl of ddH_2O. Each generated insert was first cloned into the pCR2.1 TOPO vector (Invitrogen) to allow for ease of subsequent sub-cloning. To clone each insert, which were generated with blunt ends, into the pCR2.1 TOPO vector (Invitrogen), 3' A-overhangs must be added (Section 2.3.3). Once this was done, the prepared inserts were ligated into the pCR2.1 TOPO vector (Invitrogen) (Section 2.4.2). Each TOPO construct was then

digested with the restriction enzymes whose sites were added to the 5' and 3' ends of each gene insert (Section 2.4.1) and cloned into the pCAGGS/MCS expression vector, which was also digested with the corresponding restriction enzymes in parallel (Section 2.4.3). Each construct was verified by digest screening and sequencing (Section 2.4.6) to confirm desired insert sequence and construction. A total of 8 eukaryotic protein expression plasmids were constructed in the mammalian expression vector, pCAGGS/MCS, encoding each of the viral polymerase complex proteins (PA, PB1, PB2, and NP) that were generated for the A/Brevig Mission/1/1918 (H1N1) and A/Canada/RV733/2007 viruses (Figure 9).

2.6 Cloning Strategy: Plasmid Construction for Recombinant Virus Rescue

For generation of recombinant influenza viruses, genes of the A/Brevig Mission/H1N1/1918 and A/Canada/RV733/2007 viruses were cloned into an RNA pol I (pPol) – driven plasmid (Figure 9). Briefly, cDNAs for each full length viral RNA were amplified by PCR with primers containing BsmBI restriction enzyme cut sites (Section 2.3), digested with BsmBI (Fermentas) (Section 2.4.1) and cloned into the BsmBI sites of the pPol vector (Section 2.4.3). Viral gene inserts in the pCR2.1 TOPO constructs (Section 2.5) were used as the templates for generating the pPol constructs. In these constructs, each gene in consequently flanked by the human RNA pol I promoter and the murine RNA pol I terminator. All constructs were sequenced prior to use to confirm desired sequence and construction. A total of 11 expression constructs were generated for each the A/Brevig Mission/H1N1/1918 and A/Canada/RV733/2007 viruses, one for each viral gene segment.

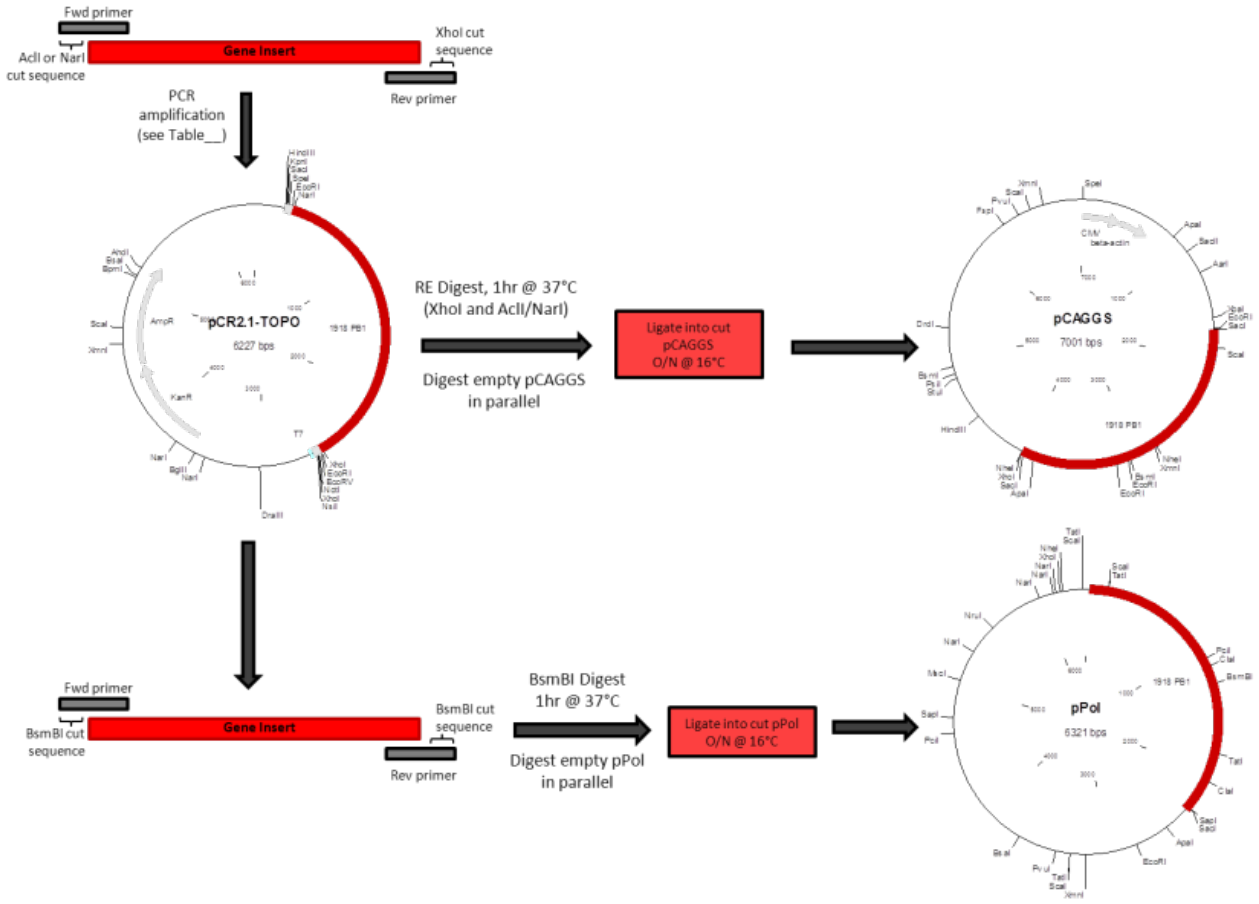

Figure 9: Cloning strategies for generation of gene expression constructs (pCAGGS) for the minigenome assay and (pPol) for reverse genetics and recombinant virus rescue. Each 1918 or RV733 Influenza RdRp gene was amplified from a pre-existing construct by PCR using specific primers to add flanking restriction sites to be used for sub-cloning. Each insert was individually cloned into the pCR2.1 TOPO vector and then subsequently removed by restriction enzyme digestion using the restriction sites added by PCR and subcloned into the pCAGGS/MCS expression vector for use in the minigenome assay. The pCR2.1 TOPO constructs were used as the template to amplify each Influenza RdRp gene by PCR during which flanking BsmBI restriction sites were added. Each gene was then digested with BsmBI in parallel with an empty pPol vector and cloned into the pPol vector for use in the generation of recombinant Influenza viruses by reverse genetics.

2.7 Construction of 1918/RV733 PB1 Chimeric genes

To analyze the contribution of the functional domains of the PB1 gene to viral transcription and replication, chimeric genes were constructed between the 1918 PB1 gene and the RV733 PB1 gene. The PB1 gene was divided into six functional domains (Figure 10). Specific primers were designed to amplify each of the PB1 functional domains of both the 1918 PB1 gene

and the RV733 PB1 gene with overlapping sequences so they could be joined together by assembly PCR (see section 2.7.1) to generate one complete chimeric PB1 gene (Appendix 1 for primers) (Figure 10). Sequences for the 1918 PB1 gene and the RV733 PB1 gene were based on GenBank sequences (Table 1 for ascension numbers) and previously determined sequence data, respectively. Primers were generated by Integrated DNA Technologies (IDT).

Each PB1 fragment was amplified by PCR (Section 2.3) using pPol constructs for each complete gene as templates. PCR products were electrophoresed on 0.7% agarose gels to confirm size and purity and subsequently cut out and purified using a QIAquick Gel Extraction kit (Qiagen) following the manufacturers protocol.

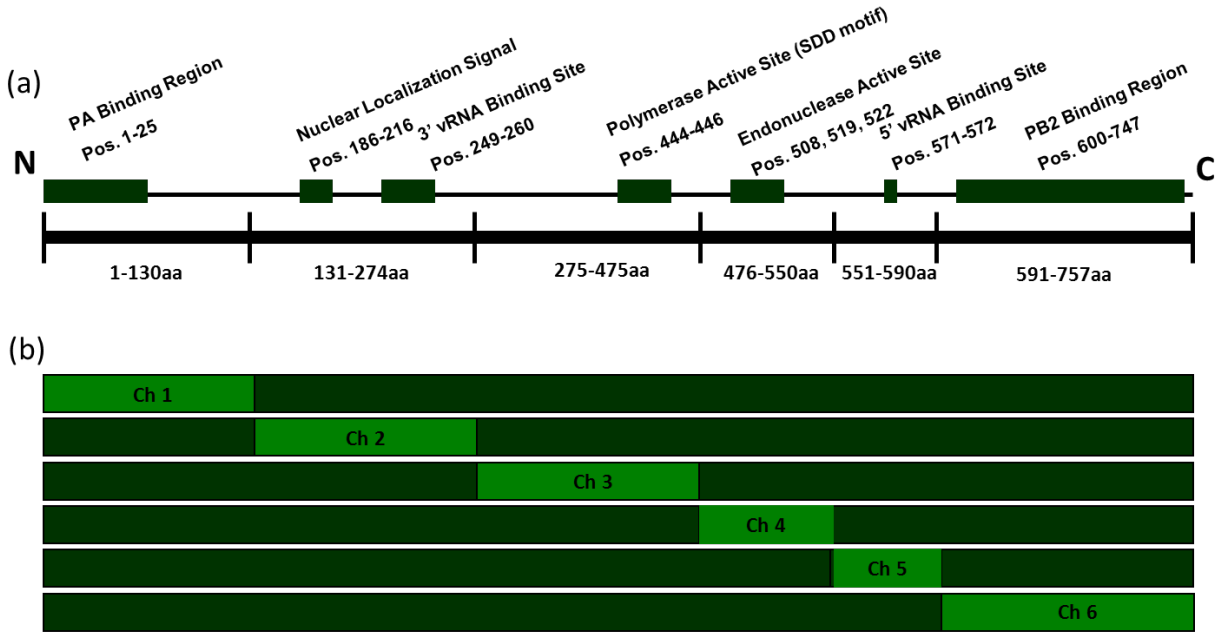

Figure 10: Influenza virus 1918/RV733 PB1 Chimeras. A schematic representation of the major functional domains of the Influenza PB1 protein (a) and design of the 1918/RV733 PB1 chimeric genes, light green denotes 1918 gene sequence and dark green denotes RV733 gene sequence (b).

2.7.1 PCR Assembly

PCR assembly was used to piece together the fragments of each PB1 gene to generate 1918/RV733 PB1 chimeric genes. Each PB1 fragment was generated with overlapping sequences of about 20 nucleotides to the fragment(s) that are intended to be adjacent to it. The purified fragment that would be required for the full chimeric gene sequence were then combined in a reaction that was prepared in the absence of primers and consisted of 2.0µl of each fragment for a given PB1 chimera (~10ng/µl), 10.0µl 5x High-Fidelity reaction buffer, 1.0µl deoxynucleotide triphosphate (dNTP) solution (10mM each), 1.5µl Dimethyl Sulfoxide (DMSO), 1.5µl magnesium chloride ($MgCl_2$), 0.5µl (1 enzyme unit) of iProof^{TM} High-Fidelity DNA polymerase and 28.5µl double-distilled water (ddH_2O). The reaction underwent 5 cycles of PCR amplification to allow the PB1 fragments to anneal together (Table 3 PCR Assembly thermocycling conditions) and extend their sequences into the adjacent fragments. The reactions were then placed on ice, 2.0µl pPol forward primer (10µM) and 2.0µl pPol reverse primer (10µM) were added and the placed back in the thermocycler for amplification of the full gene (Table 4 thermocycling parameters for PB1 Chimera PCR). The resulting PCR products were electrophoresed on a 0.7% agarose gel to confirm size and were then cut out and purified using a QIAquick Gel Extraction kit (Qiagen) following the manufacturers protocol.

Table 3: Thermocycling parameters for PCR Assembly

Number of cycles	Time	Temperature	Cycle description
1x	30sec	98°C	Activation of DNA polymerase
5x	10sec 30sec 45sec	98°C 58°C 72°C	Denaturation Annealing Elongation
1x	10min	72°C	Final elongation
1x	hold	4°C	Final cooling

Table 4: Thermocycling parameters for Chimeric PB1 PCR

Number of cycles	Time	Temperature	Cycle description
1x	30sec	98°C	Activation of DNA polymerase
40x	10sec 30sec 45sec	98°C 58°C 72°C	Denaturation Annealing Elongation
1x	10min	72°C	Final elongation
1x	hold	4°C	Final cooling

2.7.2 Cloning Strategy: PB1 Chimera Plasmid Construction for Minigenome Assay

A-overhangs on the 3' termini of PCR products were added to each assembled PB1 chimera gene (Section 2.3.3), cloned into the pCR2.1 TOPO vector (Section 2.4.2), transformed (Section 2.4.4) into chemically competent E.Coli and cultured overnight in LB media (Section 2.4.4). Plasmid DNA was extracted (Section 2.4.5) and subsequently screened by restriction enzyme digestion (EcoRI, Fermentas) and sequencing (M13 primers) to confirm the construction of each PB1 chimeric gene (Section 2.4.6). Each pCR2.1 TOPO/PB1 chimera construct was then digested with the restriction enzymes for the sites that were added to the 5’ and 3’ ends of each gene insert (Section 2.4.1) and cloned into the pCAGGS/MCS expression vector, which was also digested with the corresponding restriction enzymes in parallel (Section 2.4.3). Each construct was verified by restriction enzyme digest screening and sequencing (Section 2.4.6) to confirm desired insert sequence and construction. A total of six PB1 chimera expression constructs were generated for use in minigenome studies (Figure 10b).

2.7.3 Cloning Strategy: Plasmid Construction for 1918/RV733 Chimeric PB1 Recombinant Virus Rescue

For generation of recombinant influenza viruses which contain the above described 1918/RV733 chimeric PB1 genes, RNA polymerase I driven plasmid (pPol) constructs were generated containing one of the six chimeric PB1 genes (Figure 10). Briefly, cDNA for each full length viral RNA was amplified by PCR with primers containing BsmBI restriction enzyme cut sites (Section 2.3), digested with BsmBI (Fermentas) (Section 2.4.1) and cloned into the BsmBI sites of the pPol vector (Section 2.4.3) such that the 5'-end of the negative sense gene sequence was immediately preceded by the human PolI promoter and the 3' end of the sequence was immediately followed by the murine PolI terminator. Viral gene inserts in the pCR2.1 TOPO constructs (Section 2.8) were used as the templates for generating the pPol constructs. All constructs were sequenced prior to use to confirm desired sequence and construction.

2.8 Generation of pPol/GFP Construct

The enhanced green fluorescent protein (eGFP) was used as a reporter gene in a minigenome system. An eGFP construct, supplied by DK (commercially generated, Mr. Gene) was used as the starting template. The eGFP gene was PCR amplified using sequence specific primers that added the RV733 influenza virus NS untranslated regions to either end of the eGFP gene. The specific primers also added flanking BsmBI restriction sites for subcloning (Appendix 1 for primers, Table 1 for General PCR cycling protocol). A 5.0µl sample of the PCR product was electrophoresed on a 0.7% agarose (Invitrogen) gel to verify size and purity. The remaining PCR was purified using a QIAquick PCR purification kit (Qiagen) following the manufacturers protocol. The GFP insert was then digested in parallel with the pPol vector with BsmBI (Fermentas). A 40.0µl reaction mix consisting of 2.0µl DNA, 2.0µl BsmBI (NEB), 0.4ul BSA, 4.0µl 10X digestion buffer and 31.6µl ddH_2O was incubated for 3hrs at 55°C. Both the digested eGFP insert and the cut pPol vector were then purified using a QIAquick column purification kit (Qiagen) following

manufacturers protocol and the cut eGFP insert was then ligated into the cut pPol vector (Section 2.4.3). The ligation reaction was then transformed into competent cells. Individual colonies were grown in LB broth/100µg/ml ampicillin and plasmid DNA was extracted (Section 2.4.4 and 2.4.5). pPol/eGFP constructs were verified by restriction enzyme digest screening and DNA sequencing (Section 2.4.6).

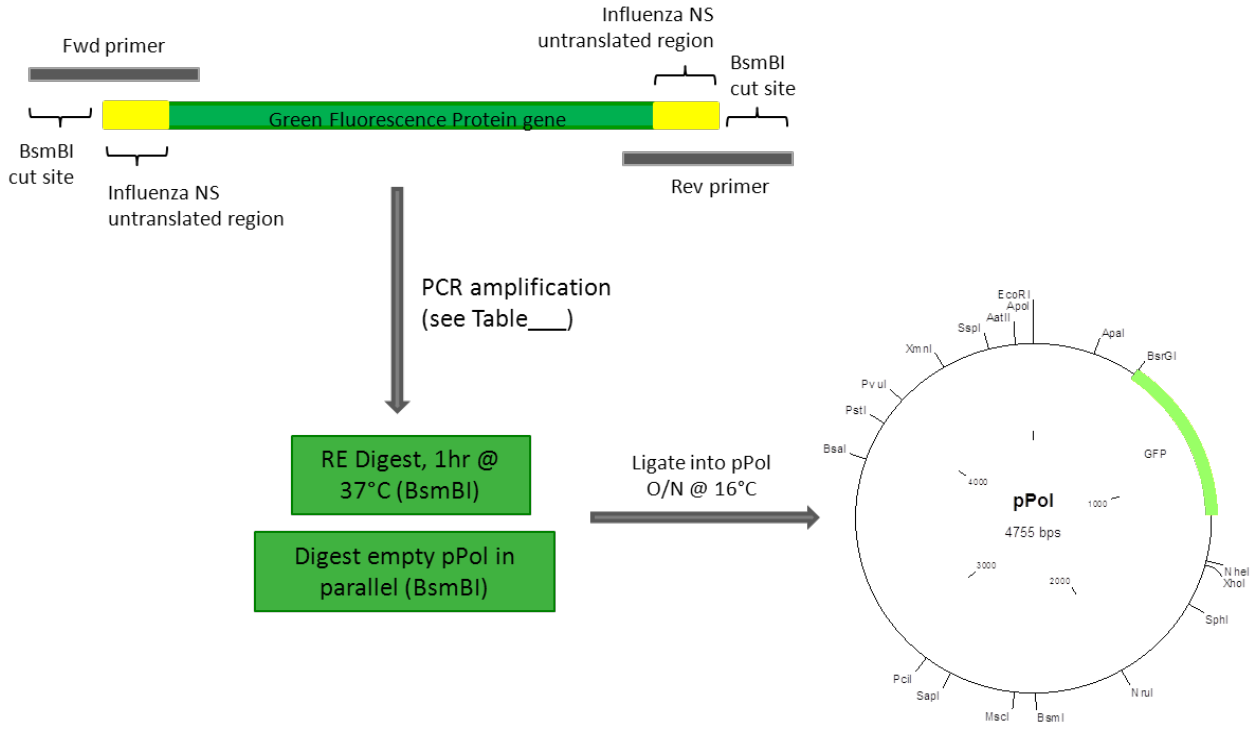

Figure 11: Cloning strategy for constructing the pPol/eGFP minigenome reporter plasmid for the 1918/RV733 minigenome assay. The enhanced green fluorescence protein (eGFP) gene was amplified by PCR with primers for the 5' and 3' ends containing the RV733 influenza NS gene untranslated regions and BsmBI restriction enzyme sites. The resulting eGFP gene PCR product was then digested with BsmBI in parallel with empty pPol vector at 37°C for 1hr and ligated into the cut pPol vector.

2.9 Generation of pPol/Firefly Luciferase Construct

The firefly luciferase (FFLuc) gene is used as a reporter gene in a second minigenome system. The FFLuc gene was amplified from a FFLuc construct provided by Charlene Ranadheera (CR) using specific primers designed to add flanking RV733 influenza NS untranslated regions to either end of the gene. BsmBI restriction sites were also added with the same set of primers for cloning into the pPol vector. FFLuc was amplified in a 50.0µl PCR reaction mixture containing 20ng FFLuc DNA template, 10.0µl 5x High-Fidelity reaction buffer, 1.0µl deoxynucleotide triphosphate (dNTP) solution (10µM each), 1.0µl dimethyl sulfoxide (DMSO), 1.0µl magnesium chloride ($MgCl_2$), 1.0µl of 10µM forward primer, 1.0µl of 10µM reverse primer, 10-20ng/µl of template plasmid DNA, 0.5µl (1 enzyme unit) of iProof^{TM} High-Fidelity DNA polymerase and the volume was brought up to 50.0µl with ddH_2O. All reactions were prepared on ice. See appendix 1 for list of primers used. General cycling conditions are outlined in table 1.

Table 5: Thermocycling parameters for PCR amplifying Firefly Luciferase

Number of cycles	Time	Temperature	Cycle description
1x	30sec	98°C	Activation of DNA polymerase
40x	10sec 30sec 40sec	98°C 60°C 72°C	Denaturation Annealing Elongation
1x	2min	72°C	Final elongation
1x	hold	4°C	Final cooling

The FFLuc amplicon (all 50.0µl) was then run on a 0.7% agarose gel to confirm size and purity. The desired band was cut out of the gel and column purified using a QIAquick Gel Extraction Kit (Qiagen) following manufacturer's protocol. The purified amplicon was then digested in parallel with the pPol vector with BsmBI (Section 2.4.1). The digested FFLuc insert and pPol vector were then purified once more using the QIAquick column purification kit (Qiagen) following manufacturer's protocol and the FFLuc insert was then ligated into pPol (Section 2.4.3). The ligation reaction was then transformed into competent cells. Individual colonies were grown in LB broth/100 µg/ml ampicillin and plasmid DNA was extracted (Section 2.4.4 and 2.4.5). pPol/FFLuc constructs were verified by digest screening and DNA sequencing (Section

2.4.6)(Figure 12). A pRL/Renilla luciferase construct was used as an internal transfection control and was generously provided by Kyle Brown (KB).

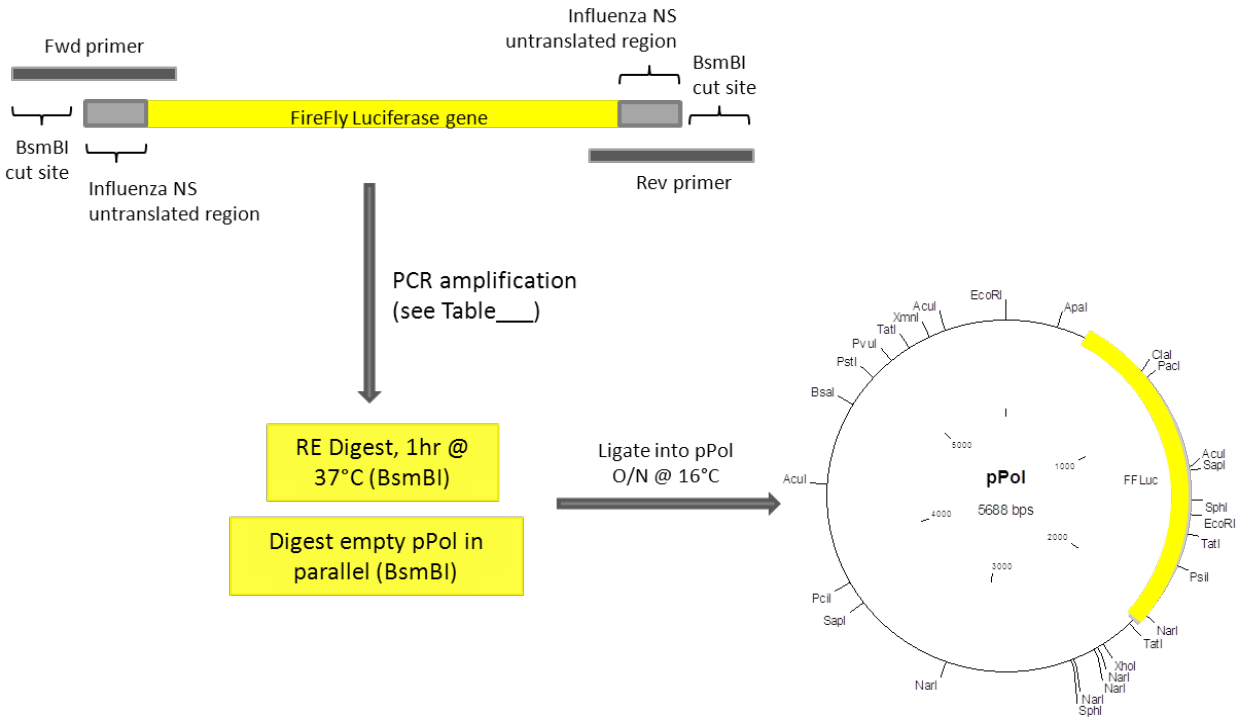

Figure 12: Cloning strategy for the generation of the pPol/FFLuc construct for the Dual-Luciferase Reporter Minigenome Assay. The luciferase gene was amplified by PCR with primers for the 5' and 3' ends containing the RV733 influenza NS gene untranslated regions and BsmBI restriction enzyme sites. The resulting luciferase gene PCR product was then digested with BsmBI in parallel with empty pPol vector at 37°C for 1hr and ligated into the cut pPol vector.

2.10 General Transfection Protocol

Human embryonic kidney 293T or 293GT cells (referred to collectively as 293(G)T) were transfected with plasmid DNA in order to express recombinant proteins. 293(G)T cells were seeded into culture plates to achieve approximately 60-80% confluency for next day use. 6-well plates (Corning) were used for reverse genetics virus rescue and 12-well plates (Corning) were used for minigenome studies. An optimized amount of *Trans*IT-LT1 (Panvera) transfection reagent was added to 200ul of Opti-MEM Reduced Serum Media (Opti-MEM, Gibco) and

incubated at room temperature for 5 min. Plasmid DNA was then added to the transfection reaction, gentle thorough mixing and incubated at room temperature for 30 min. During this time the spent media on the cells was removed and fresh Opti-MEM was added to the cells (1.0ml in 12-well plates and 2.0ml in 6-well plates). After the 30 min incubation, the transfection reaction was added to the cells by gentle pipetting. Plates were gently rocked in two-dimensions to ensure even distribution of plasmid DNA over the cells. Cells were incubated for 48 hours at 37°C with 5% CO2 and H20-saturated atmospheric conditions.

2.10.1 The GFP Minigenome System and Measurement of GFP Expression

293GT cells in 12-well culture plates were transfected with the four viral polymerase protein expression plasmids (0.5ug each), which contain the chicken Beta-actin promoter, that is recognized by the host cell transcription machinery to synthesize mRNA for each viral gene, and 0.1ug of pPol/eGFP minigenome plasmid (Figure 13). The PolI promoter in the PolI vector is recognized by the eukaryotic RNA polymerase I, which drives the first round of vRNA synthesis. These first vRNAs can then be transcribed and translated into their respective viral proteins. The viral RdRp complex then mediate the expression of the eGFP protein through recognition of the untranslated regions that flank the eGFP gene within the pPol vector to generate the viral mRNA in the same way as occurs during a viral infection. The complete set of RdRp expression plasmids minus the PB1 plasmid was used as a negative control and the pPol/eGFP construct transfected alone was used as the background eGFP signal control.

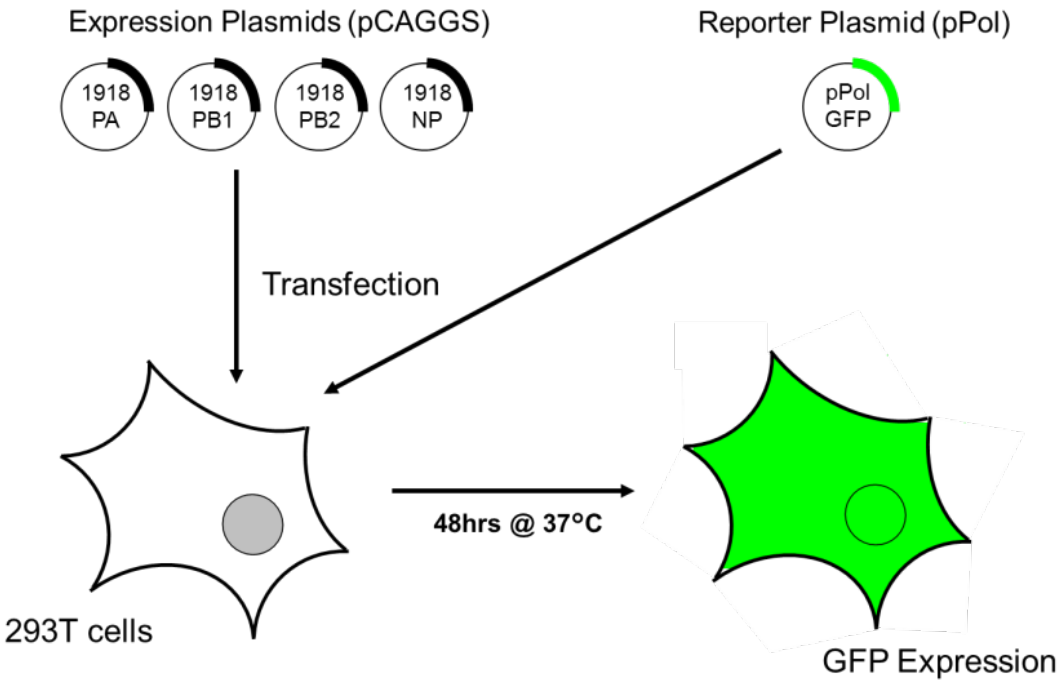

Figure 13: The general transfection method for the Influenza GFP minigenome assay. 293(G)T cells were co-transfected with the four pCAGGS expression plasmids (1.0ug each) along with the pPol/GFP reporter construct (0.1ug). Transfections were incubated at 37°C, 5% CO_2 for 48hrs. GFP expression, as a measure of transcriptional activity of the influenza RdRp, was evaluated by fluorescence microscopy and quantitated by fluorescence-activated cell sorting (FACS).

GFP expression was first visualized by fluorescence microscopy (Zeiss AxioVert 200M fluorescent microscope). Cells were analyzed without fixation and comparison between experiments was done by subjective visualization. Cells were prepared for fluorescence-activated cell sorting (FACS) (BDBiosciences LSRII) analysis after visualization by fluorescence microscopy (Zeiss). Cells were scraped from each well of a12-well culture plate and resuspended in 1.0ml of culture media. Five hundred microliters of resuspended cells were added to polystyrene test tube containing 0.5ml 4% paraformaldehyde (PFA). Cells were run through the LSRII FACS instrument and GFP positive cells were counted. Then using the High-performance FACSDiva BD software (BDbiosciences) the relative intensity of the GFP signal was measured for the population of cells that were determined to be GFP positive by selective gating. For each set of experimental conditions, three biological replicates were prepared and analyzed.

2.10.2 The Luciferase Minigenome System and Measurement of Luciferase Activity

293GT cells in 12-well culture plates were transfected with the four viral polymerase protein expression plasmids (1.0µg each), along with 0.025µg of the pPol/FFLuc reporter plasmid. As an internal control, a renilla luciferase reporter plasmid (0.01µg) was also co-transfected into the cells to normalize for transfection efficiency. Briefly, at 48hrs post-transfection, the transfection media was removed and cells were lysed by adding 250µl 1X Passive Lysis Buffer (Promega) directly to the cells. The cells were incubated for 15min at room temperature with gentle rocking. Each cell sample and buffer were then collected and transferred to a 96-well microplate. The plate was then read using the Veritas Microplate Luminometer by the sequential addition of 100.0µl LARII reagent followed by 100.0µl Stop&Glo reagent (Promega) (Figure 14). The components of the LARII and Stop&Glo reagents were supplied in the Dual-Luciferase Reporter Assay Kit (Promega) and were prepared at the time of use according to manufacturer's specifications. Three independent experiments were carried out, each performed in triplicate. Luciferase activity was expressed as Relative Light Units (RLUs) and normalized the expression of the renilla luciferase control to account for transfection efficiency.

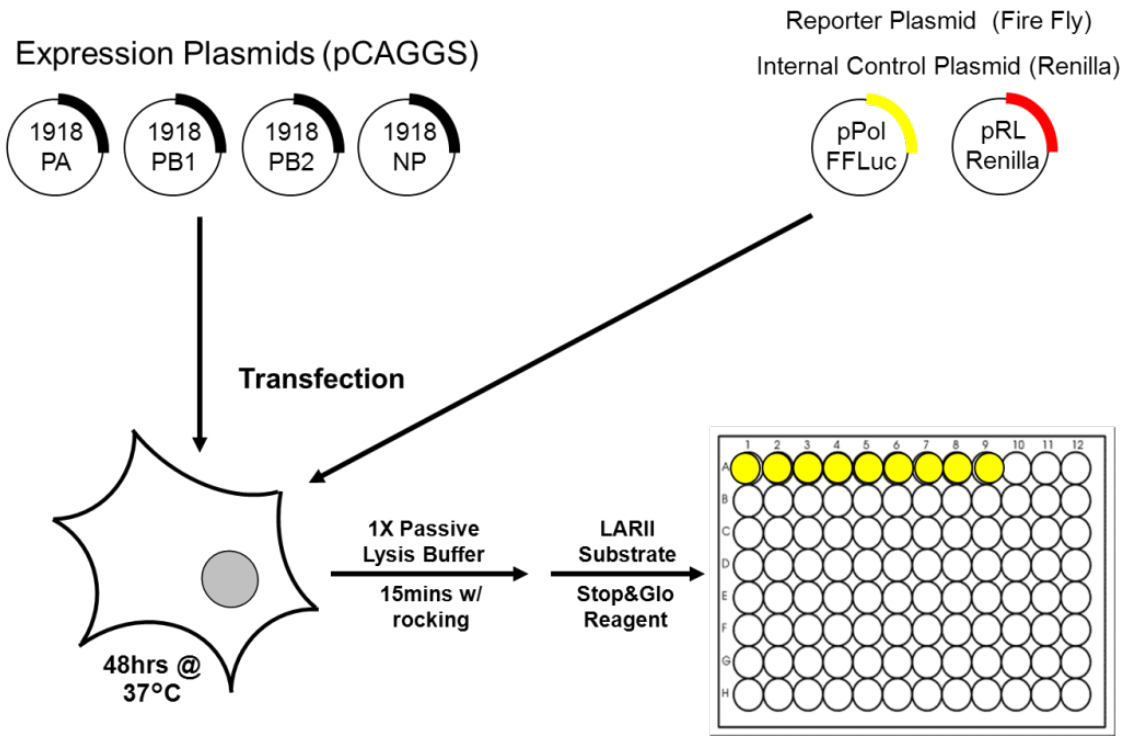

Figure 14: The general transfection method for the Influenza Dual-Reporter Luciferase minigenome assay. 293(G)T cells were co-transfected in 12-well plates with the four pCAGGS expression plasmids, pCAGGS/PA, PB1, PB2, and NP (1.0µg each) along with the pPol/FFLuc reporter construct (0.025µg) and the pRL/Renilla internal transfection control plasmid (0.01µg). Transfections were incubated at 37°C, 5% CO_2 for 48hrs. Cells were lysed with 250µl 1X Passive lysis Buffer (PBL) for 15mins with rocking, transferred to a 96-well microplate and luciferase expression was read using a Veritas Microplate Luminometer according to the Promega Dual-Luciferase Reporter assay protocol.

2.11 1918 and RV733 RdRp Transcription Kinetics

To compare the efficiency of the 1918 RdRp and the RV733 RdRp transcriptional activities a time course experiment was performed using the Dual-luciferase reporter minigenome assay. 293GT cells were transfected with the full 1918 RdRp/NP plus the luciferase minigenome or the full RV733 RdRp/NP plus the luciferase minigenome (Section 2.10.2) and cell lysates were collected at 2, 4, 6, 8, 10, 12, 16, 20, 24, 30, 36, 40, and 48hr time points. Cell lysates for each virus, at each time point was collected in triplicate. For each time point was isolated on its own plate to minimize disturbance or contamination during the transfection process. Cell lysates were collected and analyzed using the Dual-luciferase reporter assay as described in section 2.10.2.

2.12 Reverse Genetics and Recombinant Virus Rescue

All recombinant influenza viruses were generated at the National Microbiology Laboratory, Public Health Agency of Canada by a reverse genetic approach for virus rescue [47,152,154]. 293(G)T cells at 50-70% confluency were seeded in 6-well culture plates and then transfected with eight individual pPol plasmids each containing one of the eight viral genes (0.1µg each) along with four pCAGGS expression plasmids that provide the helper proteins needed to initiate viral replication (1.0µg each) (Section 2.10)(Figure 15). The helper plasmids encode each of the viral polymerase subunit and NP genes. At 48 hours post-transfection, supernatants were collected. Tosyl phenylalanyl chloromethyl ketone (TPCK)-treated trypsin was added to the supernatant (1.0µg/ml) and gently rocked for 30 min at 37°C to activate viral infectivity by cleavage of HA. TPCK-trypsin was used here as TPCK inhibits the activity of chymotrypsin and other cellular proteases that could be detrimental to infectivity. This makes it ideal for use in tissue culture as it eliminates the risk of autolysis, contamination of a sample with other proteases and allows control of the digestion by removing the trypsin from cells. One hundred microliters of activated virus supernatant was then added to 70-80% confluent MDCK cells in 12-well culture plates. MDCK culture media was minimal essential medium (MEM) supplemented with 0.1% BSA, 1% L-glutamine, and 1ug/ml TPCK-trypsin. Cells were then incubated for 48-72 hours. Efficient virus rescue was determined by the presence of cytopathic effect (CPE). Passage 2 (P2) virus stocks were prepared by infecting a 70-80% sub-confluent MDCK cell monolayer cultured with virus diluent (MEM, 0.3% BSA, and L-glutamine) containing 1.0µg/ml TPCK-trypsin in a 150cm^2 flask at a multiplicity of infection (MOI) of 0.001. Once the cells demonstrated CPE (48-72 hours post-infection), the supernatants were collected and clarified by centrifugation at 1 000xg for 10 min to remove any residual cell debris. Virus stocks were aliquoted and then stored at -80ºC.

Handling of the H1N1 human virus isolate, A/Canada/RV733/2007 was done under containment level 2 (CL-2) conditions and handling of the 1918 H1N1 Influenza virus was done under containment level 4 (CL-4) conditions as outlined in the Health Canada Laboratory Bio-

safety Guidelines handling procedures (www.hcsc.gc.ca/pphb-dgspsp/publicat/lbg-ldmbl-96/index.html). All recombinant viruses containing any 1918 virus genes were similarly produced and used in CL-4.

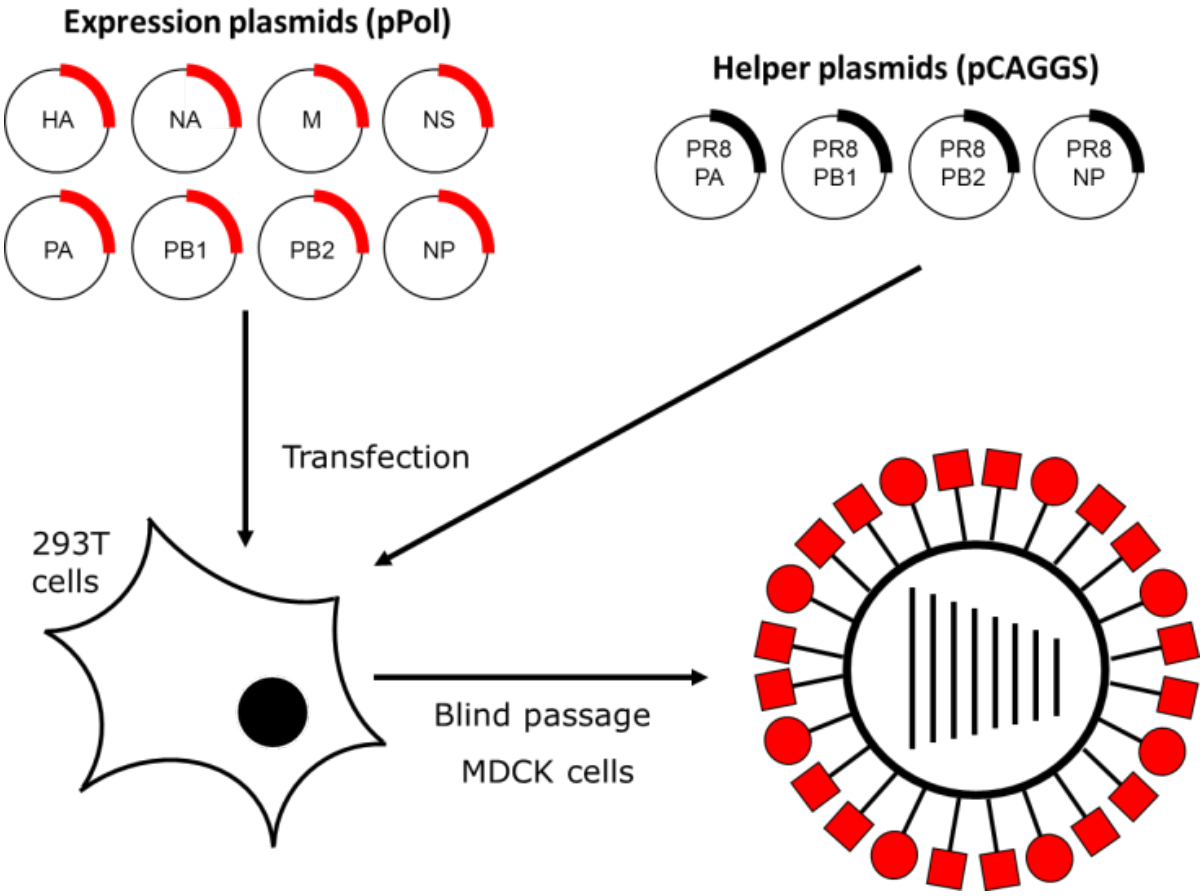

Figure 15: Method for generation of recombinant Influenza viruses by reverse genetics. 293(G)T cells at 50-70% confluency were transfected with eight individual pPol plasmids each containing one of the eight viral genes (0.1ug each) along with four pCAGGS expression helper plasmids, each with one of the viral polymerase and NP genes (1.0ug each). At 48 hours transfection supernatants were collected, TPCK-trypsin was added (1.0ug/ml) and shaken for 30 minutes at 37°C. 100ul of activated virus supernatant was added to 70-80% confluent MDCK cells. MDCK cells were then incubated for 48-72 hours and efficient virus rescue was determined by the presence of CPE.

2.13 Influenza Virus Infection

MDCK cells, cultured in MEM with 10% FBS and 1% L-glutamine were seeded in culture plates to achieve 70-80% confluency at time of infection. The culture medium was removed and the cells were washed with MEM/0.1% BSA to remove all traces of FBS. Fresh MEM/0.1%BSA was added to the cells along with 1.0 µg/ml TPCK-trypsin. MDCK cells were infected at a multiplicity of infection (generally MOI lower than 0.001) and incubated at 37°C/5% CO_2 for 48-72 hr.

2.13.1 Virus Titres: Plaque Assay

Influenza virus infectivity titres of each recombinant Influenza virus generated by reverse genetics (Section 2.11) were determined by plaque assay. MDCK cells, cultured in MEM with 10% FBS and 1% L-glutamine were seeded in 12-well plates to achieve 100% confluency for infection. An aliquot from the P2 stocks of each of the 1918/RV733 recombinant viruses were serially diluted 10-fold in MEM with 0.1% BSA from 10^{-2} dilution up to 10^{-9} dilution. The MDCK cells were washed with MEM/0.1%BSA to remove any traces of FBS. Each virus dilution was added to the MDCK cells in duplicate at 200µL/ well and incubated for 1 hour at 37^{o}C with gentle rocking every 15 minutes to distribute the medium over the cells. The viral inoculum was then removed and 1ml of a mixture of MEM (Invitrogen) supplemented with 0.1% BSA, 1% L-glutamine, and 1% low melting point agarose/0.1µg/ml TPCK-trypsin at 42ºC was overlayed onto the monolayer. Once the MEM-agar solution had solidified, the plates were inverted and incubated at 37^{o}C. Plaques were observed and counted 48-72 hr later and viral titres were calculated.

2.13.2 Influenza Virus Genotyping

Each recombinant virus that was generated was verified by sequence genotyping. Specific primers were designed to target regions of each gene of the RdRp complexes that were distinct between the 1918 and RV733 viruses (Appendix 1 for primers used). Viral RNA was extract for genotyping by RT-PCR. In brief, RNA samples for each of the recombinant influenza viruses generated by reverse genetics were brought out of the CL-4 laboratory in AVL buffer (Qiagen), as per standard CL-4 protocols for inactivation of viral samples for use in CL2, and extracted using the QIAamp Viral RNA Mini kit (Qiagen) following the manufacturer's protocol. The concentration of each RNA sample was measured using a NanoDrop ND-1000 spectrophotometer.

The genotyping RT-PCR was carried out in a two-step process using SuperScript III Reverse Transcriptase (RT; Invitrogen) and an iProof^{TM} High-Fidelity DNA polymerase PCR kit (BioRad). For the reverse transcription (RT) step a 30µl reaction mix consisting of 3.0µl 10X RT buffer (Invitrogen), 3.0µl deoxynucleotide triphosphate (dNTP mix) solution (10µM of each dNTP), 1.0µl random hexamer primer (Invitrogen), 2.0µl RT (2 enzyme units) (Invitrogen), 5.0µl RNA template and 16µl ddH_20 was first incubated at 65°C for 5 minutes and then placed on ice. The RT protocol is outlined in table 6. PCR reactions consisted of 10.0µl 10x High-Fidelity reaction buffer, 1.0µl deoxynucleotide triphosphate (dNTP) solution (10µM each), 1.0µl dimethyl sulfoxide (DMSO), 1.0µl magnesium chloride ($MgCl_2$), 1.0µl (10µM) of each genotyping primer (Appendix 1), 0.5µl (1 enzyme unit) of iProof^{TM} High-Fidelity DNA polymerase and the volume was brought up to 50.0µl with double-distilled water (ddH_2O). PCR cycling parameters are outlined in table 7. RT-PCR products were then verified by sequencing and compared to the reference sequences of the target genes to confirm the identity of each gene.

Table 6: Parameters for Reverse Transcription – Recombinant Influenza Virus Genotyping

Number of cycles	Time	Temperature	Cycle description

1x	10mins	25°C	Activation
1x	5mins	42°C	Annealing
1x	30mins	55°C	Reverse Transcription
1x	5mins	85°C	Inactivation
1x	15sec	10°C	Final cooling

Table 7: Thermocycling parameters for PCR – Recombinant Influenza Virus Genotyping

Number of cycles	Time	Temperature	Cycle description
1x	30sec	98°C	Activation of DNA polymerase
40x	10sec 30sec 40sec	98°C 60°C 72°C	Denaturation Annealing Elongation
1x	2min	72°C	Final elongation
1x	hold	4°C	Final cooling

2.14 Influenza Virus Replication Kinetics

To evaluate the replicative efficiencies of each of the recombinant Influenza viruses generated in this study as infection time course was carried out. MDCK cells were infected with each virus at an MOI of 0.001 according to the standard infection protocol (Section 2.12). Supernatants were collected for each virus in duplicate at 18hr, 24hr, 42hr and 48hr post infection and viral titres were determined by plaque assay (Section 2.12.1).

All infectious work was performed in the biosafety containment CL4 laboratory at NML/PHAC adhering to strict protocols stipulated by the Health Canada Laboratory Bio-safety Guidelines (www.hc-sc.gc.ca/pphbdgspsp/publicat/lbg-ldmbl-96/index.html).

2.15 Mouse Experiments

To study the virulence of each of the recombinant influenza viruses generated by reverse genetics in this study, groups of three mice were infected with each virus at two doses. Mice were anesthetized in an atmosphere of 5% inhalational anesthetic isoflurane in 100% oxygen for induction of anesthesia and 3% isoflurane for maintenance. Mice were infected by intranasal instillation of virus in 50.0ul MEM/0.1%BSA with either a high dose (10^5 PFU/mouse) or a low

dose (10^4 PFU/mouse) of each virus. Mice were monitored for a period of 18 days following infection for signs of disease, weighed and scored appropriately.

All animal procedures were approved by the Institutional Animal Care Committee at the National Microbiology Laboratory (NML) at the Public Health Agency of Canada (PHAC), according to the guidelines of the Canadian Council on Animal Care. Mice were monitored daily following infection and scored according to severity of clinical signs and other indicators of disease severity and lethality. The mice were scored on a scale of 0-3: 0 = no symptoms, 1=ruffled fur, slowing activity, loss of body conditions, 2=hind limb paralysis, labored breathing, hunched posture, 3= death). Based on daily scoring, mice reaching a state of disease that clearly identifies that they are unable to recover from the infection were sacrificed prior to death to prevent undue stress and suffering. All infectious work was performed in the biosafety containment BSL4 laboratory at NML/PHAC adhering to strict protocols stipulated by the Health Canada Laboratory Bio-safety Guidelines (www.hc-sc.gc.ca/pphbdgspsp/publicat/lbg-ldmbl-96/index.html).

2.16 Data Analysis

All data analysis was performed using the GraphPad Prism5 software. Raw data was inputted into the program where mean values and standard errors were calculated. Statistics were calculated using the same software program. Statistical significance between experimental data points was determined using a un-paired students t-test with a 95% confidence interval.

3.0 Results

3.1 Development of a 1918/RV733 GFP Minigenome System

3.1.1 Cloning

The minigenome reporter system allows for the analysis of the roles of specific viral gene sequences and proteins that are important in virus transcription, replication and genome packaging *in vitro*. To study the transcriptional properties of the influenza virus RdRp complex a minigenome system was employed using two different reporter systems, the green fluorescent protein (GFP) and the Dual-Luciferase reporters. Molecular cloning techniques were used to generate expression constructs for each of the RdRp and NP genes of the 1918 and RV733 Influenza viruses as well as the pPol/GFP and pPol/FFLuc reporter constructs (Section 2.5, 2.8, 2.9). Each reporter was designed to produce a RNA with influenza gene untranslated flanking sequences at either end of the open reading frame (ORF), derived from the RV733 influenza NS gene segment, that allow it to be recognized and transcribed as a viral gene by the RdRp (Figure 11 and 12).

3.1.2 GFP Reporter Minigenome System

293T cells were chosen for these minigenome studies as they are easily and efficiently transfected and are capable of efficient expression of recombinant proteins. 293T cells were co-transfected with expression plasmids of 1918 and RV733 polymerase genes and NP along with the GFP reporter construct. GFP expression, as a measure of the transcriptional activity of the RdRp complex, was evaluated by fluorescence microscopy (Figure 16) and quantitated fluorescence-activated cell sorting (FACS) (Figure 17).

The RdRp/NP of the 1918 virus showed lower reporter expression than RV733 by fluorescent microscopy and by FACS analysis. RdRp transcriptional activity was measured by

quantification of the GFP intensities of the cell population that was within a threshold that determined whether they were GFP positive. Each cell population that was determined to be GFP positive, by comparison to the appropriate controls, was gated from the non-GFP expressing cell population. Cells that were deemed GFP negative were assumed to have received an incomplete set of the RdRp/NP and reporter plasmids and thus were not able to show RdRp transcriptional activity. FACS analysis revealed that the 1918 RdRp/NP displayed GFP expression that was consistently about 3-fold less than that produced by the RV733 RdRp/NP complex (Figure 17). When analyzed using a fluorescent microscope, cells transfected with the 1918 RdRp expression plasmids showed varying levels of GFP expression. Many cells appeared bright green (<25%) while the majority of GFP positive cells displayed weak to moderate GFP expression. On the other hand, cells transfected with the RV733 RdRp expression plasmids had a more uniform level of GFP expression with >80% GFP positive cells displaying an intense green glow (Figure 16). It was also observed that after three separate transfection assays that fewer cells were GFP-positive when using the 1918 plasmids than with the RV733 plasmids. It was not determined whether this disparity between the two virus systems was due to differences in transfection efficiency with the specific plasmids or if transfection efficiency was similar but varied between the two viruses at the level of GFP-expression. As it was observed that the 1918 RdRp showed highly variable levels of expression, including many cells with much lower GFP expression than the RV733 system, it is possible that some cells had such low levels of GFP expression that it was not detectable by fluorescence microscopy, or by FACS. However, this possibility was not investigated further.

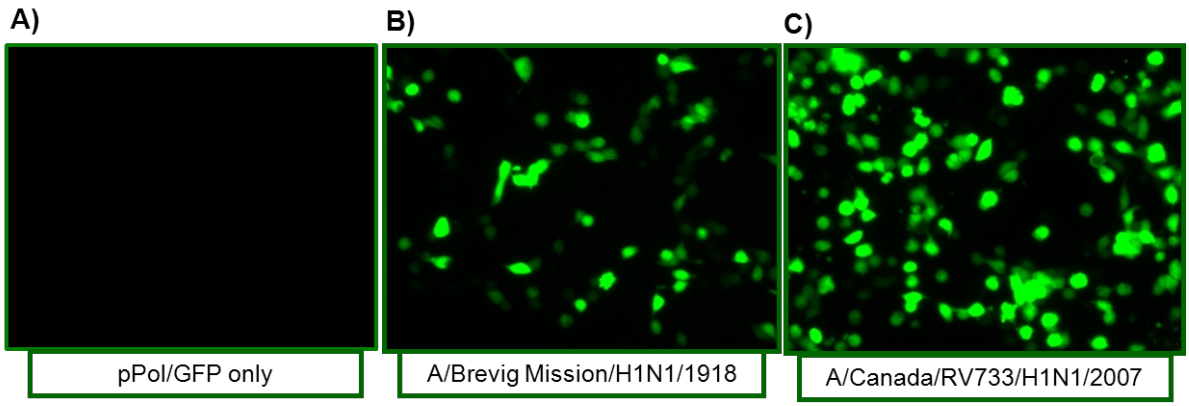

Figure 16: Fluorescence microscopy of GFP expression in 293GT cells transfected using LT1 (Mirus) transfection reagent with the RdRp and NP expression constructs (1.0µg each) and the pPol/GFP reporter construct (0.1µg) for the 1918 (B) and RV733 (C) viruses and the negative control where only the pPol/GFP reporter plasmid was transfected (0.1µg)(A). 48hrs post transfection, 20x magnification (Zeiss AxioVert 200M). Photos are representative of the outcome with 3 individual experiments, each done in triplicate.

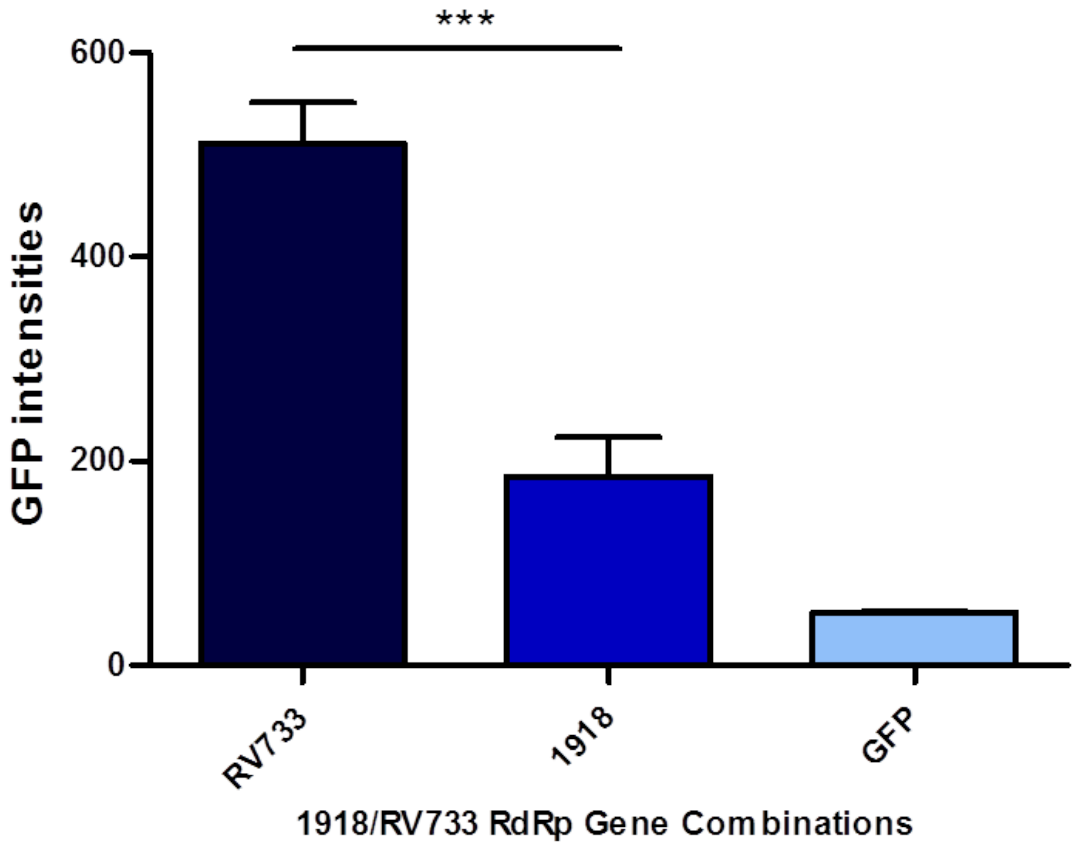

Figure 17: Optimized 1918/RV733 GFP Reporter Minigenome Assay analyzed by FACS. Total cell population was gated for GFP-positive expressing cells and relative GFP intensities were determined for the GFP positive cell population. 0.5µg of each RdRp expression plasmid for either the 1918 or RV733 genes was transfected along with 0.1µg pPol/GFP reporter plasmid into 293GT cells for 48hrs at 37°C. GFP denotes negative control containing pPol/GFP and no RdRp expression plasmids. 1918 and RV733 denote positive controls each with of the full RdRp/NP gene complement for each virus. This graph represents three independent experiments each with three biological replicates. Error bars represent the standard error of the mean of each data set. *** $p<0.0001$, unpaired student t-test, 95% confidence interval when compared to the GFP expression of the complete RV733 RdRp/NP.

To examine the contributions of each component of the RdRp/NP complex towards transcriptional activity, gene swapping experiments were conducted swapping single, then multiple gene segments for the subunits of the 1918 RdRp/NP and RV733 RdRp/NP complexes. We first investigated swapping a single 1918 RdRp/NP gene for the RV733 counterpart in the 1918 RdRp/NP genetic background followed by the swapping of a single RV733 RdRp/NP gene for the 1918 counterpart in the RV733 RdRp/NP genetic background. We then investigated swapping pairs of RdRp/NP genes to see if there are any key interactions between the subunits of the two RdRp/NP complexes under investigation here that affect the transcriptional activity of the complex as a whole.

Utilizing the GFP reporter minigenome system, gene swapping between the components of the 1918 RdRp and RV733 RdRp has revealed differences in the transcriptional activity of 1918 genes in the context of the RV733 RdRp genetic background and RV733 genes in the context of the 1918 RdRp genetic background (Figure 18).

In the context of the RV733 RdRp/NP complex, a single replacement of any gene with the 1918 counterpart revealed that the transcriptional activity was maintained to a level comparable to the complete RV733 RdRp/NP complex. Replacement of the RV733 PB1 with the 1918 PB1 or the RV733 NP with the 1918 NP maintained the full transcriptional activity of the RV733 RdRp complex. Only small decreases in transcriptional activity were observed when the RV733 PA or RV733 PB2 was replaced with the equivalent 1918 genes.

When we analyzed the single gene replacement of 1918 genes with the equivalent RV733 gene in the context of the 1918 RdRp/NP complex, dramatically different changes in transcriptional activity were observed. When the 1918 PB1 or PB2 was replaced with the equivalent RV733 genes, the 1918 RdRp transcriptional activity was severely reduced to levels comparable to the GFP negative control. However, replacing the 1918 PA gene with the RV733

PA had no effect on the activity of the 1918 RdRp/NP complex. We also observed that swapping the 1918 NP for the RV733 NP significantly increased the transcriptional activity of the 1918 RdRp nearly to the level observed for the full RV733 RdRp/NP. This result is interesting here as it suggests that the NP is a key determinant of the difference in transcriptional activity of the two RdRp complexes.

In addition to the single gene swaps in the context of each RdRp genetic background we also swapped two RdRp/NP genes at a time to assess how their interactions in pairs could affect transcriptional activity. It was observed that when pairs of RV733 genes were swapped into the 1918 RdRp, some RV733 gene pairs where able to compliment the 1918 RdRp function better than others. Swapping the 1918 PB1 and PB2 genes for the RV733 PB1 and PB2 gene abolished the transcriptional activity of the 1918 RdRp. This was similarly observed when each of those genes was swapped individually. It was also observed that the pairing of the RV733 PB1 or PB2 with any other RV733 gene resulted in the ability of these genes to function efficiently in the background of the 1918 RdRp complex. An example of this is when the RV733 PB1 is paired with the RV733 PA and the remaining genes of the 1918 RdRp complex is generated with transcriptional activity comparable to the complete RV733 RdRp/NP. However, the pairing of RV733 PB1 and NP with the remaining 1918 genes results in transcriptional activity comparable to the complete 1918 RdRp/NP. Similarly, pairing the RV733 PB2 with either the RV733 PA or NP with all other genes derived from the 1918 RdRp/NP results in high transcriptional activity comparable to the complete RV733 RdRp/NP.

The GFP reporter minigenome assay has shown that the 1918 RdRp/NP genes can complement the function of the RV733 RdRp/NP but the RV733 genes do not always compliment the 1918 RdRp/NP complex. This suggests that there are certain RdRp/NP gene combinations that are not compatible for either efficient transcriptional activity or the formation of a stable RdRp complex. However, our results have shown that the RV733 gene swaps that impair the function of the 1918RdRp/Np complex can be overcome by the addition of one other RV733 gene. This

suggests that the interactions of some of the RV733 proteins are unstable or incomplete but if another RV733 component is provided that has a more stable interaction with the 1918 components, the resulting RdRp complex will still function with the rest of the 1918 RdRp/NP complex.

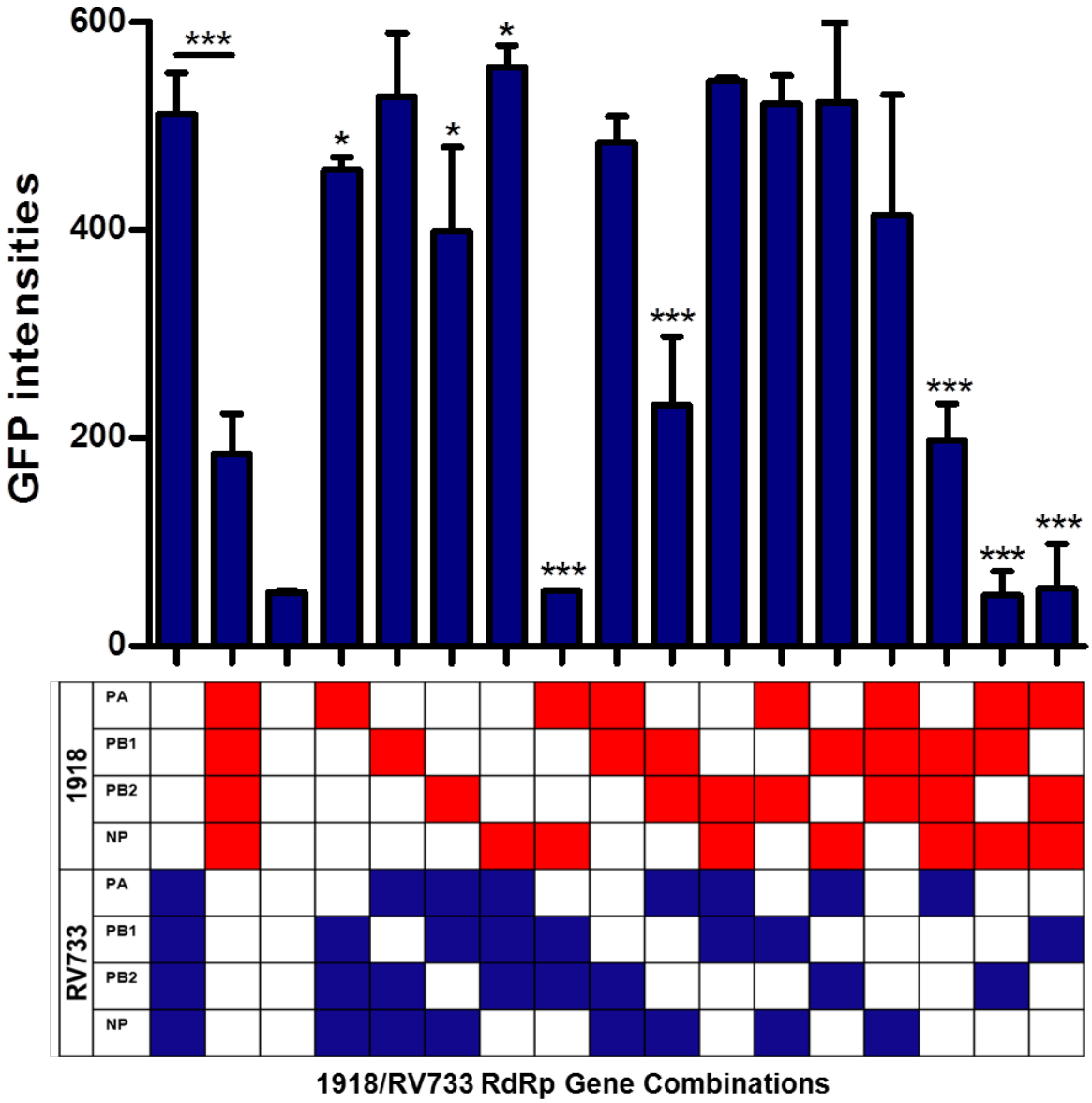

Figure 18: 1918/RV733 RdRp/NP gene combination GFP Reporter Minigenome Assay analyzed by FACS. Fourteen combinations of 1918 and RV733 RdRp/NP genes were generated and transcriptional activity was analyzed by FACS. The negative control (first column) contains pPol/GFP only and no RdRp expression plasmids. 1918 and RV733 denote positive controls (1st and 2nd column) each with the full RdRp/NP gene complement for each virus. The remaining legend represents the 1918/RV733 gene combinations present in each RdRp gene set being evaluated. 0.5µg of each RdRp expression plasmid for each the 1918 or RV733 genes was transfected along with 0.1µg pPol/GFP reporter plasmid into 293GT cells for 48hrs at 37°C. Total cell population was gated for GFP-positive expressing cells and relative GFP intensities were determined for the GFP positive cell population. This graph represents three independent experiments each with three biological replicates. Error bars represent the standard error of the mean of each data set. ***p<0.0001. * p<0.01, unpaired student t-test, 95% confidence interval. All statistical comparisons were made against the GFP expression of the complete RV733 RdRp/NP.

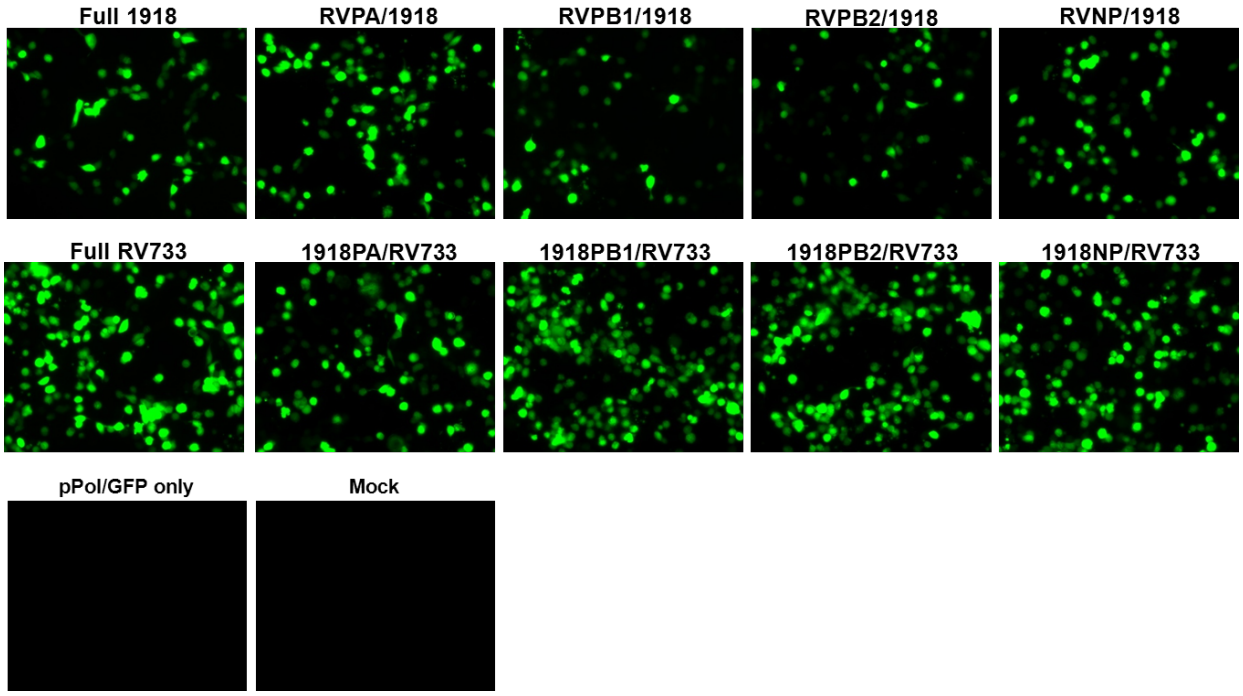

Figure 19: Fluorescent microscopy comparison of 1918/RV733 RdRp/NP gene combinations using a GFP reporter minigenome assay. Single gene swaps for each of the three RdRp genes and the NP gene were generated and their transcriptional activity was analyzed using fluorescence microscopy (Zeiss), 48hrs post transfection, 10.0µl LT1 transfection reagent (Mirus), 293GT cells, and 20x magnification.

Utilizing the expression of GFP to correlate to the transcriptional activity of the influenza RdRp complex has been a valuable and reproducible tool in this study. However, the visual analysis of GFP expression is subjective and not quantitative (Figure 19). Thus, FACS analysis was used to allow us to quantify the population of cells that were expressing GFP as well as the intensity of the GFP expression. However, the FACS protocol used here did not account for transfection efficiency or incomplete transfection. Thus we then adapted the dual-luciferase reporter minigenome system to study the transcription of the Influenza RdRp complex. The dual-luciferase reporter system utilizes a firefly luciferase as the experimental reporter and a Renilla luciferase as an internal transfection control. This allows for the normalization of experimental data to the internal control and results in greater experimental accuracy and minimizes experimental variability. The dual-luciferase reporter system also allows for rapid quantitation of luciferase expression and is becoming more widely used in the science community.

3.2 Development of a 1918/RV733 Dual Luciferase Reporter Minigenome System

3.2.1 Cloning

The pPol/FFLuc construct was generated by ligation of a PCR-amplified copy of the firefly luciferase gene into the pPol vector (Section 2.9). The same RdRp and NP expression constructs for the 1918 and RV733 viruses that were constructed for the GFP minigenome system were used with the FFLuc reporter assays. As with the GFP reporter, the FFLuc reporter was designed to produce a viral-like RNA with flanking untranslated viral gene sequences at either end of the open reading frame (ORF), derived from the RV733 influenza NS gene segment, that allow it to be recognized and transcribed as a viral gene by the RdRp (Figure 12). A pRL/Renilla firefly expression construct was also used as an internal transfection control.

3.2.2 Dual Luciferase Reporter Minigenome System

293T cells were also chosen for these minigenome studies as they are easily transfectable and are capable of efficient expression of recombinant proteins. 293T cells were co-transfected with expression plasmids of 1918 and RV733 polymerase genes and NP along with the pPol/FFLuc reporter construct and the pRL/Renilla transfection control construct (Figure 14). Each experimental data set was normalized against the expression of the Renilla luciferase to control for any variations in transfection efficiency. Luciferase expression was measured as a ratio of FireFly luciferase to Renilla luciferase in relative light units using a Veritas Microplate Luminometer. Each experimental value was first standardized by dividing the firefly luciferase signal value by the renilla luciferase internal control signal value and then normalized by subtracting the background signal value (which is also standardized). This assay was utilized in addition to the GFP reporter system as the dual luciferase reporter assay as it has a much higher sensitivity and includes a transfection control. Normalizing the activity of the experimental reporter to the activity of the internal transfection control reporter eliminates inherent assay-to-assay

variability, such as differences in the number and health of cultured cells and in the efficiencies of transfection and cell lysis, which can undermine experimental accuracy. Comparing the results of the luciferase and GFP assays will further validate the results obtained from them as well as determining the strengths and weaknesses of each assay.

We first analyzed the complete RdRp/NP for the 1918 and RV733 viruses. When we compared the activity of the 1918 RdRp/NP to that of the RV733 RdRp/NP, we found that the RdRp/NP of the 1918 virus showed reproducibly lower luciferase expression than the RdRp of the RV733 virus (Figure 20). This was consistent with what was observed using the GFP reporter minigenome assay. We then proceeded to analyze the contribution of each individual RdRp/NP gene of both 1918 and RV733 to transcriptional activity. We accomplished this by swapping each RdRp/NP gene of the 1918 virus individually with the corresponding gene of the RV733 virus. The reverse compliment of each individual gene swaps were also analyzed as well as the swapping of RdRp/NP gene pairs (Figure 21).

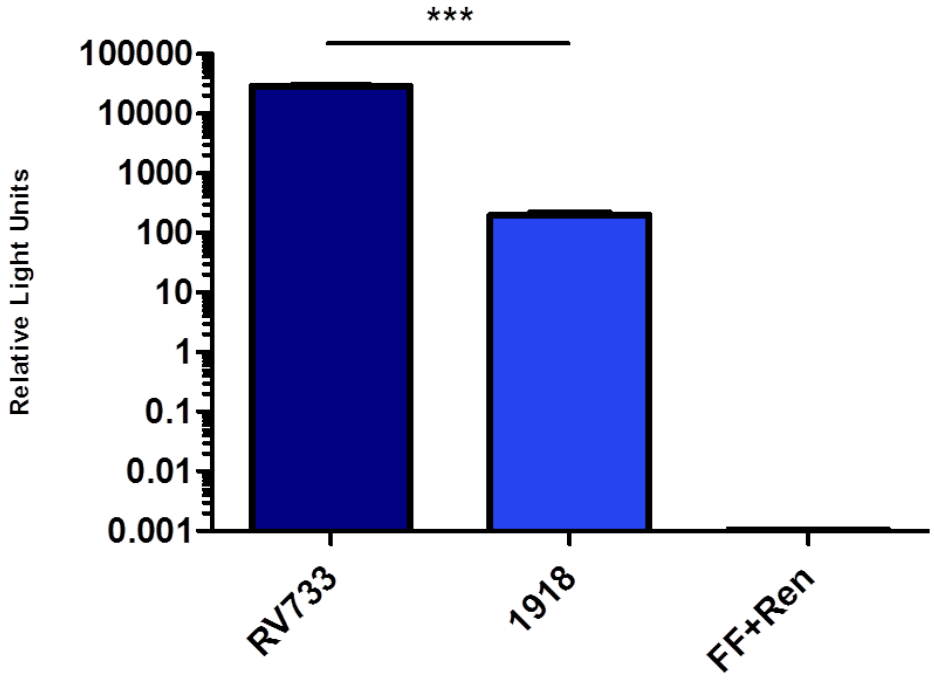

Figure 20: Optimized 1918/RV733 Dual Luciferase Reporter Minigenome Assay. 1.0μg of each RdRp expression plasmid for either the 1918 or RV733 genes, 0.025μg pPol/FFLuc and 0.01ug pRL/Renilla were transfected into 293GT cells with 10ul LT1 transfection reagent for 48hrs at 37°C. FF+Ren denotes the negative control in which only the minigenome and the internal control were transfected. 20.0ul of cell lysate at each time point was analyzed for luciferase activity according to the Dual Luciferase Reporter Assay (Promega) and luciferase expression was measured RdRp in relative light units using a Veritas Microplate Luminometer and values were normalized to a negative control. This graph represents three independent experiments each with three biological replicates and each experimental data set was normalized to the Renilla luciferase transfection control. Error bars represent the standard error of the mean. *** $p<0.0001$, unpaired student t-test, 95% confidence interval when compared to the activity of the complete RV733 RdRp/NP.

To examine the effects of swapping subunits of the RdRp/NP complex using the new Dual Luciferase Reporter assay we followed the same experimental design as was used with the GFP reporter assay. Gene swapping experiments were conducted swapping single, then multiple gene segments for the subunits of the 1918 RdRp/NP and RV733 RdRp/NP complexes and transcriptional activity resulting RdRp/NP complex was measured using the Dual Luciferase Reporter assay. We first investigated swapping a single 1918 RdRp/NP gene for the RV733 counterpart in the 1918 RdRp/NP genetic background followed by the swapping of a single RV733 RdRp/NP gene for the 1918 counterpart in the RV733 RdRp/NP genetic background. We then investigated swapping pairs of RdRp/NP genes to see if there are any key interactions

between the subunits of the two RdRp/NP complexes under investigation here that affect the transcriptional activity of the complex as a whole.

Gene swapping between the 1918 and RV733 viruses using the Dual Luciferase Reporter assay usually demonstrated very similar trends that were observed using the GFP reporter minigenome assay but with a much more dynamic range and higher sensitivity of signal detection (Figure 21). Similarly to our analysis of the GFP reporter minigenome results, gene swapping has revealed differences in the transcriptional activity of 1918 genes in the context of the RV733 RdRp genetic background and RV733 genes in the context of the 1918 RdRp genetic background.

We found that a single replacement of any one RV733 gene with the equivalent 1918 gene in the RV733 RdRp/NP appeared to have less effect on the transcriptional activity that if any single RV733 gene was swapped into the 1918 RdRp/NP. However, the minor changes in transcriptional activity that were observed in the GFP reporter minigenome system were more substantial in the dual-luciferase reporter minigenome system and in some cases appear to show a different trend in the direction (increase or decrease) of the change that occurred. In the context of the RV733 RdRp/NP, swapping the RV733 PB1 for the 1918 PB1 was the only single gene substitution that was able to maintain the transcriptional activity of the complete RV733 RdRp/NP complex. Substitution of either the RV733 PA or the RV733 PB2 for the 1918 equivalent resulted in a reduction of transcriptional activity by approximately 45% to 50%, respectively. The greatest change was observed when the RV733 NP was swapped out for the 1918 NP, resulting in nearly a 60% reduction in transcriptional activity from the complete RV733 RdRp/NP. In the context of the 1918 RdRp/NP, the replacement of the 1918 PB1 or PB2 with the RV733 equivalent yielded only minimal increases in transcriptional activity over that of the complete 1918 RdRp/NP. However, when the 1918 PA or NP was replaced with the RV733 equivalent we observed an increase in transcriptional activity over that of the complete 1918 RdRp/NP, but it was still well below the activity level of the RV733 RdRp/NP. This correlates to what was observed in the GFP

reporter minigenome and further supports our suggestion that the NP is a key determinant for the differences in transcriptional activity between the 1918 and RV733 RdRp/NP complexes.

Similarly to our analysis of the GFP reporter minigenome results, we also observed some interesting changes in transcriptional activity with the swapping of two RdRp/NP genes at a time. And consistent with the GFP reporter minigenome, it was observed that when pairs of RV733 genes were swapped into the 1918 RdRp, some RV733 gene pairs where able to complement, and in many cases augment, the 1918 RdRp function better than others in the context of these *in vitro* reporter assays. The dual-luciferase reporter minigenome revealed that swapping the 1918 PB1 and PB2 as a pair for the RV733 PB1 and PB2 maintained the low, but detectable transcriptional activity of the full 1918 RdRp/NP complex, whereas the this combination of genes showed reporter expression comparable to the negative control when utilizing the GFP reporter minigenome. Pairing of the RV733 PB2 and NP with the rest of the 1918 RdRp/NP resulted in a complex with comparable transcriptional activity to the complete RV733 RdRp/NP, which is consistent to what was observed in the GFP reporter minigenome system. Where the dual-luciferase system differs from the GFP system is when the RV733 PB1 and PA are swapped into the 1918 RdRp/NP complex. The dual-luciferase reporter minigenome revealed more than a ten-fold increase in transcriptional activity over that of the complete 1918 RdRp/NP. However the GFP reporter minigenome revealed only a 2.8-fold increase in transcriptional activity compared to that of the complete 1918 RdRp/NP. Despite the differences in the dynamic range of reporter expression that was observed in the two minigenome assays, they both reveal that the RV733 PA in combination with either the RV733 PB1 or NP can complement the other components of the 1918 RdRp/NP well enough to result in significant increases in transcriptional activity over that of the complete 1918 RdRp/NP, even reaching levels comparable to that of the RV733 RdRp/NP complex.

Overall, these results, along with the results from the GFP reporter minigenome assay, show that the 1918 RdRp/NP genes can complement the function of the RV733 RdRp/NP but the

RV733 genes do not always compliment the 1918 RdRp/NP complex. The results from the dual-luciferase reporter minigenome assay also complement the results of the GFP reporter system that suggests that there are some interactions of RV733 RdRp/NP and 1918 RdRp/NP components that suggest unstable or incomplete protein-protein interactions in the resulting polymerase complex that yield the varying levels of transcriptional activity that were observed.

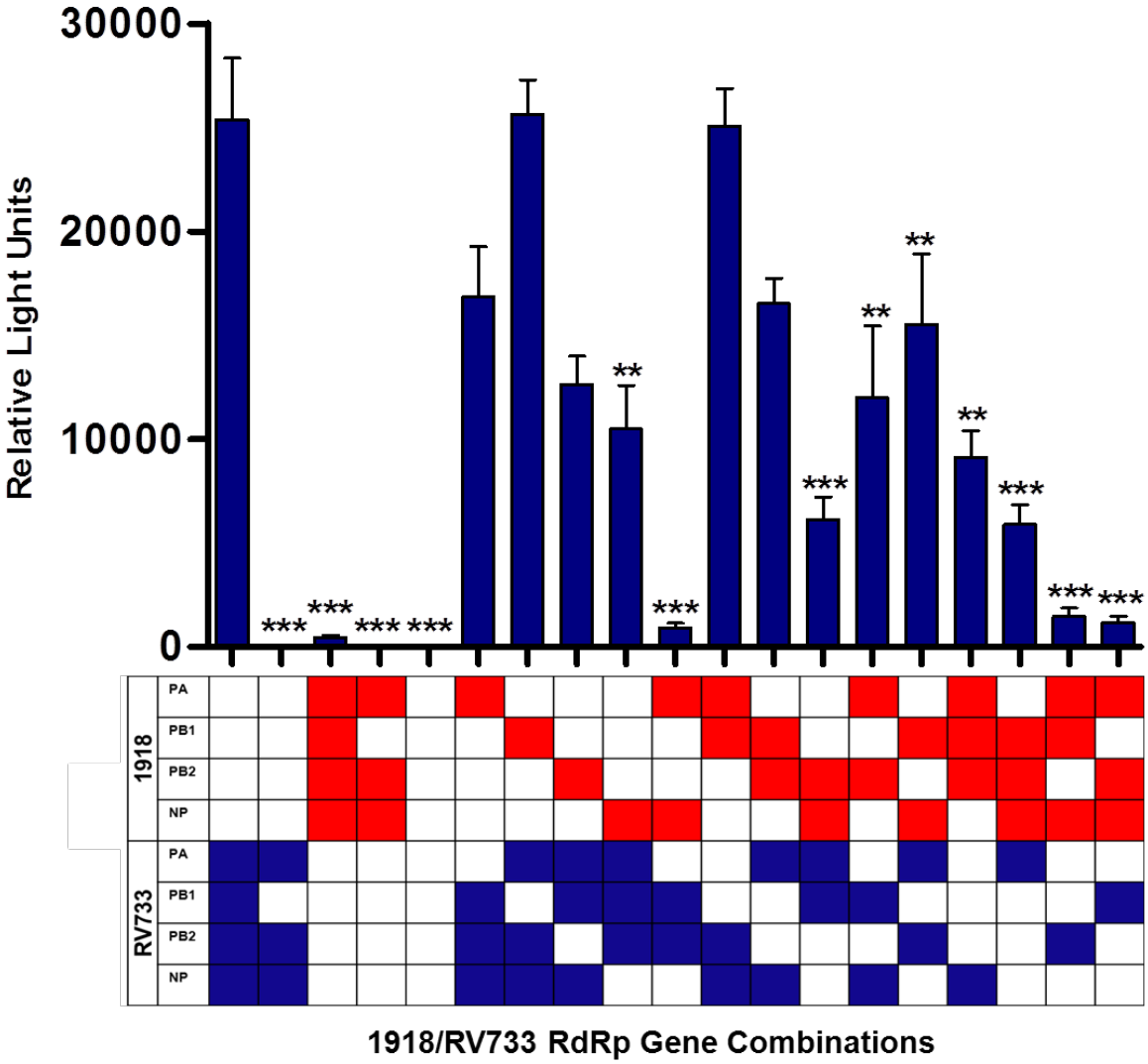

Figure 21: 1918/RV733 RdRp/NP gene combination Dual Luciferase Reporter Minigenome Assay for 14 combinations of 1918 and RV733 Influenza RdRp genes. 1918 Full and RV733 Full denote positive controls each with the full RdRp/NP gene complement for each virus followed by the 14 combinations of the 1918 and RV733 RdRp genes. The 1918 and RV733 negative denotes the full RdRp/NP gene compliment for each virus but with the exclusion of the PB1 expression plasmid. 1.0µg of each RdRp expression plasmid for either the 1918 or RV733 genes, 0.025µg pPol/FFLuc and 0.01µg pRL/Renilla were transfected into 293GT cells with 10ul LT1 transfection reagent for 48hrs at 37°C. 20.0ul of cell lysate was analyzed for luciferase activity according to the Dual Luciferase Reporter Assay (Promega) and luciferase expression was measured RdRp in relative light units using a Veritas Microplate Luminometer. This graph represents three independent experiments, each carried out in triplicate. Data was collected 48hrs post transfection and each experimental data set was normalized to the Renilla luciferase transfection control. Error bars represent the standard error of the mean. ***p<0.0001. ** p<0.001, unpaired student t-test, 95% confidence interval when compared to the activity of the complete RV733 RdRp/NP.

3.3 Viral Transcription Kinetics

To further study the properties of the transcriptional activities of the 1918 and RV733 viruses, the Dual Luciferase Reporter minigenome assay was employed for a transcription kinetics experiment. 293GT cells were transfected with the full 1918 RdRp plus the luciferase minigenome or the full RV733 RdRp plus the luciferase minigenome (Section 2.11) and cell lysates were collected at 2, 4, 6, 8, 10, 12, 16, 20, 24, 30, 36, 40, and 48hr time points. The early time points were selected because it has been reported that cRNA and mRNA are detectable by 2 hrs post infection [94], thus I hypothesized that efficient transcriptional activity would be occurring at these early time points. The time course was carried out to the 48hr time point as both the 1918 and RV733 virus reach their peak titre before this time, thus transcriptional activity should also reach a correlative peak in efficiency. A separate well was used for each time point set to minimize the disturbance of transfected cells to be collected at later time points. Luciferase expression was measured at each time point for both the 1918 and RV733 RdRp in relative light units using a Veritas Microplate Luminometer and values were normalized to a negative control (Figure 22) (Section 2.10.2).

We found that the 1918 RdRp and the RV733 RdRp share a similar transcription kinetic profile, although the absolute level of transcriptional activity at all time-points was higher for RV733 than 1918, as seen in the previous studies. Transcription products were first detected around the 8hr time point for both viruses and continue to steadily increase. The 1918 RdRp complex appeared to reach its peak transcriptional activity by 36hrs while the RV733 RdRp complex continued to increase until the experiment ended at 48hrs. The small sharp peak seen for both viruses at 4hrs could possibly be attributed to the input plasmids and their initial round of transcription to generate the RdRp complex that will transcribe the luciferase minigenome. Because there were no major differences between the transcription kinetic profile of the 1918 and RV733 viruses that would explain the differences in growth and pathogenicity properties of these

viruses, or the differences in RdRp activity in the *in vitro* reporter assays, we decided not to further investigate the transcription kinetics of the RdRp gene combinations.

/

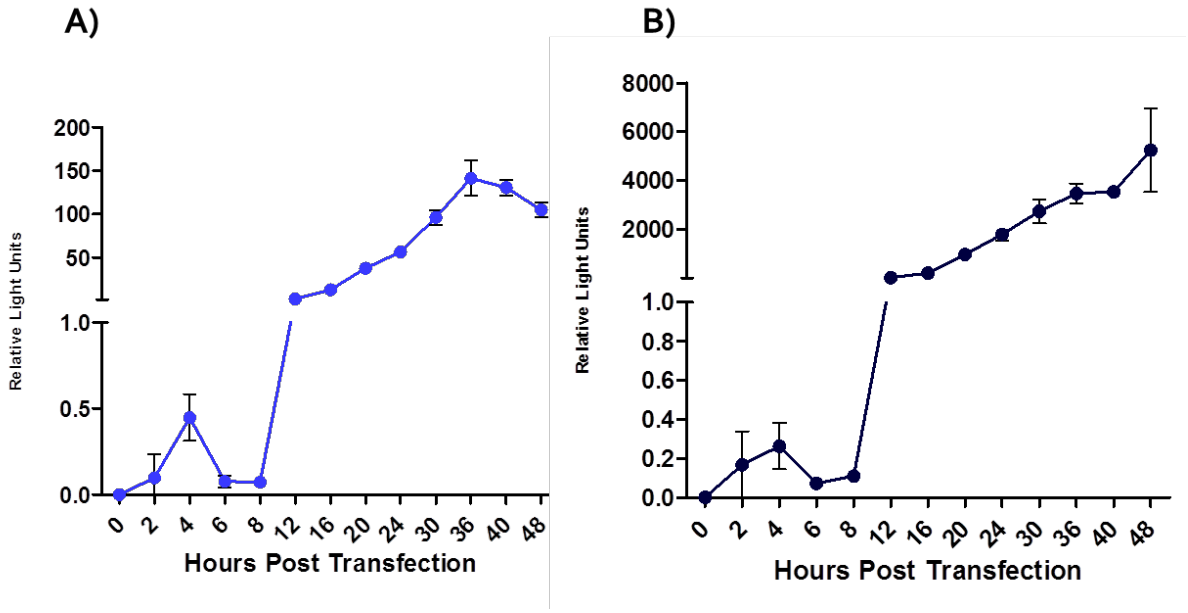

Figure 22: Time course study for the transcriptional activity of the 1918 RdRp/NP (A) and the RV733 RdRp/NP (B). 1.0ug of each expression plasmid (pCAGGS), 0.025ug pPol/FFLuc and 0.01ug pRL/Renilla were transfected into 293GT cells using 10ul LT1 transfection reagent (Mirus), incubated at 37°C and cell lysates were collected at the indicated time points. 20.0ul of cell lysate at each time point was analyzed for luciferase activity according to the Dual Luciferase Reporter Assay (Promega) and luciferase expression was measured in relative light units using a Veritas Microplate Luminometer. Experimental values were normalized to the Renilla luciferase transfection control. This graph represents three biological replicates and the error bars represent the standard error of the mean.

3.4 PB1 Chimeras

3.4.1 Cloning

To study the contribution of the key functional domains of the influenza PB1 protein to viral transcription and replication, chimeric PB1 genes were constructed between the 1918 virus and the RV733 virus. The PB1 gene was divided into six functional domains and each domain of the 1918 PB1 gene was substituted into the RV733 PB1 gene. The resulting chimeric genes were analyzed in both the 1918 RdRp/NP background and the RV733 RdRp/NP background. Each functional domain of the 1918 PB1 gene was amplified by PCR and then assembled together with the corresponding remainder of the PB1 gene from the RV733 PB1 (Figure 10). Each PB1

chimeric gene was cloned into the pCAGGS expression vector for use in both the GFP and Dual Luciferase Reporter Minigenome assays using the same molecular techniques previously outlined (Section 2.7.2). These expression constructs will then be used in minigeome studies to analyze the contribution of each function domain of PB1 to the overall transcriptional activity of the RdRp/NP complex.

3.4.2 GFP Reporter Minigenome Assay

When we transfected the PB1 chimeras, along with the remaining compliment of the RdRp/NP complex, we found that all PB1 chimeras in the RV733 background showed high levels of GFP expression comparable to that of the complete RV733 RdRp. And all PB1 chimeras in the 1918 background showed low levels of GFP expression similar to that of the complete 1918 RdRp. It was observed that PB1 chimera 1, which contains the 1918 PA binding domain, in the RV733 background had a slight decrease in GFP expression when compared to the complete RV733 RdRp. Also, the PB1 chimera 6, which contains the 1918 PB2 binding domain, in the 1918 background showed a more significant decrease in GFP expression when compared to the complete 1918 RdRp. All other PB1 chimeras in both backgrounds remained relatively unchanged from their complete RdRp counterparts as was observed by both FACS and fluorescence microscopy analysis (Figure 23 and 24).

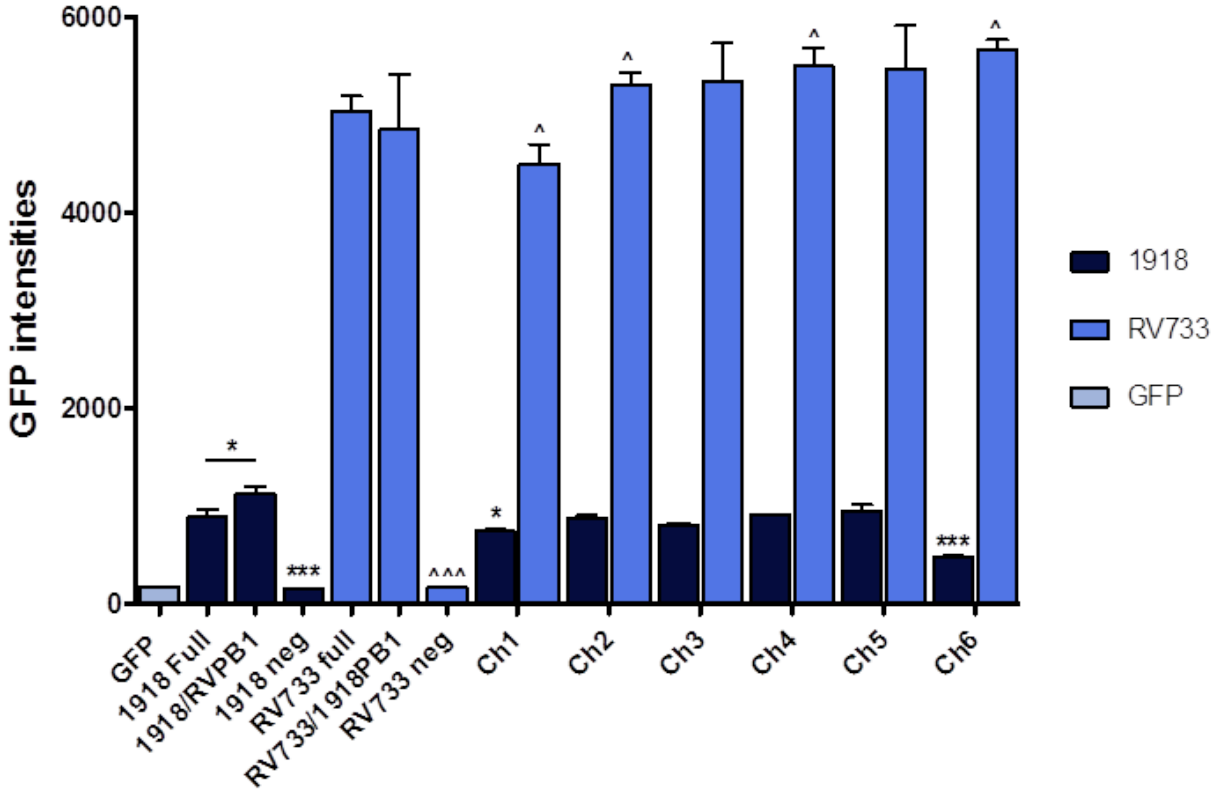

Figure 23: 1918/RV733 PB1 Chimeras in the GFP Minigenome Assay analyzed by FACS. Six chimeric PB1 proteins between the 1918 and RV733 influenza viruses were generated and their effects on RdRp transcription efficiency were analyzed using the GFP minigenome system and FACS. GFP denotes negative control containing pPol/GFP and no RdRp expression plasmids. 1918 and RV733 denote positive controls each with of the full RdRp/NP gene complement for each virus. 1918/RVPB1 denotes that the full RV733 PB1 gene was substituted into the 1918 RdRp complex and RV733/1918PB1 denotes that the full 1918 PB1 gene was substituted into the RV733 RdRp complex. The remaining legend represents each of the six chimeric PB1 genes (Ch1-Ch6) substituted into both the 1918 RdRp complex (dark blue) or the RV733 RdRp complex (light blue). 0.5µg of each RdRp expression plasmid for the 1918, RV733, or chimeric PB1 genes were transfected along with 0.1µg pPol/GFP reporter plasmid into 293GT cells for 48hrs at 37°C. Total cell population was gated for GFP-positive expressing cells and relative GFP intensities were determined for the GFP positive cell population. This graph represents three independent experiments each with three biological replicates. Error bars represent the standard error of the mean. ***p<0.0001. * p<0.01, unpaired student t-test, 95% confidence interval for comparison to the complete 1918 RdRp/NP control. ^^^p<0.0001. ^ p<0.01, unpaired student t-test, 95% confidence interval for comparison to the complete RV733 RdRp/NP control.

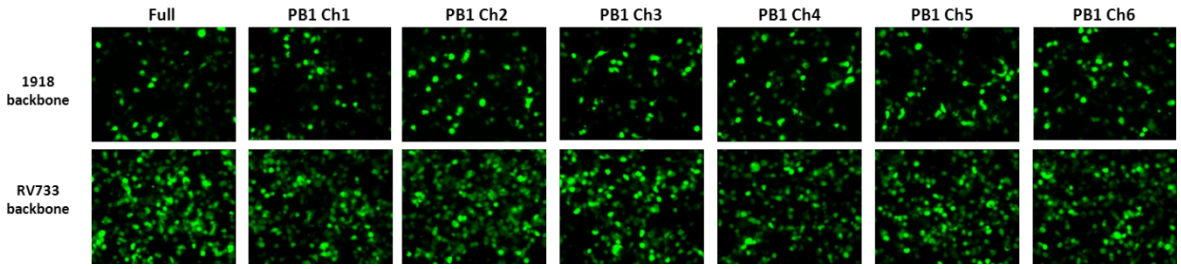

Figure 24: Comparison of six 1918/RV733 chimeric PB1 genes in either the 1918 RdRp background or the RV733 RdRp background analyzed by fluorescence microscopy. The transcriptional activity of the RdRp of both viruses with each of the PB1 chimeras was analyzed using the GFP reporter minigenome approach and analyzed by fluorescence microscopy (Zeiss). 48hrs post transfection, 10.0µl LT1 transfection reagent (Mirus), 293GT cells, 20x magnification.

3.4.3 Dual Luciferase Reporter Minigenome Assay

To further study the functional domains of the PB1 protein and transcriptional activity and validate the results of the GFP reporter assay, we again adapted the previous experiments (Section 3.4.2) to use the Dual Luciferase Reporter assay. The results obtained from the Dual Luciferase Reporter assay for analysis of the PB1 chimeras correlate with that observed in the GFP reporter assay. As a general trend, all PB1 chimeras in the 1918 background showed higher levels of luciferase expression when compared to that of the complete 1918 RdRp (Figure 25A), which is surprising considering that each chimera represents an exchange of a functionally distinct domain. However, the increases in reporter activity associated with each chimera are very modest and do not reflect a change in the general magnitude of reporter activity on a scale that distinguishes the 1918 and RV733 RdRp. Similarly in the context of the RV733 RdRp, all of the chimeras were essentially functionally equivalent to RV733 PB1 (Figure 25B), although again small differences in reporter activity were noted between the chimeras and the RV733 PB1 but these may simply be due to the compatibility between swapped domains and the rest of the protein. In no case did we observe that swapping any one domain of the PB1 significantly shifted reporter activity in a manner that would suggest that PB1 function or interaction with the other components of the RdRp were appreciably affected.

Five of the six PB1 chimeras in the RV733 background showed similar to lower levels of luciferase expression to that of the complete RV733 RdRp. PB1 chimera 1, which contains the 1918 PA binding domain yielded higher luciferase expression than the complete RV733 RdRp. However, the opposite trend was observed for the same gene combination using the GFP reporter assay. We also observed a decrease in luciferase expression with PB1 chimera 2 (Ch2), PB1 chimera 5 (Ch5) and PB1 chimera 6 (CH6) in the RV733 background when compared to the complete RV733 RdRp. These chimeric PB1 genes contained the 3' vRNA binding domain, the 5' vRNA binding domain, and the PB2 binding domain of the 1918 PB1 gene, respectively. These decreases were not observed in the GFP reporter system.

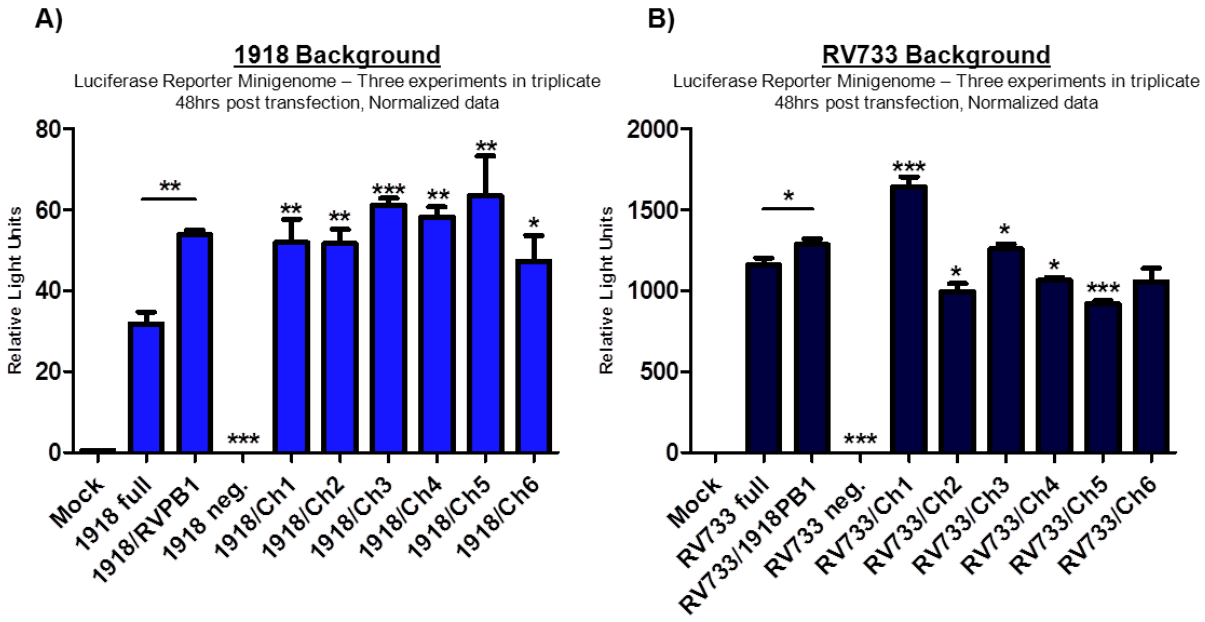

Figure 25: Analysis of the six 1918/RV733 chimeric PB1 genes in the 1918 RdRp background (A) and in the RV733 RdRp background (B) using the Dual Luciferase reporter minigenome assay. 1918 Full and RV733 Full denote positive controls each with the full RdRp/NP gene complement for each virus followed by the 14 combinations of the 1918 and RV733 RdRp genes. The 1918 and RV733 negative denotes the full RdRp/NP gene compliment for each virus but with the exclusion of the PB1 expression plasmid. 1.0µg of each RdRp expression plasmid for either the 1918 or RV733 genes, 0.025µg pPol/FFLuc and 0.01µg pRL/Renilla were transfected into 293GT cells with 10µl LT1 transfection reagent for 48hrs at 37°C. 20.0µul of cell lysate was analyzed for luciferase activity according to the Dual Luciferase Reporter Assay (Promega) and luciferase expression was measured RdRp in relative light units using a Veritas Microplate Luminometer. This graph represents three independent experiments, each carried out in triplicate. Data was collected 48hrs post transfection and each experimental data set was normalized to the Renilla luciferase transfection control. Error bars represent the standard error of the mean. ***p<0.0001. ** p<0.001, * p<0.01, unpaired student t-test, 95% confidence interval. All PB1 chimeras in the 1918 RdRp/NP background were compared to the activity of the complete 1918 RdRp/NP and all PB1 chimeras in the RV733 RdRp/NP background were compared to the activity of the complete RV733 RdRp/NP.

Both the GFP and luciferase reporter minigenome assays revealed that no single functional domain of the 1918 PB1 significantly altered the transcriptional activity of either the 1918 or RV733 RdRp/NP complex to suggest that there is one specific function region of PB1 the influences the transcriptional activity of the RdRp/NP complex as a whole. And, these results are consistent with the RdRp expression levels with the complete PB1 of either virus.

Overall, both the GFP and Luciferase reporter minigenome assays have shown that the RV733 PB1 increases the 1918 RdRp activity by nearly 2-fold compared to that of the full 1918 RdRp. This is also reflected with each of the PB1 chimeras in the 1918 background showing higher activity than the full 1918 RdRp. However, this is inconsistent from what was observed in the first GFP reporter minigenome results for the full gene swaps. That experiment showed that

the replacement of the 1918 PB1 for the RV733 PB1 in the 1918 RdRp/NP abolished transcriptional activity, while in the PB1 chimera experimental data set we observed that the RV733 PB1 in the 1918 RdRp/NP slightly increased transcriptional activity. The increase in activity was small but was consistent throughout all biological and experimental replicates. Further experiments and analysis will be required to explain these observed differences. However, we speculate that this difference might be due to the use of different plasmid preparations, as new plasmid stocks were needed to perform the PB1 chimera experiments.

3.5 1918/RV733 Recombinant Viruses

3.5.1 Virus Rescue and Titres

To further build on what we have learned from the minigenome systems we generated several 1918/RV733 recombinant viruses by swapping the genes of the RdRp complex by using reverse genetics (Section 2.12). All combinations of the 1918 and RV733 polymerase and NP genes were successfully rescued in both the 1918 and RV733 background except for the 1918 PB2 in the RV733 background (Table 8), which could not be rescued, despite several attempts. The titres of each of the 11 viruses that were successfully rescued were determined by conventional plaque assay (Section 2.13.1) and are also outlined in Table 8 below. The identity of each recombinant virus was confirmed by genetic sequencing to verify that the desired gene combinations were in fact present in each rescued virus (Section 2.13.2).

Table 8: Summary of the 1918/RV733 recombinant viruses generated by reverse genetics and their titres.

Virus	Plaque Titre* (PFU/ml)	Virus	Plaque Titre* (PFU/ml)
RV733PA/1918	$3.10x10^7$	1918PA/RV733**	$1.98x10^7$
RV733PB1/1918	$1.92x10^7$	1918PB1/RV733**	$2.45x10^7$
RV733PB2/1918	$3.75x10^6$	1918PB2/RV733**	Not rescued
RV733NP/1918	$7.95x10^6$	1918NP/RV733**	$2.55x10^7$
RV733RdRp/1918	$9.38x10^6$	1918RdRp/RV733**	$9.75x10^6$
RV733RdRp+NP/1918	$3.15x10^6$	1918RdRp+NP/RV733**	$2.42x10^7$

RV733PA/1918 denotes a virus containing the RV733 PA gene and all other genes from the 1918 virus. All recombinant viruses listed in the above table are similarly name according to their genotype.
*The titre of each virus was determined in duplicate.
**Viruses rescued with the RV733 background contained the HA of the A/USSR/90/77H1 HA as the RV733 H1 HA was not available at the time these recombinant viruses were generated.
All infectious work was performed in the biosafety containment BSL4 laboratory at NML/PHAC adhering to the strict protocols stipulated by the Health Canada Laboratory Bio-safety Guidelines.

3.5.2 1918/RV733 Recombinant Virus Replication Kinetics

To evaluate the replicative kinetics of each of the 11 1918/RV733 recombinant viruses, a time course analysis of viral replication was carried out (Figure 26). MDCK cells were infected with each of the 11 1918/RV733 recombinant viruses (Section 2.13), virus supernatants were collected at the desired time points and plaque assays were performed to determine viral titres (Section 2.13.1).

It was determined that the wild type 1918 virus reached a peak titre of $1.88x10^8$ PFU/ml by about 24 hours while the titre of the wild type RV733 also peaked at 24 hr at $4.99x10^6$ PFU/ml, 37-fold lower. When the 1918 PB1 was replaced with the RV733 PB1 in the 1918 background it was observed that this virus grew more slowly, and had nearly a log reduction in titre, when compared to the wild type 1918 virus. Conversely, when the RV733 PB1 was replaced with the 1918 PB1 in the RV733 background this virus grew more quickly than the complete RV733 virus reaching a titre of $3.9x10^7$ PFU/ml by 18hrs whereas the complete RV733 virus reached a titre of $3.47x10^6$ PFU/ml by the same time point suggesting that the 1918 PB1 conferred faster

replication kinetics on the RV733 virus. For most of the viruses, significant changes in titer were not observed after 24 hrs. However, there were some notable exceptions. The 1918NP/RV virus did continue to grow quite well past the 24hr time point, nearly increasing its titre 10-fold between 24 and 48h. This suggests that the 1918 NP gene may confer the high growth phenotype that we see with the complete 1918 virus, perhaps by increasing the virus's replicative fitness. This is also observed with the 1918RdRp+NP/RV virus, but to a lesser extent, as it too contains the 1918 NP gene along with the complete 1918 RdRp. It was also observed that the RVPB2/1918 virus titres decreased after the 24hr time point by half a log. This could be due to some instability within the RdRp complex due to the incompatibility of the RV733 PB2 protein with the rest of the 1918 subunits. Interestingly, this could reflect a general lack of compatibility between the PB2 proteins of each virus with the others RdRp complex as we could not rescue the virus containing the RV733 PB2 in the 1918 genetic background. There may be other factors involved here as well, and this could be an interesting point for further investigation. A decrease in viral titre after the 24hr time point was also observed for the RVRdRp/1918 and RVRdRp+NP/1918 viruses and this result could be linked to the fact that they also contain the RV733 PB2. However, in these recombinant viruses the RV733 PB2 is interacting with the other RdRp components from RV733 with which it apparently functions well in the RV733 virus, so this speculation would need to be confirmed by further investigation.

This growth kinetic experiment was only done once, in duplicate wells, and viral titres were determined for each virus, at each time point in duplicate. To determine the statistical significance for the changes and trends observed here, this experiment will need to be repeated and multiple replicates analyzed. Also, only the single gene swaps were analyzed. It will be both interesting and useful to perform this experiment with all of the 1918/RV733 RdRp+NP gene combinations to best interpret the trends that we already see and to solidify the determinants of transcriptional and replicative efficiency differences between the two RdRp complexes.

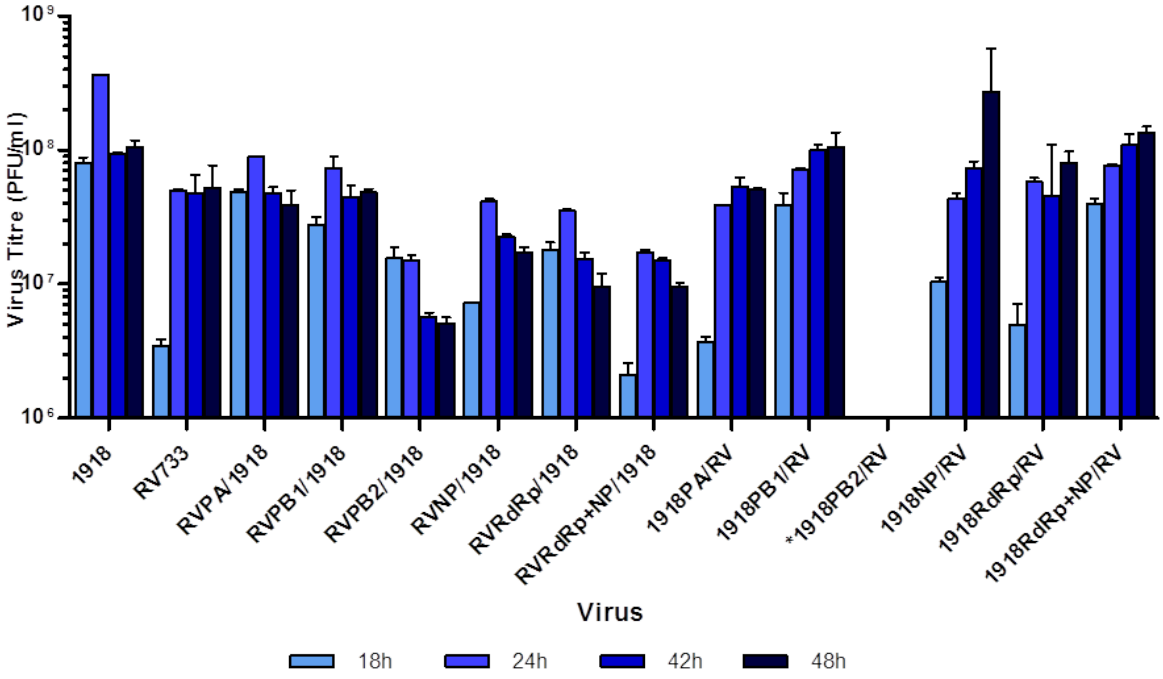

Figure 26: 1918/RV733 RdRp/NP Recombinant Viruses growth kinetics. MDCK cells were infected with each of the 11 1918/RV733 recombinant viruses at an MOI of 0.001, supernatants were collected at 18, 24, 42, and 48hrs post infection and viral titres were determined by plaque assay for each time point. Titres for each virus at each time point were collected and determined in duplicate. **We were not able to rescue the 1918PB2/RV virus, thus there is no virus titre data.* Error bars represent the standard error of the mean. All infectious work was performed in the biosafety containment BSL4 laboratory at NML/PHAC adhering to the strict protocols stipulated by the Health Canada Laboratory Bio-safety Guidelines.

3.6 Mouse Study

To study the virulence of each of the 1918/RV733 recombinant viruses generated by reverse genetics in this study, groups of 3 mice were infected at either a high dose (10^5 PFU/mouse) or a low dose (10^4 PFU/mouse) of each virus (Section 2.15). Mice were monitored for 18 days post-infection for signs of disease, which include ruffled fur, hunched posture, hind limb paralysis, labored breathing and weight loss. Sacrifices were performed prior to death due to illness when the mice reached a score based on severity of clinical signs indicating that they would not recover from the infection. All animal work was performed in the BSL4 containment laboratory at NML/PHAC adhering to the strict protocols stipulated by the Health Canada Laboratory Bio-safety Guidelines and all procedures were approved by the Institutional Animal Care Committee according to guidelines provided by the Canadian Council on Animal Care.

It was observed that the 1918 virus was 100% lethal by 6 days post infection at 10^5 PFU and by 7 to 12 days post infection at 10^4 PFU, while the RV733 was non-pathogenic in the mouse model. All viruses in the RV733 background were non-pathogenic regardless of which 1918 RdRp/NP gene(s) were exchanged for the RV733 polymerase or NP gene counterparts. None of the mice infected with these viruses exhibited clinical signs of disease that were more pronounced than those infected with the wild-type RV733 virus. On the other hand, all of the recombinant viruses in the 1918 background were pathogenic in mice (Table 9), although in this case the severity of disease was dependent on the identity of the RV733 gene(s) that it contained.

It has been previously reported that PB1 is a major determinant for the high pathogenicity phenotype associated with the 1918 influenza A virus [69,78]. However, our results were not consistent with their findings. Replacement of the 1918 PB1 with the RV733 PB1 in the 1918 background yielded a virus that was only slightly less virulent than the wild type 1918 virus. Mice infected with this virus succumbed to disease by day 12-14 at the low dose (10^4PFU/mouse) and by day 7-8 at the high dose (10^5PFU/mouse). The replicative efficiency of this virus was also reduced, as observed in our growth kinetics experiment (Figure 26). Conversely, when the 1918 PB1 was introduced into the RV733 background, the resulting virus grew much faster and to higher tires than the complete RV733 (Figure 26), but this did not correlate to an increase pathogenicity (Table 9). Based on our findings, we suggest that the 1918 PB1 is only a minor determinant of pathogenicity. However, we would also suggest that this finding must be context dependent in that the RV733 PB1 is apparently able to better substitute for the 1918 PB1 than the PB1 proteins of the viruses that were selected for the other studies.

The recombinant virus RVNP/1918 showed a greater decrease in pathogenicity than RVPB1/1918, with mice infected at the high dose dying at days 7, 8, and 17 and survival of all mice infected at the low dose, albeit with significant morbidity. This suggests that the 1918 NP

may have a role in the high growth and pathogenicity phenotypes of the 1918 virus. It was observed that replacing the 1918 RdRp with the RV733 RdRp (virus RVRdRp/1918) resulted in comparable pathogenicity to the wild-type 1918 virus, while additionally replacing the 1918 NP in the RVRdRpNP/1918 virus dramatically attenuated the virus. This demonstrates a role for the 1918 NP in pathogenicity. This role for the 1918 NP in the high growth and pathogenicity phenotype that is seen in mice is further supported by the results of the viral growth kinetic experiment where we saw a steady increase in viral titres above that of the complete RV733 virus when the 1918 NP was present. Perhaps the RV733 NP gene is missing a key element or functional domain that is present in the 1918 NP gene that allows the virus to replicate more efficiently over a longer period of time. Again, this result apparently depends on the virus that is being used as the low pathogenicity strain for comparison with the 1918 virus. In the previously published studies a role for NP in 1918 virus pathogenicity was not identified, as the NP proteins of those virus strains were able to efficiently complement the function of the 1918 virus NP in the recombinant viruses that were studied [69].

We also observed that the RVRdRp/1918 virus was comparable in pathogenicity to the wildtype 1918 virus, with mice dying at day 6 post infection at the high dose (10^5 PFU/mouse) and 3-6 day later at the low dose (10^4 PFU/mouse). This suggests that the RV733 RdRp can be an effective substitute for the 1918 RdRp with respect to pathogenicity. However, when the 1918 RdRp and NP are all replaced with the equivalent RV733 components, the resulting virus becomes partially attenuated as only one mouse died on day eight at the high dose (10^5 PFU/mouse). This further supports our above statements that suggest that the 1918 NP is a key factor for pathogenicity. Taken all together, we suggest that the NP gene has a major role in the efficient replication and high pathogenicity of the 1918 virus but that the complete 1918 RdRp/NP complex is necessary for the full pathogenicity of the 1918 virus.

Table 9: Summary of weight loss and survival of mice infected with 1918/RV733 recombinant viruses.

Virus	Low Dose (10^4)		High Dose (10^5)	
	Weight loss	Survival (Time to death)	Weight loss	Survival (Time to Death)
1918 Full*	~30%	0/3 Day 7, 12, 16	~30%	0/3 Day 6, 7, 9
RVPA/1918	~30%	0/3 Day 9 and 10	~15%	0/3 Day 6
RVPB1/1918	~30%	1/3 Day 12 and 14	~30%	0/3 Day 7 and 8
RVPB2/1918	~30%	0/3 Day 8 and 9	~20-25%	0/3 Day 5 and 6
RVNP/1918	~20%	3/3	~30%	0/3 Day 7, 8, 17
RVRdRp/1918	~30%	0/3 Day 9 and 11	~15%	0/3 Day 6
RVRdRpNP/1918	~5-10%	3/3	~25%	2/3 Day 8
RV733 Full*	none	3/3	none	3/3
1918PA/RV**	none	3/3	none	3/3
1918PB1/RV**	none	3/3	none	3/3
1918NP/RV**	none	3/3	none	3/3
1918RdRp/RV**	none	3/3	none	3/3
1918RdRpNP/RV**	none	3/3	none	3/3

RVPA/1918 denotes a virus containing the RV733 PA gene and all other genes from the 1918 virus. All recombinant viruses listed in the above table are similarly name according to their genotype.

* These viruses were not infected in parallel with the 1918/RV733 Recombinant viruses. Historical data.

Groups of 3 mice were infected with one of each of the 11 1918/RV733 recombinant viruses at either a high dose (10^5 PFU/mouse) or a low dose (10^4 PFU/mouse) and monitored for 18 days for signs of disease and weight loss (Figure 27 and 28).

All infectious work was performed in the biosafety containment BSL4 laboratory at NML/PHAC adhering to the strict protocols stipulated by the Health Canada Laboratory Bio-safety Guidelines.

**Viruses rescued with the RV733 background contained the HA of the A/USSR/90/77H1 HA as the RV733 H1 HA was not available at the time these recombinant viruses were generated.

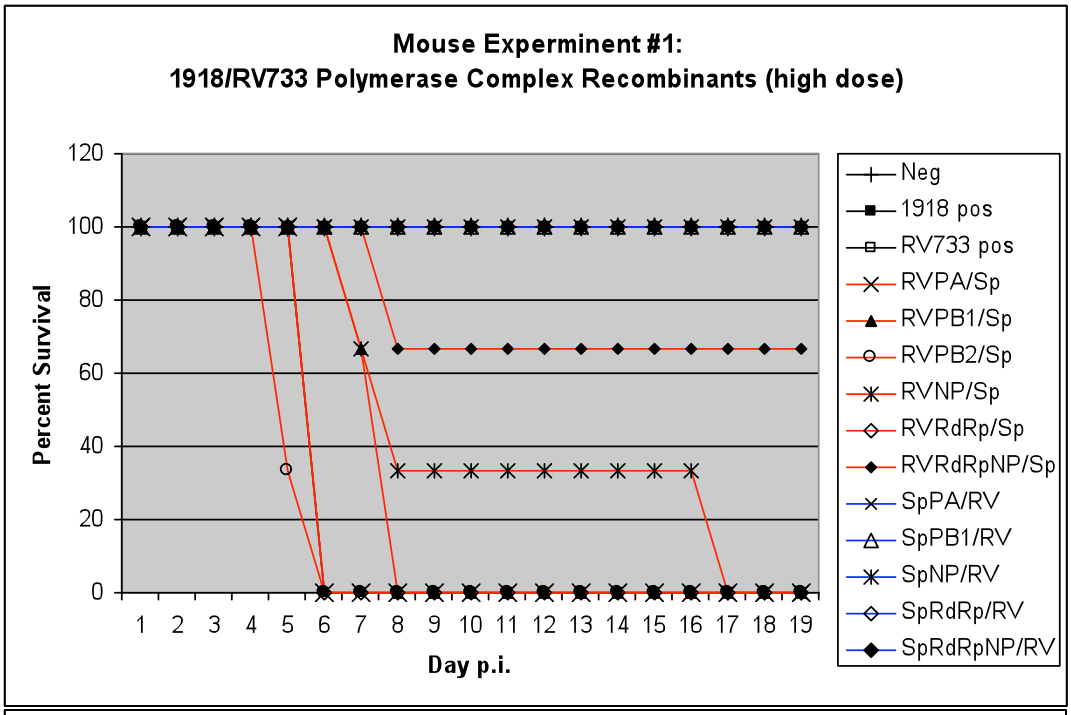

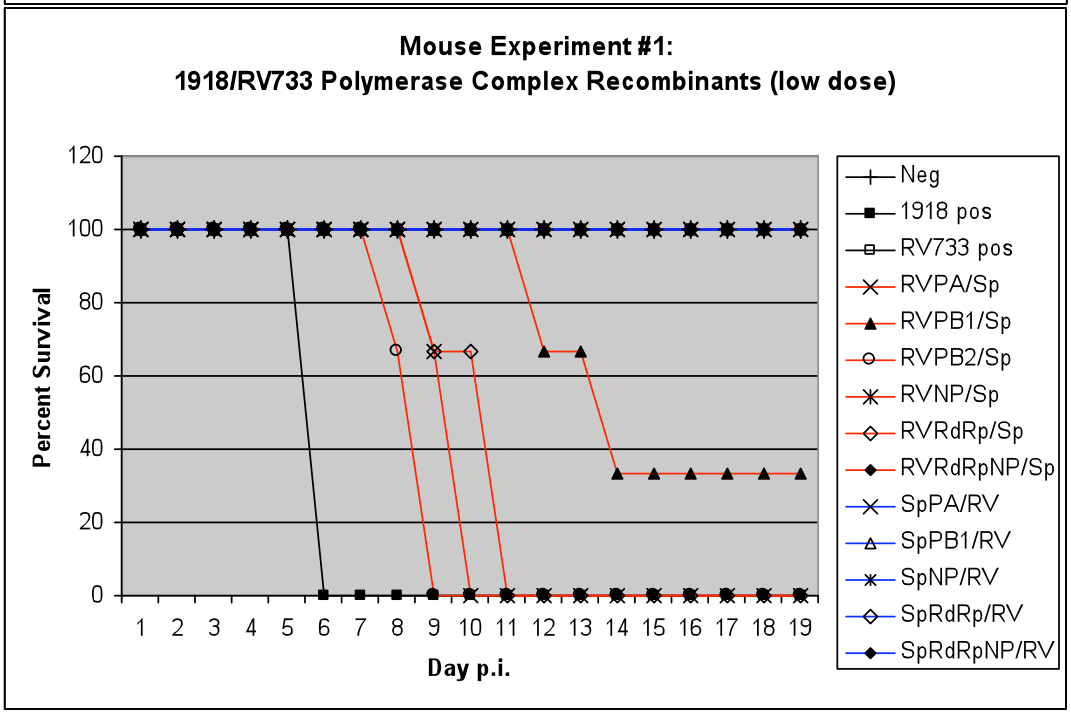

Figure 27: Survival curve for mice infected with 1918/RV733 recombinant viruses generated by reverse genetics at either a high dose (10^5 PFU/mouse) or a low dose (10^4 PFU/mouse). Groups of 3 mice were infected by intranasal instillation of virus in 50.0µl MEM/0.1%BSA with one of each of the 11 1918/RV733 recombinant viruses and monitored for 18 days for signs of disease and weight loss. All infectious work was performed in the biosafety containment BSL4 laboratory at NML/PHAC adhering to the strict protocols stipulated by the Health Canada Laboratory Bio-safety Guidelines.

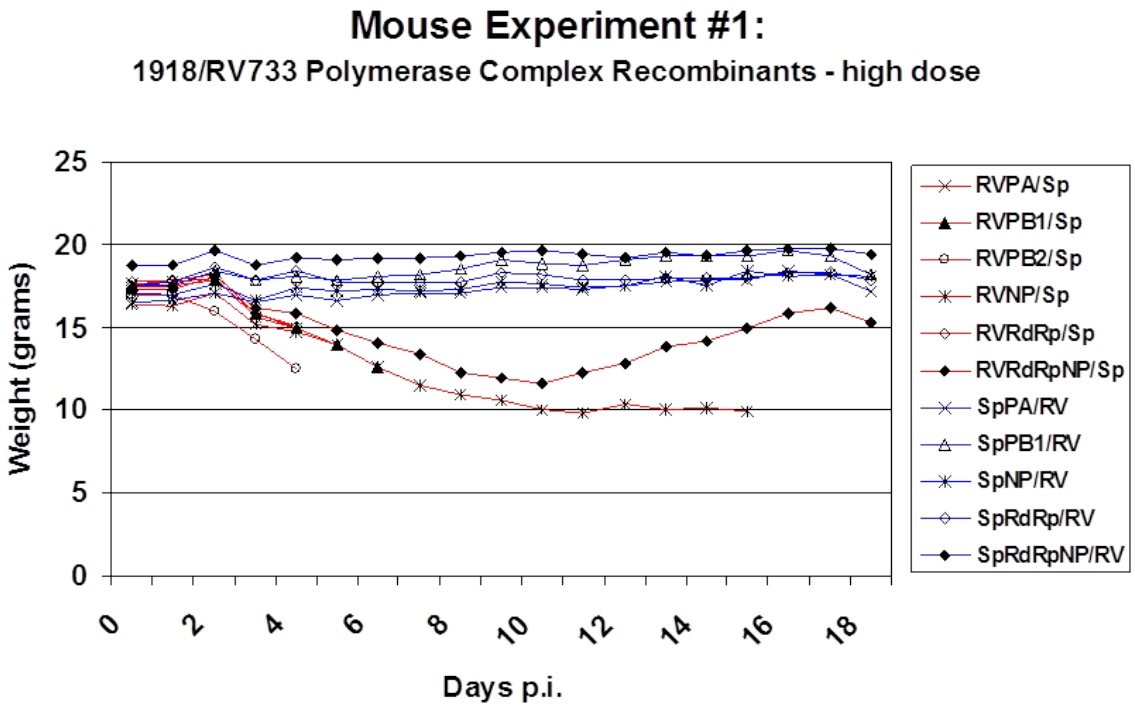

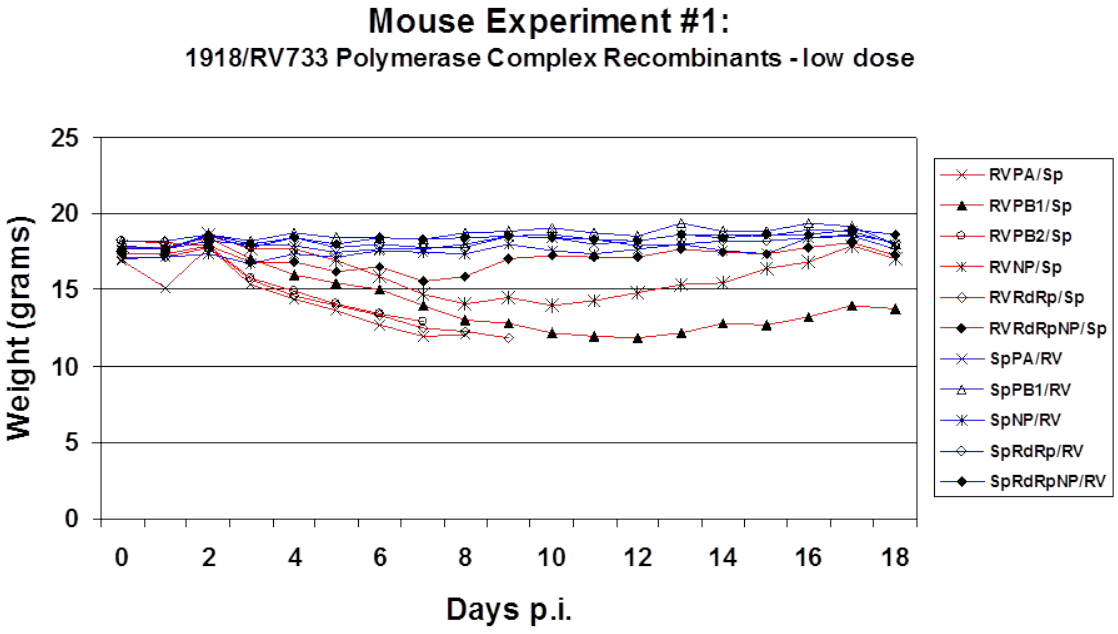

Figure 28: Weight loss curves for mice infected with 1918/RV733 recombinant viruses generated by reverse genetics at either a high dose (10^5 PFU/mouse) or a low dose (10^4 PFU/mouse). Groups of 3 mice were infected by intranasal instillation of virus in 50.0µl MEM/0.1%BSA with one of each of the 11 1918/RV733 recombinant viruses and monitored for 18 days for signs of disease and weight loss. All infectious work was performed in the biosafety containment BSL4 laboratory at NML/PHAC adhering to the strict protocols stipulated by the Health Canada Laboratory Bio-safety Guidelines.

4.0 Discussion

4.1 Experimental Rationale

The H1N1 subtype virus that caused the 1918 “Spanish Flu” pandemic was the focus of this study as nearly 50 million people died, with 500 million people being infected [81], making it one of the deadliest natural disasters in human history [6]. What made this pandemic virus unique is that most victims were healthy young adults, in contrast to most influenza outbreaks, which predominantly affect juvenile, elderly, or weakened patients. Understanding what makes these pandemic viruses different from other circulating and seasonal Influenza virus strains can help us better understand when and where they may emerge in a human population and how we can combat them with specific and effective antiviral therapies.

The influenza virus RNA-dependant RNA polymerase (RdRp) is responsible for viral RNA transcription and replication in the nucleus of infected cells. The efficiency of viral RNA synthesis, which is critical for virus replication and pathogenicity, is dependent on the assembly of the RdRp protein subunits (PA, PB1, and PB2) and the efficiency of their transcriptional activity [58,59,60]. The PB1 protein is the best characterized functionally of all the influenza polymerase subunits and contains the S-D-D amino acid motif that forms the core of the catalytic active site for polymerase activity [59,71].

The 1918 virus replicates more rapidly and to higher titer than most other influenza viruses suggesting higher transcriptional activity and several studies have also implicated the PB1 protein as a key virulence factor for this virus [69,78]. Interestingly, the 1918 PB1 gene differs from the conserved avian influenza consensus sequence by only seven amino acids [79]. It has been shown that, in a minireplicon system, the avian virus PB1 gene can support high transcriptional and replicative activity better than conventional human virus PB1 genes [155]. Thus, it has been speculated that the high similarity of the 1918 virus PB1 gene to many of the PB1 genes of avian

origin may provide an explanation for the higher transcriptional activity of the RdRp and greater virus replication that is seen in the 1918 influenza virus over some other human H1N1 viruses [69,155].

The aim of this study was too investigate the transcription and replicative properties of the 1918 RNA-dependent RNA polymerase complex by comparing it to the RdRp complex of a low virulence conventional H1N1 human virus isolate, A/Canada/RV733/2007 (RV733) beginning with a minigenome approach to study the transcriptional activity of the RdRp/NP complexes. In addition, we also generated recombinant influenza viruses by reverse genetics to study growth kinetics in vitro and pathogenesis using a mouse model to provide context for what we observed in the minigenome assays. In doing this, we hoped to identify key elements of the 1918 RdRp complex that could explain the unique growth properties and pathogenicity associated with this virus. We focused our study on the PB1 gene as it has been identified as a key virulence factor as well as play a major role in the transcriptional and replicative properties of the 1918 virus.

4.2 Transcriptional Properties of the 1918 and RV733 RNA-Dependent RNA Polymerase Complexes

The 1918 influenza virus has been previously reported to have higher replicative, and by extension, higher transcriptional capabilities over many conventional H1N1 viruses [69]. However, the results that we have presented here regarding the transcriptional activity of the 1918 RdRp/NP complex are inconsistent with previous studies. Our minigenome studies revealed that the 1918 RdRp complex had consistently lower transcriptional activity than the contemporary RV733 virus. This was observed in both the GFP reporter and dual-luciferase reporter minigenome systems (Figure 17 and 20). All reporter expression was quantified in three independent experiments, each with three technical replicates. Therefore, we are confident that the results obtained by each reporter assay are accurate.

The expression of GFP to correlate to the transcriptional activity of the influenza RdRp complex has been a valuable and reliable tool in this study. However, the visual analysis of GFP expression is subjective and not quantitative. Thus, FACS analysis was used to allow us to quantify the population of cells that were expressing GFP as well as the intensity of the GFP expression. We utilized the associated FACS software (High-performance FACSdiva) to focus our analysis on the population of cells that was determined to be GFP positive when compared to a GFP negative control as well as a negative transfection control. The efficiency of transfection is a major variable in this study since we are attempting to transfect multiple plasmids into cells at once. However, the use of the GFP system was quite labor-intensive, as it required the separate preparation and analysis by FACS of cells for each transfection reaction and a reliable; more high-throughput methodology was needed.

So we then adapted the Dual-Luciferase Reporter minigenome system to study the transcription of the Influenza RdRp complex. The Dual-Luciferase Reporter system utilizes a Fire Fly luciferase as the experimental reporter and a Renilla luciferase as an internal transfection control. This allows for the normalization of experimental data to the internal control and results in greater experimental accuracy by directly compensating for transfection efficiency as opposed to the very time consuming FACS analysis of each sample that was required for the GFP-based assay. The Dual-Luciferase reporter system also has a great dynamic range of signal detection and can be used in either cell culture based or cell-free applications in rapid quantitation of luciferase expression. For these reasons we chose to base the majority of our analysis on our findings using this assay.

For the most part, it was found that the GFP and Luciferase based systems generated comparable results for most of the gene combinations that were examined. In some cases it was observed that the magnitude of differences in reporter readout between different gene combinations was greater with the luciferase system, but this might be attributed to the greater sensitivity and wider dynamic range with the luciferase system over the GFP system. However,

for some of the gene combinations that were examined, we found significant differences in reporter expression between the GFP reporter minigenome system and the dual-luciferase reporter minigenome systems including some gene combinations that differed in the direction (i.e. greater versus less) of their magnitude of expression compared to the controls. It was not determined whether this difference in reporter expression between the two reporter assays was a function of true differences in transcriptional activity between the two reporter systems or due to some other intrinsic or technical factor. Each minigenome reporter assay was optimized individually to obtain optimal reporter expression with the lowest background signal. The ratio of each expression plasmid was kept at 1:1 for both minigenome systems. Each cell requires one copy of each RdRp/NP expression plasmid and one copy of the minigenome reporter plasmid for expression to occur. It is possible that this ratio may have not been ideal for both systems or for both viruses. Multiple biological and technical replicates were performed to confirm the results seen with each minigenome reporter system, but we cannot yet definitely rule out the possibility that the different results obtained are due to human error, although this does not appear likely as the data obtained showed reasonable and low variability between data sets. More work is needed to understand the basis of the differences between the two systems so we can more accurately understand the role of the PB1 subunit and its functional domains, and how it functions with the rest of the RdRp complex. However it should also be noted that understanding these differences and the mechanisms behind them might cause us to interpret the data we have collected here differently.

Gene swapping between the 1918 and RV733 viruses using the dual-luciferase reporter assay demonstrated very similar trends also observed using the GFP reporter minigenome assay but with a much more dynamic range and higher sensitivity of signal detection (Figure 21). The data was analyzed to show differences in the transcriptional activity of 1918 proteins in the context of the RV733 RdRp genetic background and RV733 proteins in the context of the 1918 RdRp genetic background. The replacement of any single gene in the RV733 RdRp/NP with the 1918 counterpart revealed that only the replacement of the RV733 PB1 gene with the 1918 PB1

counterpart was able to maintain the full activity of the RV733 RdRp/NP complex. Substitutions with the PA, PB2, and NP genes each showed decrease in transcriptional activity from the complete RV733 RdRp/NP of 45, 50, and 60% respectively (Figure 21). But even with these observed reductions in activity, these recombinant RdRp/NP complexes still maintain transcriptional activity well above the complete 1918 RdRp/NP complex (Figure 21). This result shows that the 1918 PB1 is capable of supporting high transcriptional activity, which is consistent with previous studies [69,79] despite the fact that our minigenome results indicate that the 1918 RdRp/NP has low transcriptional activity.

When we analyzed the single gene replacement of 1918 genes with the equivalent RV733 genes in the context of the 1918 RdRp/NP complex, dramatically different changes in transcriptional activity were observed. Each individual RV733 RdRp/NP gene was able to increase the activity of the 1918 RdRp/NP at least 2-fold over that of the complete 1918 RdRp/NP. The most interesting observation occurred when the 1918 NP was exchanged for the RV733 NP resulting in a 20-fold increase in transcriptional activity of the 1918 RdRp over that of the full 1918 RdRp/NP (Figure 21), suggesting that the NP is a key determinant of the difference in transcriptional activity of the 1918 and RV733 RdRp complexes. The RV733 PA also increased the activity of the 1918 RdRp/NP, although the increase in activity was not quite as great (13-fold increase) (Figure 21). Together these results suggest that the RV733 NP and PA can compensate for the functional deficit in the 1918 RdRp/NP that causes the very low transcriptional activity readouts in the *in vitro* reporter assays.

We also observed some interesting changes in transcriptional activity when swapping two RdRp/NP genes at a time using the dual-luciferase reporter assay. When pairs of RV733 genes were swapped into the 1918 RdRp, some RV733 gene pairs where able to complement the 1918 RdRp function better than others. The dual-luciferase reporter minigenome revealed that RV733 PB1 and PB2 in the 1918 RdRp/NP complex was able to increase the activity of the 1918

RdRp/NP slightly, but it was still well below the level of the RV733 RdRp/NP complex. However, the pairing of the RV733 PB2 and NP in the 1918 RdRp/NP resulted in a complex with comparable transcriptional activity to the complete RV733 RdRp/NP. The RV733 PB1/PA pair in the 1918 RdRp/NP complex revealed more than a ten-fold increase in transcriptional activity over that of the complete 1918 RdRp/NP. The RV733 PA and NP pair in the 1918 RdRp/NP also revealed a significant increase in activity approaching expression levels comparable to the RV733 RdRp/NP.

Our minigenome studies have given us several interesting results to explore further. We see that the RV733 PB1 and PB2, either individually or as pair are not able to significantly affect the activity of the 1918 RdRp/NP complex. This suggests that there is some unique difference between the 1918 PB1 protein and the RV733 protein that allows the 1918 PB1 to complement the RV733 RdRp/NP activity whereas the RV733 PB1 does not complement the 1918 RdRp/NP as effectively. Both the RV733 NP and PA proteins were able to significantly affect the activity of the 1918 RdRp/NP individually, but as a pair they showed an even greater increase in transcriptional activity (Figure 21). This suggests that the RV733 PA and NP can effectively compliment the other components of the 1918 RdRp/NP for efficient transcriptional activity. Our minigenome assay has also shown that the RV733 PA in combination with either the RV733 PB1 or NP can complement the other components of the 1918 RdRp/NP well enough to result in significant increases in transcriptional activity over that of the complete 1918 RdRp/NP, even reaching levels comparable to that of the RV733 RdRp/NP complex. Replacement of these 1918 RdRp components with the equivalent RV733 components seem to be able to compensate for some unknown difference between the 1918 RdRp proteins and the RV733 RdRp proteins that yield the low transcriptional activity we have observed with the complete 1918 RdRp complex. These differences between the RdRp proteins of the 1918 and RV733 viruses will be of interest to further characterize so as to better understand the specific transcriptional activity dynamics of each RdRp complex.

Despite the differences in the dynamic range of reporter expression that was observed in the two minigenome assays they both reveal the same general trends for the various RdRp/NP gene combinations. Both reporter minigenome assays have shown that the RV733 RdRp/NP proteins can complement the function of the 1918 RdRp/NP quite effectively but the 1918 genes are not always able to support the full activity of the native RV733 RdRp/NP complex. It is possible that when mixing genes from the two viruses, there are certain RdRp/NP gene combinations that are less compatible for either efficient transcriptional activity or the formation of a stable RdRp complex. Based on this idea, we could speculate that some of the interactions between the 1918 and RV733 proteins are less stable or not as complementary to function as in the native complex but if another component is provided, a more stable interaction with the remaining RV733 or 1918 components can occur and the resulting RdRp complex may function more efficiently. But, another explanation for the observed results is simply that the full RV733 RdRp/NP has very high transcriptional activity in these *in vitro* assays and when certain proteins from the 1918 RdRp/NP are substituted into the RV733 complex, the result is a complex with less activity according the function of 1918 proteins. In this explanation, it is not that the 1918 proteins are unable to function well in the RV733 complex, but rather that they have the intrinsic property of less transcriptional activity that they now confer on the RV733 complex. The distinction between the two possibilities mentioned is an interesting point for further investigation and may contribute to our understanding of the apparent very low transcriptional activity of the 1918 RdRp/NP despite the very high growth properties of the 1918 virus that we saw in the viral replication kinetics experiment.

4.3 1918/RV733 Chimeric PB1 Genes

Since previous research had identified the PB1 gene as a major contributor to the high replicative properties of the 1918 virus [69,78] we decided to look more closely at the 1918 PB1 gene and its involvement in influenza transcription and to identify the regions or molecular determinants of the protein that contributed to its role in 1918 virus pathogenesis. This portion of this project was initiated early; before we determined that PB1 was, in fact, only a minor contributor to 1918 virus pathogenesis when contrasted to the RV733 virus. However, given the significant role that had previously been demonstrated for the 1918 PB1 in viral pathogenesis, we decided to continue this part of the project as it would provide data to contrast the previously published data on PB1 and might provide some understanding for this differential role of PB1, that apparently depended on the low pathogenicity virus used for comparison to the 1918 virus. To do this we generated chimeric PB1 genes between the 1918 PB1 gene and the RV733 PB1 gene. Six major functional regions of the PB1 gene were identified and swapped from the 1918 PB1 into the RV733 PB1 to see if a change in transcriptional activity could be observed (Figure 10).

The results obtained from the Dual Luciferase Reporter assay for analysis of the PB1 chimeras generally correspond with that observed in the GFP reporter assay. As a general trend, all PB1 chimeras, as well as the RV733 PB1, in the 1918 background showed higher levels of luciferase expression than that of the complete 1918 RdRp (Figure 25A). This was surprising considering that each chimera represents an exchange of a functionally distinct domain in the RV733 PB1 with that of the 1918 PB1, yet all the chimeras apparently function equivalently to the RV733 PB1 no matter which domain is exchanged and in all cases this provided higher transcriptional activity than when the 1918 PB1 is present. However, the increases in reporter activity associated with each chimera are very modest and do not reflect a change in the general magnitude of reporter activity on a scale that distinguishes the 1918 and RV733 RdRp. Similarly in the context of the RV733 RdRp, all of the chimeras were essentially functionally equivalent to

RV733 PB1 (Figure 25B), although again small differences in reporter activity were noted between the chimeras and the RV733 PB1 but these may simply be due to the degree of compatibility between swapped domains and the rest of the protein. In no case did we observe that swapping any one domain of the PB1 significantly shifted reporter activity in a manner that would suggest that PB1 function or interaction with the other components of the RdRp were appreciably affected.

Although the differences in RV733 RdRp/NP activity with the chimeras compared to the wild type RV733 PB1 were small, there were some statistically significant decrease in luciferase expression with PB1 chimera 2 (Ch2) and PB1 chimera 5 (Ch5) in the RV733 background when compared to the complete RV733 RdRp in the luciferase reporter assays. These chimeric PB1 genes contained the 3' vRNA binding domain and the 5' vRNA binding domain, respectively. The reduction in transcriptional activity seen here could be explained by the differences in the 1918 and RV733 PB1 subunit's ability to bind RNA. If the other interactions between PB1 and the other subunits of the RdRp complex are compromised, that could also affect the ability of the PB1 to bind the viral RNA from transcription to take place. The interactions between the subunits of these two RdRp complexes would be of great interest for further study. It would be useful to understand the structure/function relationship between the RdRp subunits that we have proposed here and how their interactions dictate the activity of the complex as a whole.

4.4 Transcription Kinetics

To further study the properties of the transcriptional activities of the 1918 and RV733 viruses, the Dual Luciferase Reporter minigenome assay was employed for a transcription kinetics experiment. It was observed that the 1918 RdRp and the RV733 RdRp share a similar transcription kinetic profile, although the absolute level of transcriptional activity at all time points was higher for RV733 than 1918, as seen in the previous studies done at a single time point. Reporter expression was first detected just after the 8hr time point for both viruses and continued

to steadily increase. The 1918 RdRp complex appeared to reach its peak transcriptional activity by 36hrs while the RV733 RdRp complex continued to increase until the experiment ended at 48hrs. The small sharp peak seen for both viruses at 4hrs could possibly be attributed to the input plasmids and their initial round of transcription to generate the RdRp complex that will transcribe the luciferase minigenome.

The early time points were selected because it has been reported that cRNA and mRNA are detectable by 2 hrs post infection [94], thus I hypothesized that efficient transcriptional activity would be occurring at these early time points. The time course was carried out to the 48hr time point as this is when both the 1918 and RV733 virus reach their peak titre before this time, thus transcriptional activity should also reach a correlative peak in efficiency when, or even before, peak titers are observed.

Because there were no major differences between the transcription kinetic profile of the 1918 and RV733 viruses that would explain the differences in growth and pathogenicity properties of these viruses, or the differences in RdRp activity in the *in vitro* reporter assays, we decided not to further investigate the transcription kinetics of the RdRp gene combinations.

4.5 The Minigenome System

The minigenome reporter systems correlates transcriptional activity to the production of mRNA produced from the viral RNA template, but provides little insight into the efficiency of the RdRp to replicate the cRNA intermediate and the vRNA genome. We speculate that the 1918 RdRp may be more efficient at producing cRNA and vRNA rather than mRNA. This could explain why the 1918 virus, which is so efficient at replicating, would have this apparent low transcriptional activity. Kawakami and co-workers have shown using a strand-specific real-time RT-PCR assay that mRNA is produced primarily in the early stages of infection and in later

stages of infection mRNA synthesis stops and genome replication reactions dominate (ie, production of cRNA and vRNA) [94,156]. This is further supported by the proposed “switching mechanisms” which suggests that newly synthesized NP stabilizes the cRNA so efficient genome replication can occur [95,97]. It is possible that differential activities of the 1918 and RV733 NP in the regulation of influenza transcription and replication is reflected in the results of 1918/RV733 RdRp/NP gene swapping using our two minigenome systems, as well as our analysis of 1918/RV733 RdRp/NP recombinant virus growth kinetics (to be discussed below). Both reporter minigenome systems revealed that substituting the RV733 NP for the 1918 NP significantly increased the activity of the 1918 RdRp/NP complex (Figure 18 and 21). This suggests that the NP is a key determinant of the difference in transcriptional activity of the two RdRp complexes. It is possible that there is some unknown property that differentiates the 1918 NP from the RV733 NP that allows for more efficient transcriptional activity of a given RdRp complex. Although this was not investigated for the purposes of this dissertation, a more detailed look at the NP could be carried out by generating 1918/RV733 NP chimeric genes to study the functional domains of the NP and what effect they have on transcriptional activity, similarly to the generation and analysis of the 1918/RV733 PB1 chimeras.

Another possible explanation for the unexpected low transcriptional activity of the 1918 RdRp is a potential design flaw in our minigenome reporter system. The pPol reporter constructs were designed so that the reporter gene is flanked by the untranslated regions of an influenza NS sequence, so that it can be recognized by the viral polymerase complex that is generated from the pCAGGS expression plasmids. This untranslated region contains the promoter sequence that the viral polymerase recognizes and binds too. In our minigenome system the NS untranslated regions were derived from the RV733 influenza virus sequence. One suggestion to explain our observed results is that that the low reporter expression that we observed from the 1918 RdRp complex in both of our minigenome system that we interpreted as low transcriptional activity could in actuality be due to an inability of the 1918 RdRp to efficiently recognize the RV733 promoter sequence. If the 1918 RdRp is not able to recognize or bind efficiently to the promoter region then

efficient transcription cannot occur and low levels of reporter expression will result. The RV733 RdRp was able to yield high levels of reporter expression as it recognizes and efficiently binds it complementary promoter region on the reporter plasmid. However, alignment of the NS untranslated regions from the 1918 virus and the RV733 virus reveals only one nucleic acid residue difference. Further investigation is required to determine if this one residue difference is enough to affect recognition and/or binding. To support this explanation of our unexpected findings, the reporter plasmid should be reconstructed with the untranslated regions of the 1918 NS sequences, or perhaps even an unrelated NS sequence that is equally different from both the 1918 and RV733 sequences.

After analyzing all of our data and interpreting it as best we could, we still believe that the 1918 RdRp/NP is capable of highly efficient transcriptional activity. Despite what our two minigenome reporter systems tell us, there are numerous peer reviewed studies in the literature as well as our own viral growth kinetics study (described below) that supports this. We have suggested several reasons to why we did not see the expected high transcriptional activity, but further investigation will be needed to understand this anomaly. It is perhaps that we are failing to take into consideration some minor point in designing a minigenome assay to study the transcriptional activity of the 1918 RdRp/NP complex. This is quite intriguing as the minigenome assay system used in this study has been well established in the literature for evaluating the activity of influenza RdRp/NP activity, as well as the 1918 virus [47,59,152] which all suggest that the 1918 RdRp/NP has high transcriptional activity. Yet we continued to observe very negligible activity in both of the reporter assays described in this study. We speculate that there must be some specific requirement of the minigenome assay that is needed by the 1918 RdRp/NP for efficient transcriptional activity that our comparison RdRp/NP from the RV733 virus does not need. While it is not clear why the 1918 RdRp/NP displayed such low activity in out *in vitro* reporter assays, we have been able to shed some light on the critical interactions between the subunits of the RdRp/NP and the involvement of each of those subunits in supporting efficient transcriptional activity.

4.6 Replication Kinetics

To further build on what we have learned about the transcriptional properties of the 1918 and RV733 viruses from the minigenome systems we generated several 1918/RV733 recombinant viruses to study their replicative properties. All combinations of the individual exchanges of 1918 and RV733 polymerase and NP genes were successfully rescued in both the 1918 and RV733 background except for the 1918 PB2 in the RV733 background (Table 8), which could not be rescued, despite several attempts. We speculated that the 1918PB2/RV virus did not rescue because this combination of RdRp genes was the least favorable for viral replication, possibly due to instability in the RdRp complex that contains these proteins, which itself would be of interest to investigate further for a better understanding the basis for compatibility between the components of the RdRp complex.

To evaluate the replicative efficiencies of each of the 11 1918/RV733 recombinant viruses, an infection time course was carried out. Our results are consistent with what Watanabe and coworkers [78] report in that the combination of all of the 1918 RdRp/NP genes, rather than any single gene substitution into a low pathogenic contemporary H1N1 virus was more effective at transferring and maintaining 1918-like replicative efficiencies. It was determined that the wild type 1918 virus reached a peak titre of 1.88×10^8 PFU/ml by about 24 hours while the titre of the wild type RV733 also peaked at 24 hr at 4.99×10^6 PFU/ml, 37-fold lower. When the 1918 PB1 was replaced with the RV733 PB1 in the 1918 background this virus grew more slowly, and had nearly a log reduction in titre, when compared to the wild type 1918 virus. This suggests that the 1918 PB1 has a role in supporting the high replication efficiency of the 1918 virus. When the RV733 PB1 was replaced with the 1918 PB1 in the RV733 background we found that this virus grew more quickly than the complete RV733 virus, reaching much higher titres than the complete RV733 virus (Figure 26). This further supports our suggestion that the 1918 PB1 is capable of supporting the high replication efficiency associated with the 1918 virus as we were able to confer this property into another virus system. Interestingly, this role for the 1918 PB1 is mirrored in the

results from our minigenome studies. As described above, we suggest that the 1918 PB1 is capable of supporting high transcriptional activity when it is substituted into the RV733 RdRp/NP complex (Figure 21). This is consistent with the accepted concept that high transcriptional activity correlates to high replicative fitness.

It was also observed that the RVPB2/1918 virus titres decreased after the 24hr time point by half a log. This could be due to some instability within the RdRp complex due to the incompatibility of the RV733 PB2 protein with the rest of the 1918 subunits. Although there are likely other factors involved here as well, such as influences from the other subunits of the RdRp complex (described above). A decrease in viral titres after the 24hr time point was also observed for the RVRdRp/1918 and RVRdRp+NP/1918 viruses, which again may be linked to the fact that they both contain the RV733 PB2. However, this idea would not be consistent with the fact that in these latter two viruses, the RV733 PB2 is acting together with most or all of its usual partner proteins from the RV733 RdRp/NP and it would be expected that the RV733 PB2 would be well adapted to function in the context of the RV733 RdRp/NP. Therefore, we should not rule out the possibility of independent reasons for the reduced replication rates and possible instability shown by the decreasing titers at time points after 24hr with these viruses. However, it is not possible to provide further reasonable speculation regarding this possibility based on the data we have available.

One of our most significant and novel finding was a novel role for the NP in viral replication with our growth kinetics study. We observed that the 1918NP/RV virus continued to grow quite well past the 24hr time point, increasing its titre by nearly 10-fold, whereas many of the other recombinant viruses reached their peak titres by the 24hr time point (Figure 26). This suggests that the 1918 NP gene may contribute to the high growth phenotype that we see with the complete 1918 virus, perhaps by increasing the virus's replicative fitness. This is also observed with the 1918RdRp+NP/RV virus, as it too contains the 1918 NP gene along with the complete 1918 RdRp. However, it is clear that this recombinant virus exhibited faster growth

kinetics and replication to higher titer than either the parental RV733 virus or recombinant 1918RdRp/RV, clearly supporting a role for the 1918 NP. This role for the 1918 NP was mirrored in our minigenome studies as we revealed that NP may also have a significant role in the regulation of the transcriptional activity of an RdRp complex (described above). Another significant point about the 1918RdRp+NP/RV virus is that it exhibits faster growth kinetics, when comparing growth at the 18h time point, than the RV733 virus, much the same as was observed for the 1918PB1/RV virus, suggesting that this effect might be attributed to the presence of the 1918 PB1. However, the 1918RdRp/RV virus, which also has the 1918 PB1, did not exhibit these enhanced growth kinetics. This observation highlights the complex interaction that exists between the RdRp proteins that can result in somewhat variable and unpredictable outcomes when the proteins from different viruses are mixed.

4.7 Pathogenicity

The 1918 virus was 100% lethal by as early as 6 days post infection while the RV733 was non-pathogenic. The RV733 PB1 in a 1918 genetic background yielded lower viral titres and slower growth kinetics *in vitro.* While this recombinant virus did exhibit reduced pathogenicity *in vivo*, compared to the complete 1918 virus, the attenuation due to the RV733 PB1 replacement was slight resulting in a 1-2 day delay in the time to death and survival of one animal at the lowest dose evaluated. However, the small group size of mice infected with each virus is not sufficient to evaluate the statistical significance of the outcome and repeating the experiment with larger group sizes will be required to confirm these results with enough confidence to conclude that the RV733 PB1 attenuated the 1918 virus. Conversely, the 1918 PB1 in a RV733 genetic background resulted in increased viral titers and more rapid growth kinetics, but a concomitant increase in pathogenicity was not observed. This suggests that the 1918 PB1 gene segment is essential for the high growth phenotype but is only a minor contributor to the pathogenicity of the

complete 1918 wild-type virus as the substituting of the 1918 PB1 gene into a low pathogenic influenza virus did not confer 1918 pathogenicity characteristics.

Building on our viral growth kinetics findings, our preliminary mouse study has revealed a novel role for the NP in pathogenicity. We found that the substitution of the RV733 NP for the 1918NP significantly reduced the pathogenicity of the 1918 virus, more so than when the 1918 PB1 was substituted for the RV733PB1. Previous studies have shown PB1 to be a key factor in the pathogenicity of the 1918 virus [69,78]. However, our studies suggest that the 1918 PB1 plays only a minor role in pathogenicity and that the 1918 NP is critical for the high pathogenicity and high growth phenotype of the 1918 virus, at least in the context of the RV733 virus that we selected for comparison. To our knowledge, a role for the NP in pathogenicity has not been previously described for influenza viruses. Structural and stabilization roles have been extensively described for the NP protein in the transcription and replication of influenza viruses [58,95]. The NP serves as the structural basis of the vRNPs complexes by interacting with both the viral RNA as well as each of the RdRp subunits. A more interesting role for the NP protein is in regulating the switch from transcription to replication during an influenza virus infection [95]. Two mechanisms have been proposed for this regulatory role, both of which involve the stabilization of cRNA by the NP protein, allowing for more vRNA to be produced [58]. Based on this we suggest that it is possible that the transcriptional activity and replication efficiency of the 1918 virus is influenced significantly by the ability of the1918 NP protein to stabilize cRNA much more efficiently that the RV733 NP and that is why we see more efficient replication of the 1918 virus as compared to the RV733 virus. More experiments will need to be performed to determine the specific role of NP in the differences in transcriptional activity between the 1918 and RV733 RdRp complexes.

Growth kinetics analysis of each 1918/RV733 recombinant virus revealed that swapping the 1918 PB1 into the RV733 virus background yielded a virus able to grow more rapidly than the complete RV733 virus. In contrast, swapping in the RV733 PB1 to the 1918 virus background had

the opposite effect yielding a virus with reduced titres compared to the complete 1918 virus. Taken all together we suggest that the 1918 PB1 does contributes to the high growth properties associated with the 1918 virus and it is able to confer that property when substituted into the RV733 virus genetic background and the RV733 PB1 is not capable of supporting the high replicative properties of the 1918 virus. However, these results did not seem to correlate to pathogenicity. The RV733PB1/1918 virus, while attenuated compared to the parental 1918 virus, was still highly pathogenic in mice. These results are inconsistent with what was previously reported that PB1 is one of the key determinants of the pathogenicity of the 1918 virus [69]. It is also important to consider that the results present here are specific to the virus being used for comparison against the 1918 virus. Pappas and co-workers compared the 1918 virus to another low pathogenic H1N1 influenza strain, A/Texas/36/91 (Tx/91). They showed that PB1 was important for pathogenicity but NP did not detectably contribute to pathogenicity. But, in our study we found the NP to be more significant for efficient replication and pathogenicity and the PB1 to play only a minor role when we compared the 1918 virus to the RV733 virus. Since we did not have access to the Tx/91 virus we were not able to compare it to the RV733 virus to see what differences existed between these viruses that could explain why our results were so different from what had been previously reported. We suggest that the various subunits of the RV733 RdRp/NP complex can efficiently complement the 1918 RdRp/NP complex differently than those of the Tx/91 virus. Our results show that the RV733 PB1 can be exchanged for the 1918 PB1 and the activity of the 1918 RdRp/NP measured in the *in vitro* reporter assay does not change significantly, and the RV733 NP seems able to significantly increase the activity of the 1918 RdRp/NP. In the study done by Pappas and co-workers, we can see that the Tx/NP can replace the 1918 NP effectively as viral replication and pathogenicity were not significantly affected. But the Tx/PB1 cannot replace the 1918 PB1 without significantly reducing replication efficiency and attenuating the virus. A possible interpretation of the outcomes from my study and the previously published data is that the RV733 PB1 is more similar to the 1918 PB1 that the Tx/91 PB1, hence the RV733 is more readily able to complement the 1918 RdRp/NP. Similarly, the RV733 NP is less like the 1918 NP than that of the Tx/91 NP in some key functional/structural property and is

less able to complement the full function of the 1918 RdRp/NP than the Tx/91 NP. While we have no information as yet regarding these key differences/similarities in the low pathogenicity virus proteins compared to the 1918 counterparts, it will be very interesting to pursue this idea further.

Overall, our study has shown that none of the 1918 RdRp/NP genes were individually able to confer 1918 pathogenicity to the RV733 virus and the that the full 1918 RdRp/NP complex is required for 1918 pathogenicity, although several of the proteins, in particular PA and PB2 and to a less degree PB1, can be functionally substituted with those of a low pathogenicity virus without affecting 1918 virus pathogenicity. From these studies we have identified the 1918 NP as a key determinant of 1918 virus pathogenicity, which is a novel finding in that the NP has not previously been found to a major determinant of viral pathogenicity for any other influenza virus. But it is also important to consider the virus to which the 1918 virus is being compared to as the structure/function relationships that exist between the subunits of the RdRp/NP complex are likely virus specific and interchanging of subunits can drastically change the activity and efficiency of the complex as a whole. This latter observation is an important point for the understanding and interpreting studies that seek to identify determinants of pathogenicity. While determinants that are identified in similar studies are often taken as absolute and essential features that define the differences between pathogenic and non-pathogenic viruses, our results have demonstrated that the differences that define pathogenicity can be context dependent. These determinants of pathogenicity can also be dependent upon the similarities between not only the pathogenic virus and non-pathogenic virus but also by differences between non-pathogenic virus strains that are used for comparison.

4.8 Influence of PB1-F2

In our analysis of the activities of the 1918 and RV733 RdRp/NP complexes we found that the 1918 PB1 is important in the high replication kinetics of the 1918 virus, consistent with it role that was reported previously. However, the 1918 RdRp/NP unexpectedly exhibited lower transcriptional activity than the RV733 complex in the *in vitro* reporter assays, a property that was not linked to the activity of the 1918 PB1, despite the central role for PB1 in transcriptional activity This is inconsistent with previous reports on the role of the PB1 subunit in the transcription and replication properties of the 1918 virus, thus we speculate that there are other factors involved in these processes.

The increased virulence of the 1918 virus has been associated with the function of its full length PB1-F2 protein, which is generated from an alternate open reading frame of the PB1 gene [81]. Increased polymerase activity has also been linked to PB1-F2, as it is known to interact directly with PB1 [83,87]. Thus we must acknowledge the influence of the PB1-F2 in all of the transcription and replication activities of the 1918 virus. Previously it had been shown that when the 1918 virus was compared to the low pathogenic A/Texas/36/91 (Tx/91) virus, which does not possess a functioning PB1-F2, that the Tx/91 PB1 was not able to efficiently replace the 1918 PB1 in the 1918 virus genetic background, and pathogenicity was reduced [69]. This suggested that the presence of a functioning PB1-F2 contributes to pathogenicity. This was further supported by Conenello and co-workers who demonstrated that the single mutation of S66N in PB1-F2, which does not affect the protein sequence of PB1, was sufficient to increase the median lethal dose (LD_{50}) in mice by more than 1000-fold, demonstrating a dramatic reduction in pathogenicity [84]. However, our results have shown that you can replace the 1918 PB1 gene, with its functioning PB1-F2, with the RV733 PB1 gene that does not have a functioning PB1-F2, without significantly affecting the pathogenicity of the virus (Table 9). From this we can conclude that the RV733 PB1 can complement the 1918 PB1 in pathogenicity even though it does not possess a functioning PB1-F2. This suggests that the RV733 PB1 protein functions differently

than the 1918 PB1 protein in the context of the RdRp complex and has some mechanism to compensate for the activity that PB1-F2 would contribute to pathogenicity.

In addition to the direct demonstration that the 1918 virus can be attenuated by mutation of a key amino acid in PB1-F2, further studies have provided some idea of how PB1-F2 functions and may contribute to pathogenesis. These studies are worth noting as we consider the ways that the RV733, without a functional PB1-F2, may contribute to pathogenesis. It has been shown that the PB1-F2 N66S contributes to the delay of innate immune responses through direct interactions with key modulators of interferon signaling responses. The 1918 PB1-F2, containing S66, has been shown to suppress interferon-stimulated genes and thus down regulate the early interferon response to infection by either a traditional interferon antagonistic mechanism or by an inhibition mechanism of transcription factors for interferon-stimulated genes [157]. Either of these proposed mechanisms would then allow for prolonged viral replication and the development of irreversible pulmonary immunopathology [157]. These findings are consistent with that is observed for highly pathogenic influenza strains, such as the 1918 virus [84,158].

Smith and co-workers explored the role of PB1-F2 further by studying it's *in vivo* effects on viral growth properties by utilizing a recombinant A/Puerto Rico/8/34 (PR8; H1N1) virus that has been modified to express the 1918 PB1-F2 protein, which was called PR8-PB1-F2 (1918) [159]. PR8 is a mouse-adapted virus and is already highly pathogenic in mice. However, mice infected with PR8-PB1-F2 (1918) had increased viral replication kinetics, reaching peak viral titres a full 24hr sooner than the wild-type PR8 virus [159]. This is consistent with what we observed in our *in vitro* growth kinetics study. When we introduced the 1918 PB1 (along with its functioning PB1-F2 gene) into the RV733 background, the resulting recombinant virus displayed a significant increase in replication efficiency over that of the wild-type RV733 virus (Section 3.5.2)(Figure 26) suggesting that the 1918 PB1 is a key determinant of the high growth phenotype associated with the 1918 virus. We can further speculate that these viral growth properties are also influenced by the presence of the 1918 PB1-F2.

Based on our results, we suggest that the RV733 RdRp/NP may not require its own PB1-F2 for efficient transcription and replication and that it must have some other compensatory mechanism that allows it to function efficiently. We have shown in our mouse study that the RVPB1/1918 recombinant virus remained nearly as highly pathogenic, despite the absence of a functioning a PB1-F2 protein, as the complete 1918 virus possesses. The RV733 RdRp/1918 recombinant virus was also at least as highly pathogenic as the RVPB1/1918 virus, if not slightly more pathogenic, suggesting that the RV733 PB1 may also be adapted to function best with the RV733 PA and PB2 components. However, it is evident that the RV733 RdRp complex is able to function efficiently with the remaining 1918 genes and maintain the high pathogenic phenotype associated with the complete 1918 virus even without the help of PB1-F2. Overall, our results lead us to speculate that PB1-F2 is not absolutely essential to elicit the high pathogenic phenotype of the 1918 virus when we compliment the 1918 RdRp proteins with those from the RV733 virus. The ability of the RV733 PB1 to effectively replace the 1918 PB1, despite its lack of PB1-F2 is an important result. Further understanding how the RV733 PB1 is able to dispense with the PB1-F2 protein but still maintain the high pathogenicity phenotype of the 1918 virus will be a significant area for further investigation and will be very useful for further elucidating the still ambiguous function of the PB1-F2 protein.

4.9 Future Directions

We expected that since the 1918 virus is able to grow to very high titres very quickly that this would correlate to high transcriptional activity, likely mediated by the 1918 PB1 subunit. But this was not observed. The minigenome systems that we employed in these studies are designed in a manner that is consistent with the many systems that have been reported in the literature [47,59,152]. So, we must either accept that the 1918 RdRp/NP must have high transcriptional activity, consistent with the growth properties of the 1918 virus, or we must consider the low transcriptional activity displayed in our minigenome assays is a novel property of the 1918 RdRp

complex. Regardless, we must acknowledge that we do not fully understand the requirements for 1918 RdRp/NP activity and that the minigenome is inadequate to model the 1918 RdRp/NP transcriptional activity, despite the fact that it appears to be adequate for modeling the RdRp/NP activity of other influenza viruses. Either possibility is very fascinating, as it does not fit into the model of influenza transcription/genome replication that is currently accepted. The minigenome reporter system correlates transcriptional activity to the production of mRNA produced from the viral RNA template, but provides little insight into the efficiency of the RdRp to replicate the cRNA intermediate and the vRNA genome. One intriguing speculation to explore further, that was mentioned above briefly, is that the 1918 RdRp is more efficient at producing cRNA and vRNA rather than mRNA and that this somehow translates into increased viral replication kinetics, despite the possibility that less viral proteins are made due to reduced mRNA levels. However, it is possible that increased vRNA production early in the viral life cycle could ultimately result in more mRNA, suggesting a different regulation of transcriptional/genome replication events for the 1918 virus than for other influenza virus strains that have been studied. Thus, it would be interesting to investigate the highly regulated balance of the production of each species of RNA during the course of an influenza infection.

To investigate this, we have begun to develop the Strand-Specific Real-time RT-PCR assay that was pioneered by Kawakami and co-workers [94] that would allow monitoring of all RNA species that are produced during actual viral replication. We mimicked their experimental and primer design by utilizing tagged primers to be able to distinguish between the three species of RNA present during an Influenza virus infection. In the whole viruses system, we decided to target the RNAs of the NA segment as it is highly conserved between the 1918 and RV73 viruses. Thus, we could design primers that target the same region of the NA segment for both viruses. It will also be possible to compare the RNA replication events that occur in the minigenome to live virus replication. In the minigenome system, we will target the GFP sequence, as it is the reporter for transcriptional activity and will be present in every experimental scenario. The luciferase gene will also be targeted so we can continue to compare these two reporter

systems on a more detailed level and to perhaps better understand the differences in the results we have obtained from these two systems in this study. By using this Strand-Specific Real-time RT-PCR assay to analyse the transcription and replication dynamics of both the whole virus infectious system and the minigenome system we can hope to further validate the minigenome system as a valuable tool to study high containment viruses in a biosafety-level 2 setting.

To verify our findings from the minigenome assays and to complete our analysis of the transcriptional activity of the 1918 RdRp complex, the pPol reporter constructs will need to be reconstructed to contain the NS untranslated region sequences from the 1918 virus. This will give us a more representative readout of transcriptional activity of the 1918 RdRp as this will ensure proper recognition and efficient binding of the RdRp to the promoter region. This could be further explored by utilizing the NS sequences from other influenza viruses that are unrelated to both 1918 and RV733 to try to ensure equal recognition and binding of the both RdRp complexes to the promoter region.

Watanabe and co-workers [78] have investigated the role of the 1918 polymerase complex in the growth of the virus. In this study they compared the 1918 virus to A/Kawasaki/173/2001 (K173), another contemporary human H1N1 virus. They showed that replacing the K173 PB1 with the 1918 PB1, resulted in a recombinant virus with higher replication efficiency and was able to grow in both the upper and lower respiratory tract of macaques like the 1918 virus (whereas, the K173 can only grow in the upper respiratory tract at relatively low titres), showing that the 1918 PB1 is able to confer the 1918 virus high growth phenotype and tissue tropism in another virus system. This influence of the 1918 PB1 on viral growth is consistent with what we observed in our study comparing the 1918 virus to the RV733 virus. Thus, it would be very interesting to build on this and determine the effect on replication kinetics in the lungs of mice.

We would also like to generate recombinant viruses that contain each of the six chimeric PB1 genes that were generated in this study. It would be interesting to see what influence the chimeric PB1 genes have on viral replication and pathogenicity and if it correlates to the transcriptional activity findings from this study. We would expect similar correlations from the PB1 chimeras to what we observed in the minigenome reporter systems as well as what we observed with the full gene swaps in both the minigenome reporter systems and the whole virus infectious system. Since we have suggested that the 1918 virus is more efficient in generating vRNA (replication) than mRNA (transcription), we predict that this will more obviously seen using the PB1 chimeras as they showed us that altering the specific interactions between the RdRp subunits can affect transcriptional activity significantly, while replication is less affected and conversely, transcriptional activity can be maintained while replication is impaired. This will also support the "switching model" for regulation of viral transcription and replication and show that the balance of transcription and replication differs between the 1918 and RV733 viruses.

The recombination of the 1918 gene segments with the gene segments of different viruses will yield different protein-protein interactions, different protein-RNA interactions and different virus-host interactions. All of which will affect transcriptional activity, replication efficiency and pathogenicity of the recombinant virus. Thus the results obtained from such comparisons are subjective and must be analyzed completely and carefully to determine what is scientifically significant. But ultimately, with careful analysis, we have uncovered some very intriguing findings that have open many doors to further exciting studies and a great understanding of the unique characteristics of the 1918 pandemic influenza virus.

5.0 References

1. Palase P, Shaw, ML. (2007) Orthomyxoviridae: The Viruses and Their Replication. In: Knipe DM HP, editor. Fields Virology. 5th ed. Philidelphia, PA: Lippincott Williams & Wilkins. pp. 1648-1678.
2. Kawaoka Y, Neumann G (2012) Influenza viruses: an introduction. Methods Mol Biol 865: 1-9.
3. Myers KP, Olsen CW, Gray GC (2007) Cases of swine influenza in humans: a review of the literature. Clin Infect Dis 44: 1084-1088.
4. Goday A, Jensen AB, Culianez-Macia FA, Mar Alba M, Figueras M, et al. (1994) The maize abscisic acid-responsive protein Rab17 is located in the nucleus and interacts with nuclear localization signals. Plant Cell 6: 351-360.
5. Acheson NH (2007) Fundamentals of Molecular Virology; Witt K, editor: John Wiley & Sons, Inc.
6. Taubenberger JK, Kash JC (2010) Influenza virus evolution, host adaptation, and pandemic formation. Cell Host Microbe 7: 440-451.
7. David M. Knipe PPMH, MD; Diane E. Griffin, MD, PhD; Robert A. Lamb, PhD, ScD; Malcolm A. Martin, MD; Bernard Roizman, ScD; Stephen E. Straus, MD (2007) Fields Virology. In: David M. Knipe PPMH, MD; Diane E. Griffin, MD, PhD; Robert A. Lamb, PhD, ScD; Malcolm A. Martin, MD; Bernard Roizman, ScD; Stephen E. Straus, MD editor. 5th ed: Lippincott Williams & Wilkins (LWW).
8. Kawaoka Y, Neumann, G., Wright, PF. (2007) Orthomyxoviruses. In: Knipe DM HP, editor. Fields Virology. 5th ed. Philidelphia, PA: Lippincott Williams & Wilkins. pp. 1691-1740.
9. Li Q, Sun X, Li Z, Liu Y, Vavricka CJ, et al. (2012) Structural and functional characterization of neuraminidase-like molecule N10 derived from bat influenza A virus. Proc Natl Acad Sci U S A 109: 18897-18902.
10. Gorai T, Goto H, Noda T, Watanabe T, Kozuka-Hata H, et al. (2012) F1Fo-ATPase, F-type proton-translocating ATPase, at the plasma membrane is critical for efficient influenza virus budding. Proc Natl Acad Sci U S A 109: 4615-4620.
11. Van Epps HL (2006) Influenza: exposing the true killer. J Exp Med 203: 803.
12. Baudin F, Bach C, Cusack S, Ruigrok RW (1994) Structure of influenza virus RNP. I. Influenza virus nucleoprotein melts secondary structure in panhandle RNA and exposes the bases to the solvent. EMBO J 13: 3158-3165.
13. Ahmed MU, Chawdhury FA, Hossain M, Sultan SZ, Alam M, et al. (2010) Monitoring antimicrobial susceptibility of Neisseria gonorrhoeae isolated from Bangladesh during 1997-2006: emergence and pattern of drug-resistant isolates. J Health Popul Nutr 28: 443-449.
14. Fahy WA, Farnworth E, Yeldrem KP, Melling GS, Grennan DM (2006) Pneumococcal and influenza vaccination in patients with rheumatic conditions and receiving DMARD therapy. Rheumatology (Oxford) 45: 912-913.
15. Brands R, Visser J, Medema J, Palache AM, van Scharrenburg GJ (1999) Influvac: a safe Madin Darby Canine Kidney (MDCK) cell culture-based influenza vaccine. Dev Biol Stand 98: 93-100; discussion 111.

16. Ahmed US, Junaidi B, Ali AW, Akhter O, Salahuddin M, et al. (2010) Barriers in initiating insulin therapy in a South Asian Muslim community. Diabet Med 27: 169-174.
17. Salahuddin N, Irfan M, Khan S, Naeem M, Haque AS, et al. (2010) Variables predictive of outcome in patients with acute hypercapneic respiratory failure treated with noninvasive ventilation. J Pak Med Assoc 60: 13-17.
18. Poole EL, Medcalf L, Elton D, Digard P (2007) Evidence that the C-terminal PB2-binding region of the influenza A virus PB1 protein is a discrete alpha-helical domain. FEBS Lett 581: 5300-5306.
19. Takizawa N, Morita M, Adachi K, Watanabe K, Kobayashi N (2009) Induction of immune responses to a human immunodeficiency virus type 1 epitope by novel chimeric influenza viruses. Drug Discov Ther 3: 252-259.
20. Sawabuchi T, Suzuki S, Iwase K, Ito C, Mizuno D, et al. (2009) Boost of mucosal secretory immunoglobulin A response by clarithromycin in paediatric influenza. Respirology 14: 1173-1179.
21. Heikkinen T, Booy R, Campins M, Finn A, Olcen P, et al. (2006) Should healthy children be vaccinated against influenza? A consensus report of the Summits of Independent European Vaccination Experts. Eur J Pediatr 165: 223-228.
22. Gilbert R, Ghosh K, Rasile L, Ghosh HP (1994) Membrane anchoring domain of herpes simplex virus glycoprotein gB is sufficient for nuclear envelope localization. J Virol 68: 2272-2285.
23. Klenk HD, Rott R, Orlich M, Blodorn J (1975) Activation of influenza A viruses by trypsin treatment. Virology 68: 426-439.
24. Kobasa D, Takada A, Shinya K, Hatta M, Halfmann P, et al. (2004) Enhanced virulence of influenza A viruses with the haemagglutinin of the 1918 pandemic virus. Nature 431: 703-707.
25. Baum LG, Paulson JC (1991) The N2 neuraminidase of human influenza virus has acquired a substrate specificity complementary to the hemagglutinin receptor specificity. Virology 180: 10-15.
26. Rogers GN, Paulson JC (1983) Receptor determinants of human and animal influenza virus isolates: differences in receptor specificity of the H3 hemagglutinin based on species of origin. Virology 127: 361-373.
27. Couceiro JN, Paulson JC, Baum LG (1993) Influenza virus strains selectively recognize sialyloligosaccharides on human respiratory epithelium; the role of the host cell in selection of hemagglutinin receptor specificity. Virus Res 29: 155-165.
28. Wagner R, Wolff T, Herwig A, Pleschka S, Klenk HD (2000) Interdependence of hemagglutinin glycosylation and neuraminidase as regulators of influenza virus growth: a study by reverse genetics. J Virol 74: 6316-6323.
29. Pinto LH, Holsinger LJ, Lamb RA (1992) Influenza virus M2 protein has ion channel activity. Cell 69: 517-528.
30. Matlin KS, Reggio H, Helenius A, Simons K (1981) Infectious entry pathway of influenza virus in a canine kidney cell line. J Cell Biol 91: 601-613.
31. Zhirnov OP, Grigoriev VB (1994) Disassembly of influenza C viruses, distinct from that of influenza A and B viruses requires neutral-alkaline pH. Virology 200: 284-291.

32. Hayden FG, Hay AJ (1992) Emergence and transmission of influenza A viruses resistant to amantadine and rimantadine. Curr Top Microbiol Immunol 176: 119-130.
33. Moeller A, Kirchdoerfer RN, Potter CS, Carragher B, Wilson IA (2012) Organization of the influenza virus replication machinery. Science 338: 1631-1634.
34. Hsu MT, Parvin JD, Gupta S, Krystal M, Palese P (1987) Genomic RNAs of influenza viruses are held in a circular conformation in virions and in infected cells by a terminal panhandle. Proc Natl Acad Sci U S A 84: 8140-8144.
35. Compans RW, Content J, Duesberg PH (1972) Structure of the ribonucleoprotein of influenza virus. J Virol 10: 795-800.
36. Jones IM, Reay PA, Philpott KL (1986) Nuclear location of all three influenza polymerase proteins and a nuclear signal in polymerase PB2. EMBO J 5: 2371-2376.
37. Mukaigawa J, Nayak DP (1991) Two signals mediate nuclear localization of influenza virus (A/WSN/33) polymerase basic protein 2. J Virol 65: 245-253.
38. Nath ST, Nayak DP (1990) Function of two discrete regions is required for nuclear localization of polymerase basic protein 1 of A/WSN/33 influenza virus (H1 N1). Mol Cell Biol 10: 4139-4145.
39. Cros JF, Garcia-Sastre A, Palese P (2005) An unconventional NLS is critical for the nuclear import of the influenza A virus nucleoprotein and ribonucleoprotein. Traffic 6: 205-213.
40. O'Neill RE, Jaskunas R, Blobel G, Palese P, Moroianu J (1995) Nuclear import of influenza virus RNA can be mediated by viral nucleoprotein and transport factors required for protein import. J Biol Chem 270: 22701-22704.
41. Noda T, Kawaoka Y (2010) Structure of influenza virus ribonucleoprotein complexes and their packaging into virions. Rev Med Virol 20: 380-391.
42. Chan WH, Ng AK, Robb NC, Lam MK, Chan PK, et al. (2010) Functional analysis of the influenza virus H5N1 nucleoprotein tail loop reveals amino acids that are crucial for oligomerization and ribonucleoprotein activities. J Virol 84: 7337-7345.
43. Ye Q, Krug RM, Tao YJ (2006) The mechanism by which influenza A virus nucleoprotein forms oligomers and binds RNA. Nature 444: 1078-1082.
44. Salahuddin P, Khan AU (2010) Structure function studies on different structural domains of nucleoprotein of H1N1 subtype. Bioinformation 5: 28-30.
45. Martin-Benito J, Area E, Ortega J, Llorca O, Valpuesta JM, et al. (2001) Three-dimensional reconstruction of a recombinant influenza virus ribonucleoprotein particle. EMBO Rep 2: 313-317.
46. Weber F, Kochs G, Gruber S, Haller O (1998) A classical bipartite nuclear localization signal on Thogoto and influenza A virus nucleoproteins. Virology 250: 9-18.
47. Neumann G, Fujii K, Kino Y, Kawaoka Y (2005) An improved reverse genetics system for influenza A virus generation and its implications for vaccine production. Proc Natl Acad Sci U S A 102: 16825-16829.
48. Fodor E, Crow M, Mingay LJ, Deng T, Sharps J, et al. (2002) A single amino acid mutation in the PA subunit of the influenza virus RNA polymerase inhibits endonucleolytic cleavage of capped RNAs. J Virol 76: 8989-9001.

49. Neumann G, Zobel A, Hobom G (1994) RNA polymerase I-mediated expression of influenza viral RNA molecules. Virology 202: 477-479.
50. Dias A, Bouvier D, Crepin T, McCarthy AA, Hart DJ, et al. (2009) The cap-snatching endonuclease of influenza virus polymerase resides in the PA subunit. Nature 458: 914-918.
51. Hsu JT, Yeh JY, Lin TJ, Li ML, Wu MS, et al. (2012) Identification of BPR3P0128 as an inhibitor of cap-snatching activities of influenza virus. Antimicrob Agents Chemother 56: 647-657.
52. Perez DR, Donis RO (1995) A 48-amino-acid region of influenza A virus PB1 protein is sufficient for complex formation with PA. J Virol 69: 6932-6939.
53. Li ML, Ramirez BC, Krug RM (1998) RNA-dependent activation of primer RNA production by influenza virus polymerase: different regions of the same protein subunit constitute the two required RNA-binding sites. EMBO J 17: 5844-5852.
54. Guilligay D, Tarendeau F, Resa-Infante P, Coloma R, Crepin T, et al. (2008) The structural basis for cap binding by influenza virus polymerase subunit PB2. Nat Struct Mol Biol 15: 500-506.
55. Perez DR, Donis RO (2001) Functional analysis of PA binding by influenza a virus PB1: effects on polymerase activity and viral infectivity. J Virol 75: 8127-8136.
56. Poon LL, Pritlove DC, Fodor E, Brownlee GG (1999) Direct evidence that the poly(A) tail of influenza A virus mRNA is synthesized by reiterative copying of a U track in the virion RNA template. J Virol 73: 3473-3476.
57. Zheng H, Lee HA, Palese P, Garcia-Sastre A (1999) Influenza A virus RNA polymerase has the ability to stutter at the polyadenylation site of a viral RNA template during RNA replication. J Virol 73: 5240-5243.
58. Vreede FT, Jung TE, Brownlee GG (2004) Model suggesting that replication of influenza virus is regulated by stabilization of replicative intermediates. J Virol 78: 9568-9572.
59. Chu C, Fan S, Li C, Macken C, Kim JH, et al. (2012) Functional analysis of conserved motifs in influenza virus PB1 protein. PLoS One 7: e36113.
60. Turner SJ, Diaz G, Cross R, Doherty PC (2003) Analysis of clonotype distribution and persistence for an influenza virus-specific CD8+ T cell response. Immunity 18: 549-559.
61. Heinzinger NK, Bukinsky MI, Haggerty SA, Ragland AM, Kewalramani V, et al. (1994) The Vpr protein of human immunodeficiency virus type 1 influences nuclear localization of viral nucleic acids in nondividing host cells. Proc Natl Acad Sci U S A 91: 7311-7315.
62. Ohtsu Y, Honda Y, Sakata Y, Kato H, Toyoda T (2002) Fine mapping of the subunit binding sites of influenza virus RNA polymerase. Microbiol Immunol 46: 167-175.
63. Gonzalez S, Zurcher T, Ortin J (1996) Identification of two separate domains in the influenza virus PB1 protein involved in the interaction with the PB2 and PA subunits: a model for the viral RNA polymerase structure. Nucleic Acids Res 24: 4456-4463.
64. Biswas SK, Nayak DP (1996) Influenza virus polymerase basic protein 1 interacts with influenza virus polymerase basic protein 2 at multiple sites. J Virol 70: 6716-6722.

65. Hemerka JN, Wang D, Weng Y, Lu W, Kaushik RS, et al. (2009) Detection and characterization of influenza A virus PA-PB2 interaction through a bimolecular fluorescence complementation assay. J Virol 83: 3944-3955.
66. Schlatt S, Weinbauer GF (1994) Immunohistochemical localization of proliferating cell nuclear antigen as a tool to study cell proliferation in rodent and primate testes. Int J Androl 17: 214-222.
67. Panagakos FS, Kumar S (1994) Nuclear localization of tumor necrosis factor-alpha in human osteoblast-like cells. Biochem Biophys Res Commun 201: 1445-1450.
68. Huet S, Avilov SV, Ferbitz L, Daigle N, Cusack S, et al. (2010) Nuclear import and assembly of influenza A virus RNA polymerase studied in live cells by fluorescence cross-correlation spectroscopy. J Virol 84: 1254-1264.
69. Pappas (2008) Single gene reassortants identify a critical role for PB1, HA, and NA in the high virulence of the 1918 pandemic influenza virus. PNAS 105: 3064-3069.
70. Cherian MG (1994) The significance of the nuclear and cytoplasmic localization of metallothionein in human liver and tumor cells. Environ Health Perspect 102 Suppl 3: 131-135.
71. Biswas SK, Nayak DP (1994) Mutational analysis of the conserved motifs of influenza A virus polymerase basic protein 1. J Virol 68: 1819-1826.
72. Takemoto Y, Tashiro S, Handa H, Ishii S (1994) Multiple nuclear localization signals of the B-myb gene product. FEBS Lett 350: 55-60.
73. Pante N, Bastos R, McMorrow I, Burke B, Aebi U (1994) Interactions and three-dimensional localization of a group of nuclear pore complex proteins. J Cell Biol 126: 603-617.
74. Sugiyama K, Obayashi E, Kawaguchi A, Suzuki Y, Tame JR, et al. (2009) Structural insight into the essential PB1-PB2 subunit contact of the influenza virus RNA polymerase. EMBO J 28: 1803-1811.
75. Wunderlich K, Mayer D, Ranadheera C, Holler AS, Manz B, et al. (2009) Identification of a PA-binding peptide with inhibitory activity against influenza A and B virus replication. PLoS One 4: e7517.
76. Maeda Y, Hatta M, Takada A, Watanabe T, Goto H, et al. (2005) Live bivalent vaccine for parainfluenza and influenza virus infections. J Virol 79: 6674-6679.
77. Shinya K, Suto A, Kawakami M, Sakamoto H, Umemura T, et al. (2005) Neurovirulence of H7N7 influenza A virus: brain stem encephalitis accompanied with aspiration pneumonia in mice. Arch Virol 150: 1653-1660.
78. Rubino IA, Dotti A, Greco E, Zanna V, Fieramonti E, et al. (1995) Styles of regulation in the bipolar spectrum. Percept Mot Skills 81: 419-428.
79. Taubenberger JK, Reid AH, Lourens RM, Wang R, Jin G, et al. (2005) Characterization of the 1918 influenza virus polymerase genes. Nature 437: 889-893.
80. Yamaguchi K, Hisano M, Isojima S, Irie S, Arata N, et al. (2009) Relationship of Th1/Th2 cell balance with the immune response to influenza vaccine during pregnancy. J Med Virol 81: 1923-1928.
81. Matheny C, Day ML, Milbrandt J (1994) The nuclear localization signal of NGFI-A is located within the zinc finger DNA binding domain. J Biol Chem 269: 8176-8181.

82. Mazur I, Anhlan D, Mitzner D, Wixler L, Schubert U, et al. (2008) The proapoptotic influenza A virus protein PB1-F2 regulates viral polymerase activity by interaction with the PB1 protein. Cell Microbiol 10: 1140-1152.
83. Zamarin D, Ortigoza MB, Palese P (2006) Influenza A virus PB1-F2 protein contributes to viral pathogenesis in mice. J Virol 80: 7976-7983.
84. Conenello GM, Zamarin D, Perrone LA, Tumpey T, Palese P (2007) A single mutation in the PB1-F2 of H5N1 (HK/97) and 1918 influenza A viruses contributes to increased virulence. PLoS Pathog 3: 1414-1421.
85. Coleman JR (2007) The PB1-F2 protein of Influenza A virus: increasing pathogenicity by disrupting alveolar macrophages. Virol J 4: 9.
86. Yamada H, Chounan R, Higashi Y, Kurihara N, Kido H (2004) Mitochondrial targeting sequence of the influenza A virus PB1-F2 protein and its function in mitochondria. FEBS Lett 578: 331-336.
87. Zamarin D, Garcia-Sastre A, Xiao X, Wang R, Palese P (2005) Influenza virus PB1-F2 protein induces cell death through mitochondrial ANT3 and VDAC1. PLoS Pathog 1: e4.
88. Subbarao EK, London W, Murphy BR (1993) A single amino acid in the PB2 gene of influenza A virus is a determinant of host range. J Virol 67: 1761-1764.
89. Shinya K, Hamm S, Hatta M, Ito H, Ito T, et al. (2004) PB2 amino acid at position 627 affects replicative efficiency, but not cell tropism, of Hong Kong H5N1 influenza A viruses in mice. Virology 320: 258-266.
90. Fleming DM, Pannell RS, Cross KW (2005) Mortality in children from influenza and respiratory syncytial virus. J Epidemiol Community Health 59: 586-590.
91. Sanz-Ezquerro JJ, Zurcher T, de la Luna S, Ortin J, Nieto A (1996) The amino-terminal one-third of the influenza virus PA protein is responsible for the induction of proteolysis. J Virol 70: 1905-1911.
92. Ovcharenko AV, Zhirnov OP (1994) Aprotinin aerosol treatment of influenza and paramyxovirus bronchopneumonia of mice. Antiviral Res 23: 107-118.
93. Paterson D, Fodor E (2012) Emerging Roles for the Influenza A Virus Nuclear Export Protein (NEP). PLoS Pathog 8: e1003019.
94. Kawakami E, Watanabe T, Fujii K, Goto H, Watanabe S, et al. (2011) Strand-specific real-time RT-PCR for distinguishing influenza vRNA, cRNA, and mRNA. J Virol Methods 173: 1-6.
95. Barrett T, Wolstenholme AJ, Mahy BW (1979) Transcription and replication of influenza virus RNA. Virology 98: 211-225.
96. Beaton AR, Krug RM (1986) Transcription antitermination during influenza viral template RNA synthesis requires the nucleocapsid protein and the absence of a 5' capped end. Proc Natl Acad Sci U S A 83: 6282-6286.
97. Perez JT, Varble A, Sachidanandam R, Zlatev I, Manoharan M, et al. (2010) Influenza A virus-generated small RNAs regulate the switch from transcription to replication. Proc Natl Acad Sci U S A 107: 11525-11530.
98. Huang X, Liu T, Muller J, Levandowski RA, Ye Z (2001) Effect of influenza virus matrix protein and viral RNA on ribonucleoprotein formation and nuclear export. Virology 287: 405-416.
99. Ye Z, Liu T, Offringa DP, McInnis J, Levandowski RA (1999) Association of influenza virus matrix protein with ribonucleoproteins. J Virol 73: 7467-7473.

100. Baudin F, Petit I, Weissenhorn W, Ruigrok RW (2001) In vitro dissection of the membrane and RNP binding activities of influenza virus M1 protein. Virology 281: 102-108.
101. Lamb RA, Lai CJ (1980) Sequence of interrupted and uninterrupted mRNAs and cloned DNA coding for the two overlapping nonstructural proteins of influenza virus. Cell 21: 475-485.
102. Yasuda J, Nakada S, Kato A, Toyoda T, Ishihama A (1993) Molecular assembly of influenza virus: association of the NS2 protein with virion matrix. Virology 196: 249-255.
103. O'Neill RE, Talon J, Palese P (1998) The influenza virus NEP (NS2 protein) mediates the nuclear export of viral ribonucleoproteins. EMBO J 17: 288-296.
104. Robb NC, Smith M, Vreede FT, Fodor E (2009) NS2/NEP protein regulates transcription and replication of the influenza virus RNA genome. J Gen Virol 90: 1398-1407.
105. Lamb RA, Choppin PW (1980) A ninth unique influenza virus-coded polypeptide. Philos Trans R Soc Lond B Biol Sci 288: 327-333.
106. Yea C, Adachi D, Johnson G, Nagy E, Gharabaghi F, et al. (2007) Design of a single tube RT-PCR assay for the diagnosis of human infection with highly pathogenic influenza A(H5) viruses. J Virol Methods 139: 220-226.
107. Enami M, Sharma G, Benham C, Palese P (1991) An influenza virus containing nine different RNA segments. Virology 185: 291-298.
108. Bancroft CT, Parslow TG (2002) Evidence for segment-nonspecific packaging of the influenza a virus genome. J Virol 76: 7133-7139.
109. Duhaut SD, McCauley JW (1996) Defective RNAs inhibit the assembly of influenza virus genome segments in a segment-specific manner. Virology 216: 326-337.
110. Odagiri T, Tashiro M (1997) Segment-specific noncoding sequences of the influenza virus genome RNA are involved in the specific competition between defective interfering RNA and its progenitor RNA segment at the virion assembly step. J Virol 71: 2138-2145.
111. Morens DM, Taubenberger JK, Fauci AS (2009) The persistent legacy of the 1918 influenza virus. N Engl J Med 361: 225-229.
112. Schultz-Cherry S, Dybdahl-Sissoko N, Neumann G, Kawaoka Y, Hinshaw VS (2001) Influenza virus ns1 protein induces apoptosis in cultured cells. J Virol 75: 7875-7881.
113. Neumann G, Watanabe T, Ito H, Watanabe S, Goto H, et al. (1999) Generation of influenza A viruses entirely from cloned cDNAs. Proc Natl Acad Sci U S A 96: 9345-9350.
114. Gomez-Puertas P, Albo C, Perez-Pastrana E, Vivo A, Portela A (2000) Influenza virus matrix protein is the major driving force in virus budding. J Virol 74: 11538-11547.
115. Wagner R, Matrosovich M, Klenk HD (2002) Functional balance between haemagglutinin and neuraminidase in influenza virus infections. Rev Med Virol 12: 159-166.
116. Harris A, Forouhar F, Qiu S, Sha B, Luo M (2001) The crystal structure of the influenza matrix protein M1 at neutral pH: M1-M1 protein interfaces can rotate in the oligomeric structures of M1. Virology 289: 34-44.

117. Sha B, Luo M (1997) Structure of a bifunctional membrane-RNA binding protein, influenza virus matrix protein M1. Nat Struct Biol 4: 239-244.
118. Palese P, Tobita K, Ueda M, Compans RW (1974) Characterization of temperature sensitive influenza virus mutants defective in neuraminidase. Virology 61: 397-410.
119. Watanabe T, Watanabe S, Neumann G, Kida H, Kawaoka Y (2002) Immunogenicity and protective efficacy of replication-incompetent influenza virus-like particles. J Virol 76: 767-773.
120. Basler CF, Reid AH, Dybing JK, Janczewski TA, Fanning TG, et al. (2001) Sequence of the 1918 pandemic influenza virus nonstructural gene (NS) segment and characterization of recombinant viruses bearing the 1918 NS genes. Proc Natl Acad Sci U S A 98: 2746-2751.
121. Hale BG, Randall RE, Ortin J, Jackson D (2008) The multifunctional NS1 protein of influenza A viruses. J Gen Virol 89: 2359-2376.
122. Bergmann M, Garcia-Sastre A, Carnero E, Pehamberger H, Wolff K, et al. (2000) Influenza virus NS1 protein counteracts PKR-mediated inhibition of replication. J Virol 74: 6203-6206.
123. Garcia-Sastre A (2004) Identification and characterization of viral antagonists of type I interferon in negative-strand RNA viruses. Curr Top Microbiol Immunol 283: 249-280.
124. Garcia-Sastre A (2001) Inhibition of interferon-mediated antiviral responses by influenza A viruses and other negative-strand RNA viruses. Virology 279: 375-384.
125. Garcia-Sastre A, Egorov A, Matassov D, Brandt S, Levy DE, et al. (1998) Influenza A virus lacking the NS1 gene replicates in interferon-deficient systems. Virology 252: 324-330.
126. Eccles R (2005) Understanding the symptoms of the common cold and influenza. Lancet Infect Dis 5: 718-725.
127. Chaipan C, Kobasa D, Bertram S, Glowacka I, Steffen I, et al. (2009) Proteolytic activation of the 1918 influenza virus hemagglutinin. J Virol 83: 3200-3211.
128. Kido H, Okumura Y, Yamada H, Mizuno D, Higashi Y, et al. (2004) Secretory leukoprotease inhibitor and pulmonary surfactant serve as principal defenses against influenza A virus infection in the airway and chemical agents up-regulating their levels may have therapeutic potential. Biol Chem 385: 1029-1034.
129. Wilson IA, Cox NJ (1990) Structural basis of immune recognition of influenza virus hemagglutinin. Annu Rev Immunol 8: 737-771.
130. Knossow M, Skehel JJ (2006) Variation and infectivity neutralization in influenza. Immunology 119: 1-7.
131. de Jong JC, Palache AM, Beyer WE, Rimmelzwaan GF, Boon AC, et al. (2003) Haemagglutination-inhibiting antibody to influenza virus. Dev Biol (Basel) 115: 63-73.
132. Irwin DE, Weatherby LB, Huang WY, Rosenberg DM, Cook SF, et al. (2001) Impact of patient characteristics on the risk of influenza/ILI-related complications. BMC Health Serv Res 1: 8.

133. Kilbourne ED, Pokorny BA, Johansson B, Brett I, Milev Y, et al. (2004) Protection of mice with recombinant influenza virus neuraminidase. J Infect Dis 189: 459-461.
134. Bosch BJ, Bodewes R, de Vries RP, Kreijtz JH, Bartelink W, et al. (2010) Recombinant soluble, multimeric HA and NA exhibit distinctive types of protection against pandemic swine-origin 2009 A(H1N1) influenza virus infection in ferrets. J Virol 84: 10366-10374.
135. Strutt TM, McKinstry KK, Dibble JP, Winchell C, Kuang Y, et al. (2010) Memory CD4+ T cells induce innate responses independently of pathogen. Nat Med 16: 558-564, 551p following 564.
136. Wilkinson TM, Li CK, Chui CS, Huang AK, Perkins M, et al. (2012) Preexisting influenza-specific CD4+ T cells correlate with disease protection against influenza challenge in humans. Nat Med 18: 274-280.
137. Wang ML, Skehel JJ, Wiley DC (1986) Comparative analyses of the specificities of anti-influenza hemagglutinin antibodies in human sera. J Virol 57: 124-128.
138. Moscona A (2005) Neuraminidase inhibitors for influenza. N Engl J Med 353: 1363-1373.
139. Hayden FG, Treanor JJ, Fritz RS, Lobo M, Betts RF, et al. (1999) Use of the oral neuraminidase inhibitor oseltamivir in experimental human influenza: randomized controlled trials for prevention and treatment. JAMA 282: 1240-1246.
140. Gubareva LV, Kaiser L, Hayden FG (2000) Influenza virus neuraminidase inhibitors. Lancet 355: 827-835.
141. Colman PM, Varghese JN, Laver WG (1983) Structure of the catalytic and antigenic sites in influenza virus neuraminidase. Nature 303: 41-44.
142. Octaviani CP, Li C, Noda T, Kawaoka Y (2011) Reassortment between seasonal and swine-origin H1N1 influenza viruses generates viruses with enhanced growth capability in cell culture. Virus Res 156: 147-150.
143. Qi L, Davis AS, Jagger BW, Schwartzman LM, Dunham EJ, et al. (2012) Analysis by single-gene reassortment demonstrates that the 1918 influenza virus is functionally compatible with a low-pathogenicity avian influenza virus in mice. J Virol 86: 9211-9220.
144. Shinya K, Ebina M, Yamada S, Ono M, Kasai N, et al. (2006) Avian flu: influenza virus receptors in the human airway. Nature 440: 435-436.
145. Yaesoubi R, Cohen T (2011) Dynamic health policies for controlling the spread of emerging infections: influenza as an example. PLoS One 6: e24043.
146. Chen R, Holmes EC (2006) Avian influenza virus exhibits rapid evolutionary dynamics. Mol Biol Evol 23: 2336-2341.
147. Potier S, Robbe-Saul S, Boulanger Y (1980) Structural studies on aminoacyl-tRNA synthetases. A tentative correlation between the subunit size and the occurrence of repeated sequences. Biochim Biophys Acta 624: 130-141.
148. Laver G, Garman E (2002) Pandemic influenza: its origin and control. Microbes Infect 4: 1309-1316.
149. Taubenberger JK, Reid AH, Krafft AE, Bijwaard KE, Fanning TG (1997) Initial genetic characterization of the 1918 "Spanish" influenza virus. Science 275: 1793-1796.

150. Reid AH, Fanning TG, Hultin JV, Taubenberger JK (1999) Origin and evolution of the 1918 "Spanish" influenza virus hemagglutinin gene. Proc Natl Acad Sci U S A 96: 1651-1656.
151. Taubenberger JK, Baltimore D, Doherty PC, Markel H, Morens DM, et al. (2012) Reconstruction of the 1918 influenza virus: unexpected rewards from the past. MBio 3.
152. Fodor E, Devenish L, Engelhardt OG, Palese P, Brownlee GG, et al. (1999) Rescue of influenza A virus from recombinant DNA. J Virol 73: 9679-9682.
153. Rouillard JM, Lee W, Truan G, Gao X, Zhou X, et al. (2004) Gene2Oligo: oligonucleotide design for in vitro gene synthesis. Nucleic Acids Res 32: W176-180.
154. Hoffmann E, Stech J, Guan Y, Webster RG, Perez DR (2001) Universal primer set for the full-length amplification of all influenza A viruses. Arch Virol 146: 2275-2289.
155. Naffakh N, Massin P, Escriou N, Crescenzo-Chaigne B, van der Werf S (2000) Genetic analysis of the compatibility between polymerase proteins from human and avian strains of influenza A viruses. J Gen Virol 81: 1283-1291.
156. Shapiro GI, Gurney T, Jr., Krug RM (1987) Influenza virus gene expression: control mechanisms at early and late times of infection and nuclear-cytoplasmic transport of virus-specific RNAs. J Virol 61: 764-773.
157. Conenello GM, Tisoncik JR, Rosenzweig E, Varga ZT, Palese P, et al. (2011) A single N66S mutation in the PB1-F2 protein of influenza A virus increases virulence by inhibiting the early interferon response in vivo. J Virol 85: 652-662.
158. Flynn KJ, Belz GT, Altman JD, Ahmed R, Woodland DL, et al. (1998) Virus-specific CD8+ T cells in primary and secondary influenza pneumonia. Immunity 8: 683-691.
159. Smith AM, Adler FR, McAuley JL, Gutenkunst RN, Ribeiro RM, et al. (2011) Effect of 1918 PB1-F2 expression on influenza A virus infection kinetics. PLoS Comput Biol 7: e1001081.

6.0 Appendices

Appendix 1: Summary of Primers

Purple: Restriction enzymes cut sites incorporated into primers
Green: Random nucleotide sequence
Orange: Influenza NS untranslated region
Black: Target ORF gene sequence
Red: 1918 Influenza virus gene sequence
Blue: RV733 Influenza virus gene sequence

Primer Name	Use	Primer Sequence (5'-3')	Method	Notes
PA1918F	Clone influenza viral gene into pCAGGS expression vector for minigenome system	GCATCAACGTTATGGAAGACTTTGTGCG	PCR	
PA1918R		CGATCCTCGAGCTATCTCAGTGCATGTGTGAG	PCR	
PB11918F		GCATCGGCGCCATGGATGTCAATCCGACTTTAC	PCR	
PB11918R		CGATCCTCGAGCTACTTTTGCCGTCTGAGCTC	PCR	
PB21918F		GCATCAACGTTATGGAAAGAATAAAAGAACTAAGGGATC	PCR	
PB21918R		CGATCCTCGAGCTAATTGATGGCCATCCGAATTC	PCR	
NP1918F		GCATCAACGTTATGGCGTCTCAAGGCACC	PCR	
NP1918R		CGATCCTCGAGTTAATTGTCGTACTCCTCTGCATTGTCTCCG	PCR	
PARV733F		GCATCAACGTTATGGAAGATTTTGTGCGACAATG	PCR	
PARV733R		CGATCCTCGAGCTATCTCAATGCATGTGTTAGG	PCR	
PB1RV733F		GCATCGGCGCCATGGATGTCAATCCGACATTAC	PCR	
PB1RV733R		CGATCCTCGAGCTATTTTTGCCGTCTGAGGTC	PCR	
PB2RV733F		GCATCAACGTTATGGAAAGAATAAAAGAGCTAAG	PCR	
PB2RV733R		CGATCCTCGAGTTAATTGATGGCCATCCGAATTC	PCR	
NPRV733F		GCATCAACGTTATGGCGTCCCAAG	PCR	
NPRV733R		CGATCCTCGAGTTAATTGTCGTACTCCTCTG	PCR	
GFP fwd	Clone GFP into pPol for minigenome system	TATTCGTCTCAGGGAGCAAAAGCAGGGTGGCAAAGACATAATGGTGAGCAAGGG	PCR	
GFP rev	Clone GFP into pPol for minigenome system	ATATCGTCTCGTATTAGTAGAAACAAGGGTGTTTTTTATCACTATTACTTGTACAG	PCR	
FFLucfwd	Clone FFLuc gene into pPol for minigenome system	TATTCGTCTCAGGGAGCAAAAGCAGGGTGGCAAAGACATAATGGAAGACGCCAAAAACATAAAGAAAGGCC	PCR	
FFLucrev	Clone FFLuc gene into pPol for minigenome system	ATATCGTCTCGTATTAGTAGAAACAAGGGTGTTTTTTATCACTATTACAATTTGGACTTTCCGCCCTTCTTGG	PCR	
M13 fwd	Sequencing pCR2.1 TOPO constructs	GTA AAACGACGGCCAGT	Sequencing	
M13 rev	Sequencing pCR2.1 TOPO constructs	GTT TTCCCAGTCACGAC	Sequencing	
pPolfwd	Cloning into pPol vector and PB1 chimera PCR	TATTCGTCTCAGGGAGCGAAAGCAGGCA	PCR	
pPolrev	Cloning into pPol vector and PB1 chimera PCR	TTTACGGAACAAAGATGATTATGCTCTGCTATA	PCR	
Ch1PB1intfwd	PB1 chimera PCR	CAAGGCCGACAGACCTATGACTGGACTCTAAATAGGAACC	PCR	Use with primer pPolrev
Ch1PB1intrev	PB1 chimera PCR	GTTCCGGCTGTCTGGATACTGACCTGAGATTT	PCR	Use with primer

		ATCCTTGG		pPolfwd
Ch2PB1int1fwd	PB1 chimera PCR	CAAGGCCGACAGACCTATGACTGGACTCTAAA TAGGAACC	PCR	Use with primer Ch2PB1int2rev
Ch2PB1int1rev	PB1 chimera PCR	GTTCCGGCTGTCTGGATACTGACCTGAGATTT ATCCTTGG	PCR	Use with primer pPolfwd
Ch2PB1int2fwd	PB1 chimera PCR	CAGGATTGCCAGTTGGAGGAAATGAGAAGAAA GCAAAG	PCR	Use with primer pPolrev
Ch2PB1int2rev	PB1 chimera PCR	GTCCTAACGGTCAACCTCCTTTACTCTTCTTTC GTTTC	PCR	Use with primer Ch2PB1int1fwd
Ch3PB1int1fwd	PB1 chimera PCR	CAATCAGGATTGCCAGTTGGAGGTAATGAGAA GAAAGCC	PCR	Use with primer Ch3PB1int2rev
Ch3PB1int1rev	PB1 chimera PCR	GTTAGTCCTAACGGTCAACCTCCATTACTCTTC TTTCGG	PCR	Use with primer pPolfwd
Ch3PB1int2fwd	PB1 chimera PCR	CGAACCTGTAAGCTGCTTGGAATTAATATGAG CAAAAAG	PCR	Use with primer pPolrev
Ch3PB1int2rev	PB1 chimera PCR	GCTTGGACATTCGACGAACCTTAATTATACTCG TTTTTC	PCR	Use with primer Ch3PB1int1fwd
Ch4PB1int1fwd	PB1 chimera PCR	CCTGTAAGCTGCTTGGAATCAATATGAGCAAG AAAAAGTC	PCR	Use with primer Ch4PB1int2rev
Ch4PB1int1rev	PB1 chimera PCR	GGACATTCGACGAACCTTAGTTATACTCGTTCT TTTTCAG	PCR	Use with primer pPolfwd
Ch4PB1int2fwd	PB1 chimera PCR	GCTCAAATGGCCCTTCAGTTGTTCATCAAAGAT TACAGG	PCR	Use with primer pPolrev
Ch4PB1int2rev	PB1 chimera PCR	CGAGTTTACCGGGAAGTCAACAAGTAGTTTCT AATGTCC	PCR	Use with primer Ch4PB1int1fwd
Ch5PB1int1fwd	PB1 chimera PCR	GCTCAAATGGCCCTTCAGTTATTTATAAAAGAT TACAGG	PCR	Use with primer Ch5PB1int2rev
Ch5PB1int1rev	PB1 chimera PCR	CGAGTTTACCGGGAAGTCAATAAATATTTTCTA ATGTCC	PCR	Use with primer pPolfwd
Ch5PB1int2fwd	PB1 chimera PCR	CTCCAAAGCTGGGCTGTTGGTCTCTGATGGAG	PCR	Use with primer pPolfwd
Ch5PB1int2rev	PB1 chimera PCR	GAGGTTTCGACCCGACAACCAGAGACTACCCT	PCR	Use with primer Ch5PB1int1fwd
Ch6PB1int1fwd	PB1 chimera PCR	AAAGCTGGGCTGTTGGTCTCCGACGGA	PCR	Use with primer pPolrev
Ch6PB1int1rev	PB1 chimera PCR	TTTCGACCCGACAACCAGAGGCTGCCT	PCR	Use with primer pPolfwd
PB1fwd	Genotyping	GCCTGCTGCA ACAGCATTG G	RT-PCR and sequencing	Random hexamer primer used in RT step
PB1rev	Genotyping	C CTGGGG TTGCAATTGC	RT-PCR and sequencing	Random hexamer primer used in RT step
PAfwd	Genotyping	CACATATACTATCTGGAAAAGGCC	RT-PCR and sequencing	Random hexamer primer used in RT step
PArev	Genotyping	GAATCCATCCACATAGGCTC	RT-PCR and sequencing	Random hexamer primer used in RT step
PB2fwd	Genotyping	CATGGAACCTTTGGCCCTG	RT-PCR and sequencing	Random hexamer primer used in RT step
PB2rev	Genotyping	TCATCATTCCTCACTTCCCCA	RT-PCR and sequencing	Random hexamer primer used in RT step
NPfwd	Genotyping	CTGGAAGAACATCCCAGCG	RT-PCR and sequencing	Random hexamer primer used in RT step
NPrev	Genotyping	GATCCCACGTTTGATCA CCTG	RT-PCR and sequencing	Random hexamer primer used in RT step

Appendix 2: TrackIt 1Kb Plus DNA Ladder

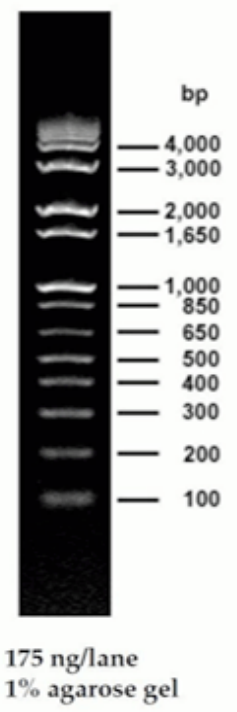

Appendix 3: Recipes

6x DNA Gel Loading buffer
30% Glycerol (dissolved in water)
0.25% Bromophenol Blue

SOC medium
20 g Bacto Tryptone
5 g Bacto Yeast Extract
2 ml 5M NaCl
2.5 ml M KCl
10 ml 1M $MgCl_2$
10 ml 1M $MgSO_4$
20 ml 1M Glucose
900 ml water
Adjust to 1000 ml

LB Broth
10 g tryptone
5 g yeast extract
10 g NaCl
Adjust volume to 1000 ml